2022

Associations of feline paramyxoviruses with pathological lesions in cat kidneys

Aisyah Nikmatuz Zahro
Faculty of Veterinary Science

ASSOCIATIONS OF FELINE PARAMYXOVIRUSES WITH PATHOLOGICAL LESIONS IN CAT KIDNEYS

Miss Aisyah Nikmatuz Zahro

A Thesis Submitted in Partial Fulfillment of the Requirements
for the Degree of Master of Science in Veterinary Science and technology
FACULTY OF VETERINARY SCIENCE
Chulalongkorn University
Academic Year 2022

ความสัมพันธ์ของฟีไลน์พารามิกโซไวรัสกับพยาธิสภาพในไตแมว

น.ส.อาซิยาห์ นิคมาตุส ซาห์โร

วิทยานิพนธ์นี้เป็นส่วนหนึ่งของการศึกษาตามหลักสูตรปริญญาวิทยาศาสตรมหาบัณฑิต
สาขาวิชาวิทยาศาสตร์ทางการสัตวแพทย์และเทคโนโลยี ไม่สังกัดภาควิชา/เทียบเท่า
คณะสัตวแพทยศาสตร์ จุฬาลงกรณ์มหาวิทยาลัย
ปีการศึกษา 2565

Thesis Title	ASSOCIATIONS OF FELINE PARAMYXOVIRUSES WITH PATHOLOGICAL LESIONS IN CAT KIDNEYS
By	Miss Aisyah Nikmatuz Zahro
Field of Study	Veterinary Science and technology
Thesis Advisor	Associate Professor Doctor SOMPORN TECHANGAMSUWAN, Ph.D.
Thesis Co Advisor	Doctor CHUTCHAI PIEWBANG, Ph.D.

Accepted by the FACULTY OF VETERINARY SCIENCE, Chulalongkorn University in Partial Fulfillment of the Requirement for the Master of Science

..... Dean of the FACULTY OF VETERINARY SCIENCE

(Professor Doctor SANIPA SURADHAT, Ph.D.)

THESIS COMMITTEE

..... Chairman

(Associate Professor Doctor NOPADON PIRARAT, Ph.D.)

..... Thesis Advisor

(Associate Professor Doctor SOMPORN TECHANGAMSUWAN, Ph.D.)

..... Thesis Co-Advisor

(Doctor CHUTCHAI PIEWBANG, Ph.D.)

..... Examiner

(Professor Doctor ANUDEP RUNGSIPIPAT, Ph.D.)

..... External Examiner

(Doctor SURANGKANANG CHAIYASAK, Ph.D.)

อาซิยาห์ นิคมาตุส ซาห์โร : ความสัมพันธ์ของฟีไลน์พารามิกโซไวรัสกับพยาธิสภาพในไตแมว. (ASSOCIATIONS OF FELINE PARAMYXOVIRUSES WITH PATHOLOGICAL LESIONS IN CAT KIDNEYS) อ.ที่ปรึกษาหลัก : รศ. ดร.สมพร เตชะงามสุวรรณ, อ.ที่ปรึกษาร่วม : ดร.ฉัตรชัย ผิวบาง

พารามิกโซไวรัสในแมวประกอบด้วย 3 ไวรัสหลัก ได้แก่ ฟีไลน์พารามิกโซไวรัส (FPaV) ฟีไลน์มอบิลลิไวรัสชนิดที่ 1 (FeMV-1) และ 2 (FeMV-2) ซึ่งมีการศึกษามาก่อนหน้าว่าอาจมีความสัมพันธ์กับโรคไตในแมว อย่างไรก็ตาม ขบวนการทางพยาธิวิทยาของการเกิดโรคยังไม่ทราบแน่ชัด การศึกษานี้มีวัตถุประสงค์ในการหาความสัมพันธ์ของการติดเชื้อพารามิกโซไวรัสกับพยาธิสภาพในไตแมว โดยทำการเก็บตัวอย่างชิ้นเนื้อไตจากแมวที่เข้ารับการชันสูตรซากที่ภาควิชาพยาธิวิทยา คณะสัตวแพทยศาสตร์ จุฬาลงกรณ์มหาวิทยาลัย แบ่งลักษณะทางจุลพยาธิวิทยาของไตออกเป็น 2 กลุ่ม คือกลุ่มปกติ และกลุ่มที่มีพยาธิสภาพ ทำการตรวจคัดกรองเบื้องต้นหาการติดเชื้อพารามิกโซไวรัสด้วยวิธีปฏิกิริยาลูกโซ่แบบย้อนกลับ (RT-PCR) ด้วยไพรเมอร์ชนิด Res-Mor-Hen pan-primer และไพรเมอร์ที่มีความจำเพาะกับพารามิกโซไวรัสแต่ละชนิด สำหรับไตที่ให้ผลบวกจะทำการย้อมด้วยสีพิเศษชนิด Periodic acid-Schiff (PAS) และ Masson Trichrome (MT) เพื่อดูความเสียหายของฐานเยื่อบุไตและการแทรกของเนื้อเยื่อเกี่ยวพันในไต ทำการย้อมด้วยเทคนิคอิมมูโนฮิสโตเคมี (IHC) และอินไซตูไฮบริไดเซชั่น (ISH) เพื่อดูการปรากฏของไวรัสแอนติเจนและสารพันธุกรรมไวรัส ทำการย้อมดู Apoptotic activity โดยดูการแสดงออกของ cleaved caspase 3 ทำการให้คะแนนแบบกึ่งคุณภาพสำหรับตัวอย่างที่พบพารามิกโซไวรัสกับคุณลักษณะทางจุลพยาธิวิทยา ได้แก่ การอักเสบของไต เซลล์บุท่อไตเสียหาย การแทรกของเนื้อเยื่อเกี่ยวพันและ Apoptotic activity หาความสัมพันธ์ทางสถิติด้วย Spearman correlation coefficient (p>0.05) ผลการศึกษาพบว่ามีไตแมว 9 ตัวให้ผลบวกต่อการตรวจด้วย RT-PCR และเป็น FeMV-1 ทั้งหมด อีกทั้งไตยังแสดงรอยโรคทางพยาธิวิทยา โดยพบเซลล์อักเสบชนิดลิมโฟไซท์และพลาสมาเซลล์แทรกเข้ามาในเนื้อเยื่อระหว่างท่อไต การย้อมด้วย IHC และ ISH พบให้ผลบวกในไตแมว 7 ตัว และ 9 ตัว ตามลำดับ บริเวณที่ให้ผลบวกพบทั้งในส่วนที่เป็นนิวเคลียสและไซโตพลาสมของเยื่อ

สาขาวิชา วิทยาศาสตร์ทางการสัตวแพทย์และเทคโนโลยี ลายมือชื่อนิสิต .....

ปีการศึกษา 2565 ลายมือชื่อ อ.ที่ปรึกษาหลัก .....

ลายมือชื่อ อ.ที่ปรึกษาร่วม .....

6378504031 : MAJOR VETERINARY SCIENCE AND TECHNOLOGY
KEYWORD: Cat Immunohistochemistry In situ hybridization Kidney Paramyxovirus Pathology

Aisyah Nikmatuz Zahro : ASSOCIATIONS OF FELINE PARAMYXOVIRUSES WITH PATHOLOGICAL LESIONS IN CAT KIDNEYS. Advisor: Assoc. Prof. Dr. SOMPORN TECHANGAMSUWAN, Ph.D. Co-advisor: Dr. CHUTCHAI PIEWBANG, Ph.D.

Paramyxoviruses in cats composing of feline paramyxovirus (FPaV), feline morbillivirus genotype 1 (FeMV-1), and feline morbillivirus genotype 2 (FeMV-2). These viruses had been recently suggested to be associated with kidney disease in cats. However, pathological consequence of infection is remained restricted. This study aimed to investigate the association of paramyxovirus infection and pathological consequence in cats' kidney. Renal fresh tissues were collected from routine necropsy in Department of Pathology, Faculty of Veterinary Science, Chulalongkorn University. Then, tissues were histopathologically categorized into normal group and pathologic group. To screen paramyxovirus infection, reverse-transcription polymerase chain reaction (RT-PCR) assays using Res-Mor-Hen pan-primer set and specific primer set for each virus were carried out. Then, RT-PCR positive cases were employed for special staining determination using Periodic acid-Schiff (PAS) and Masson Trichrome (MT), followed by immunohistochemistry (IHC) and *in situ* hybridization (ISH). Furthermore, apoptotic activity assay was employed to detect the expression of cleaved caspase 3. Semiquantitative scorings were carried out for positive cases according to histopathological parameters such as degree of interstitial inflammation, tubular detachment, fibrosis, and apoptotic activity. The statistic data was evaluated using Spearman correlation coefficient with two-tailed test and $p<0.05$. The result of molecular detection revealed that

Field of Study: Veterinary Science and technology — Student's Signature .....

Academic Year: 2022 — Advisor's Signature .....

Co-advisor's Signature .....

ACKNOWLEDGEMENTS

I would like to express my deepest appreciation and gratitude to my Principle Thesis Advisor Associate Professor Doctor Somporn Techangamsuwan for her sincerity and patience guiding me for this past two year of my master study. Furthermore, I am deeply indebted to my Thesis Advisor Dr. Chutchai Piewbang for encouragement he gives me so I keep trying and not giving up on bad days. I feel so grateful for becoming part of Animal Virome and Diagnostic Development Research Group (AVDD), a place to grow not only as a beginner in scientific life, but also as a person.

My gratitude for my senior Wichan Dankaona, Panida Poonsin, Sabrina Wahyu Wardhani, Pattiya Lohavicharn, Tin Van Nguyen for teach me about laboratory activities, countless thoughtful ideas, and cheering me up everyday.

I would like to extend my deepest gratitude for all lecturers and staffs of Department of Pathology, Faculty of Veterinary Science, Chulalongkorn University for warm welcome and sincere help that I always receive during my study.

I am also grateful to Graduate School of Chulalongkorn University for giving me opportunity to elevate my knowledge and capability through scholarship program of Graduate Scholarship Program for ASEAN or Non-ASEAN countries. Furthermore, this research is supported by the 90th Anniversary of Chulalongkorn University Scholarship under the Ratchadapisek Somphot Endowment Fund.

I am extremely grateful to my friends Chairani Ridha Maghfiroh, Quang Trung Lee, Kiitipath Supchukun and Eaint Min Phyu for all wonderful experiences I had in Thailand.

Moreover, special thanks to all my senior and friends from Indonesia. Last but not the least, my deeply gratitude for my parents and my family in Indonesia. This wouldn't be possible to happen without their supports.

Sincerely,

Aisyah Nikmatuz Zahro

TABLE OF CONTENTS

LIST OF TABLES

Page

LIST OF FIGURES

Page

CHAPTER 1
INTRODUCTION

Pets become important part of human life and offer many benefits such as improving both mental and physical health of the owner and offer a promising economic impact (Sterneberg-van der Maaten et al., 2016). According to data compiled by The European Pet Food Industry Federation (FEDIAF) in 2020, it was estimated that around 88 million household in Europe continent had at least one pet animal in their house. Among those pet animals, cat is the most favorable animal to be raised as pet compared to other animals (FEDIAF, 2020). In 2017, surveying in pet ownership and demographic distribution by American Veterinary Medical Association (AVMA) revealed that cats were nominated as the second most favorable pet to be kept in American households (AVMA, 2018).

Cat, either pure-breed or crossbreed, is possessed by many health issues. A study conducted in England classified the most common health problems in cats such as periodontal problem (13.9%), flea infestation (8%), obesity (6.7%), heart murmur (5%), traumatic injury (4.6%), nail clip (3.7%), chronic kidney disease (3.6%), cat bite injury (3.6%), abscess (3.2%), and cat bite abscess (3.2%) (O'Neill et al., 2014). As a terrestrial animal, it is also vulnerable to many exposures from infectious agent from environment such as *Echinococcosis* (Bonelli et al., 2018) and *Dematiaceous* fungal infections (Bouljihad et al., 2002).

Compared to other animal species, cats are prone to be vulnerable to renal disease or renal failure (Sugisawa et al., 2016). This vulnerability associates with several factors such as dietary, breed predisposition, congenital disease and acquired illness (Finch et al., 2016). Regarding the duration of disease progression, cats could suffer from acute and chronic renal failures. Acute renal failure is the loss of kidney function in short period, whereas chronic renal failure is loss of kidney function in longer course (Newman, 2012). Acute renal failure or known as acute kidney injury (AKI) is the consequence of exposure of insults such as nephrotoxic substance, ischemia, obstruction, neoplasia, and infection, onto that kidney undergoes self-repairment mechanism to compensate the loss. In contrast, chronic renal failure or

known as chronic kidney disease (CKD) is the stage that kidney fails to serve self-repairment mechanism any longer (Monaghan et al., 2012).

In human medicine, infections damage the kidney in several pathways such as direct alteration on renal tissue structure, formation of antigen-antibody complex, and triggering systemic inflammatory response syndrome (SIRS) (Prasad and Patel, 2018). In cats, infectious agents such as virus, bacteria, parasite can cause injuries in feline kidney, even further, it can initiate CKD (Hartmann et al., 2020). Kidney injuries initiate inflammatory response associated with cytokines and chemokines secretion which aim to repair the damage and activating pro-fibrotic reaction. Although this mechanism is expected to repair the damage, in contrast, incomplete action or prolonged response would generate fibrosis (inverted result) (Black et al., 2019). Among those infectious agents, viral pathogen takes essential role in feline medicine (Beatty and Hartmann, 2021). Accordance with its nature as an obligate parasite, virus hijacks host metabolism system and use them as the instrument to survive, by undergo replication inside the host cell then shed to environment. Thus, virus is able to infect animal population rapidly (Bruggeman, 2007; Zwart and Elena, 2015).

Recently, viruses from family *Paramyxoviridae* have been notified to have an association with the kidney disease in cats. Those viral pathogens are feline morbillivirus genotype 1 (FeMV-1), feline morbillivirus genotype 2 (FeMV-2), and feline paramyxovirus (FPaV) (Sieg et al., 2015; Hartmann et al., 2020; Piewbang et al., 2020). The evidence revealed that these viruses can be molecularly detected in kidney of cats possessed both with and without renal diseases (Sieg et al., 2015; McCallum et al., 2018). To date, the suspicious viruses have been discovered in some continents such as Asia, Europe, and United States (Sieg et al., 2015; McCallum et al., 2018; Mohd Isa et al., 2019; Balbo et al., 2021). However, the pathologic alteration and viral distribution of the suspicious viruses on infected renal tissue remain restricted. Therefore, it is worthy to perform viral molecular, pathological and immunohistochemical investigations of suspicious viruses that could be associated with feline kidney disease.

Objectives of study

1. To investigate the occurrence of paramyxoviruses (FeMV-1, FeMV-2, FPaV) in feline kidneys by molecular detection
2. To study the pathological alteration of feline kidneys associated with the presence of paramyxoviruses by histopathological examination, special staining determination and apoptotic activity evaluation
3. To localize and evaluate the viral distribution of paramyxoviruses in kidney tissues by performing immunohistochemistry (IHC) and *in situ* hybridization (ISH) techniques

Keywords (Thai): แมว อิมมูโนฮิสโตเคมี อินไซตูไฮบริไดเซชั่น ไต พารามิกโซไวรัส พยาธิวิทยา
Keywords (English): Cat, Immunohistochemistry, *In situ* hybridization, Kidney, Paramyxovirus, Pathology

Hypothesis

The paramyxoviruses will be detected and localized in the feline kidneys by molecular and immunological investigations. The associated pathological changes will be elucidated accordingly.

CONCEPTUAL FRAMEWORK

ASSOCIATIONS OF FELINE PARAMYXOVIRUSES WITH PATHOLOGICAL LESIONS IN CAT KIDNEYS

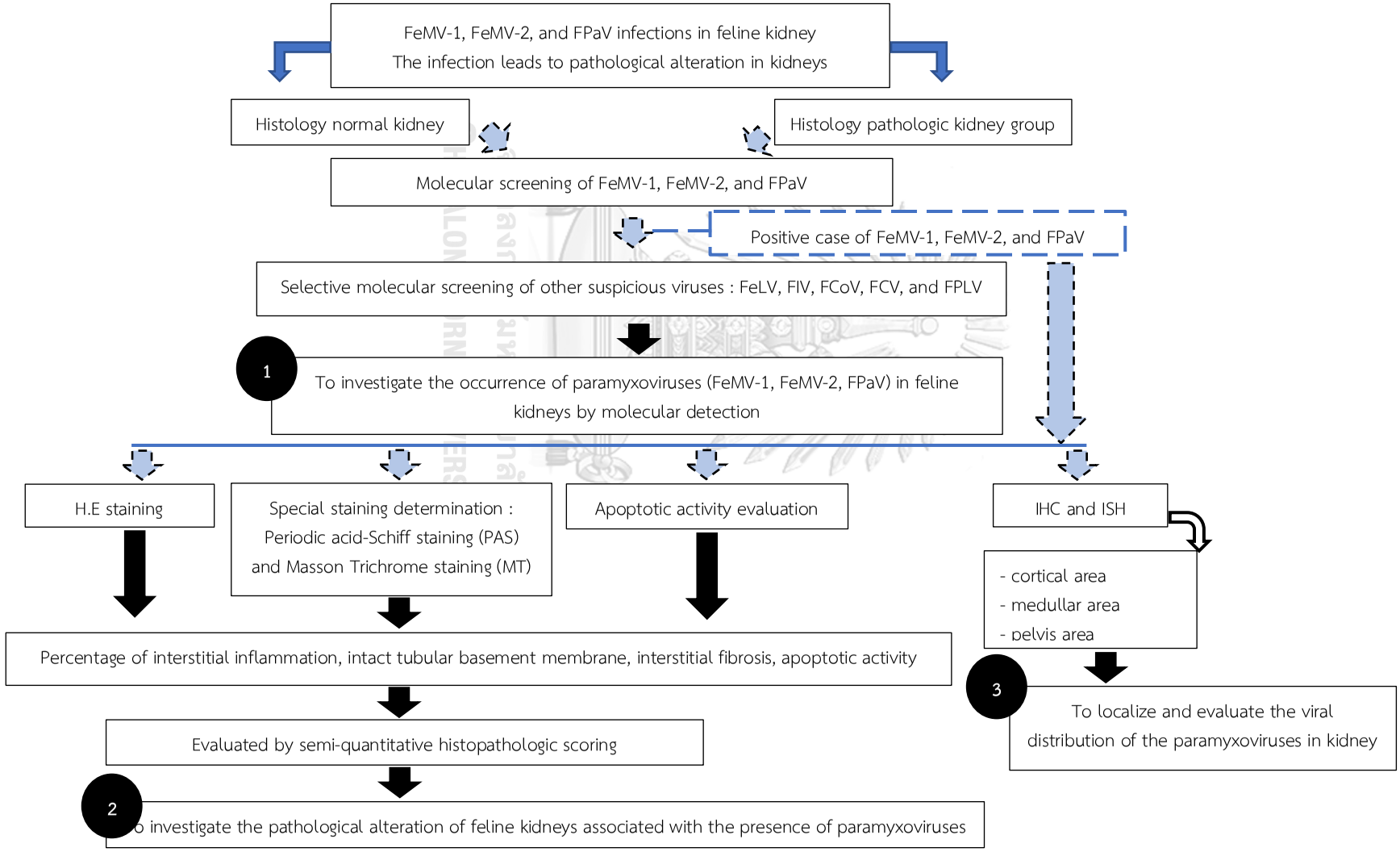

Advantages of the study

1. Provide the information regarding infection of FeMV-1, FeMV-2, and FPaV viruses that can be detected in feline kidney
2. Provide the information that associates with pathological alteration on renal tissue regarding the paramyxovirus infection
3. Reveal viral localization and distribution of paramyxoviruses in feline kidney

CHAPTER 2
LITERATURE REVIEW

Pathology and associated immune response of feline kidney

Kidney is a pair of complex organs that serve several physiological functions such as excretory, secretory, and metabolism regulation in mammals. Kidneys are susceptible for various insults that affect its physiologic anatomy and function, generating pathologic condition on kidney (Newman, 2012). Regarding the period of the insults, pathological condition of kidney is differentiated into two types which are acute kidney injury (AKI) and chronic kidney disease (CKD) (Chen et al., 2020). AKI is the disturbance on kidney that result in both anatomical and/or functional damage of kidney occurred in short-certain period (Makris and Spanou, 2016; Chen et al., 2020). AKI is a reversible condition in both human and animal with life expectancy around 50% (Long et al., 2016; Chen et al., 2020). Furthermore, CKD is the disturbance on kidney that occurred for certain-longer period than the AKI (approximately 3 months) that affect the structural and function of kidneys (Bartges, 2012). CKD is an irreversible condition occurring on all ages but the prevalence is higher in older animals (Bartges, 2012). It is the most common renal disease in cats (Reynolds and Lefebvre, 2013). Beforehand in human medicine, AKI and CKD are acknowledged as two separated cases, in which episodic AKI could lead to CKD. However, some evidence proves that both cases are the risk factor for each other. AKI contributes on the occurrence of CKD and vice versa (Hsu and Hsu, 2016). This similar situation can also be found in cats and dogs. International Renal Interest Society (IRIS) reported that AKI and CKD are no longer two different separate systems because they share common biomarkers which are existing in both illnesses (Segev, 2022).

There are several etiologies could damage kidney, such as feline polycystic kidney disease (FPKD), amyloidosis, dysplasia, renal lymphoma, nephrotoxic agent and infectious agents such as virus, bacteria as well as parasite (Monaghan et al., 2012; Reynolds and Lefebvre, 2013; Lawson et al., 2015; Hartmann et al., 2020) . The damage leads to hypoxia which followed by diminishing of ATP storage in the affected area. This condition initiates the decreasing of glomerular filtration rate (GFR). The reduction of ATP triggers the elevation of intracellular calcium level. The ATP reduction also induces the activation of protease and phospholipase which aim to lead the accumulation of reactive oxygen species and free radicals that initiate tissue damage. The sequence of this event triggers the response of inflammatory system by producing cytokines and chemokines, followed by initiation of tissue repairing process in which benefits for the kidney but also alter the kidney structure, by leaving scar mark on renal tissue. Further, the continuing of hypoxia generating extensive inflammatory response due to the presence of apoptosis and necrosis of tubular epithelial cells, which damage the endothelial cell, lead to activity enhancement of vasoconstriction components. The endothelial damaging increases the expression of P- and E-selectin and intracellular adhesion molecule-1 (ICAM-1) which the mediators of endothelial-leukocytes interaction. These mediators regulate the leukocytes to ischemic area. This event accelerates the inflammatory cascades; generate congestion that deteriorates the ischemia, given rise to the damage of tubular epithelial cells. In contrast, after this sequence of threats, the GFR returns to normal. However, the apoptotic activity would remain, but the blood flow returns to normal, which landmark of tissue repairment. Although the GFR returns to normal rate, there would be possibility that residual of the injury is remained (Monaghan et al., 2012). This acute response usually present unnoticeable because the compensatory mechanism still working and clinical signs are absent. If the insult

reoccurs, the response will reach threshold point then the kidney could not compensate the damage (Cowgill et al., 2016; Chen et al., 2020).

As known that CKD is very common in cats and the prevalence increases in senior cats, until now the pathogenesis of CKD remains unsolved. In other animal, it is suggested that CKD is initiated by the presence of chronic primary renal disease such as amyloidosis that is found in cats as well. Despite the presence of primary renal insult, in cats, inherent factors such as breed predisposition and congenital condition might initiate CKD. Moreover, external factors such as acute insults and aging play a role to prolong the disease (Brown et al., 2016). Commonly, CKD in cats is often diagnosed on final stage when the impaired kidneys are unable to compensate the damage and the irreversible injury has been demonstrated (Chen et al., 2020). CKD gives rise to the pathological alteration of glomeruli, tubules, vasculature, and interstitial tissues of kidney. Tubulointerstitial damage (TID) is the hallmark of shifting between CKD and end-stage renal disease. The pathological response that initiate TID is an infiltration of mononuclear cell, tubular injury, and interstitial fibrosis (Yabuki et al., 2010). TID is the sequelae of myofibroblast activity that produce extracellular matrix (ECM). This myofibroblastic cell is an underlying component of wound healing and fibrous connective tissue synthesis in many organs such as kidney (Bascands and Schanstra, 2005; Yabuki et al., 2010). Myofibroblast has its origin from interstitial fibroblast. Under physiological condition, interstitial fibroblast has a role in managing the homeostasis of ECM. Once the insult appears in renal interstitial area, fibroblastic cell undergo transformation to become myofibroblast. This myofibroblast proliferates and responds to the chronic injury by producing fibrous tissue that would generate fibrosis (Strutz and Zeisberg, 2006; Lawson et al., 2015).

Regarding the immune response on pathological kidney, the sterile insults (toxins, ischemia, and trauma) damage the renal tissue by generating apoptosis and

necrosis of the renal cell (Kurts et al., 2013). Apoptosis is programmed cell death that is physiologically occurs and aims to maintain the homeostasis of cell population in tissue (Ludes et al., 2021; Obeng, 2021). In contrast, necrosis is pathological cell death that induced by extreme environment such as injury (Syntichaki and Tavernarakis, 2002). Necrotic renal cell releases the damage-associated molecular pattern (DAMP) filling the extracellular area. DAMP activates the pattern recognition receptors (PRRs) expressed on renal cell. This activation triggers several cellular responses in renal tissue such as mononuclear cell e.g; dendritic and macrophage cells that mostly founded in most kidney disease including AKI and infections. Furthermore, endothelial cell, mesangial cell, and podocyte cell will produce tumor necrosis factor (TNF) as well as interleukin-6 (IL-6) that associates with glomerular disease. In addition, endothelial cell and mesangial cell will produce interferon alpha (IFN-alpha). Eventually, tubular epithelial cell also gives rise to response on the insult by producing TNF and IL-6 as well (Kurts et al., 2013).

Kidney is part of urinary tract systems that exhibits high chance of infection. Regarding this risk factor, kidney is protected by various resident immune cells to prevent the infections (Abraham and Miao, 2015). The viral infection associated to kidney Injury can occur for short period (acute) or long period (chronic). It causes pathological condition directly or indirectly as the consequence of local or systemic inflammatory response. Once the virus inserts its genetic material in the host cell, this genomic material plays a role as pathogen associated molecular patterns (PAMPs). Following the viral invasion, the PAMPs will be recognized by intracellular pattern recognition receptors such as Toll-like receptors (TLRs) and retinoic acid-inducible gene 1-like receptors (RLRs) of innate immune system. The outcome of this action is the host cell undergo endocytic-lysosomal degradation objected to eliminate the viral genome or induce apoptosis to eradicate infected cell. Further, the pattern recognition also serves the secretion of interferon and interleukin that

modulate and activate T and B lymphocyte cells of acquired immune system. The consequence of this robust response is massive cytokine activation and interstitial inflammation, given rise to acute renal failure. The chronic response of this infection would extend the inflammatory response followed by fibrosis. Moreover, antibody-antigen complex that is deposited in the microvasculature may generate immune-complex glomerulonephritis (ICGN). In this sequela, adaptive immune cell such as natural killer (NK) cell might be recruited and aggravate renal tissue damage by cell-mediated killing-mechanism aiming for the infected cell. Further, epithelial cells loss due to apoptosis or cell-mediated killing-mechanism initiate tissue recovery by arranging deposition of temporary matrix, inducing epithelial cells proliferation, and fibroblast and remodeling matrix recruitment. This sequence of response would deteriorate the normal renal tissue and affecting the kidney function. Despite the inflammatory response, the virus would also hijack the cellular homeostasis of infected renal cell to support the viral replication that causing dysregulation of tissue repairment process (Bruggeman, 2019).

Paramyxovirus associated to feline kidney disease

Paramyxovirus is a single-stranded negative-sense enveloped RNA virus member of family *Paramyxoviridae*, order *Mononegavirales*. It infects various host range such as mammals, birds, fish and reptiles. According to International Committee on Taxonomy of Viruses (ICTV), family *Paramyxoviridae* is comprised of four subfamilies which are *Avulavirinae*, *Rubulavirinae*, *Orthoparamyxovirinae* and *Metaparamyxovirinae* (Rima et al., 2019). Among family of *Paramyxoviridae* member, some viruses are associated to disease in both human and animals, even has zoonotic potential such as Nipah and Hendra viruses (Thibault et al., 2017). Furthermore, several paramyxoviruses are notifiable to be associated with severe disease in human such as respiratory syncytial virus (RSV), human metapneumovirus

(hMPV), human parainfluenza virus (hPIV) (Chen et al., 2021), and measles virus (Naim, 2015).

In the veterinary field, paramyxoviruses also associated with diseases in animals such as newcastle disease, canine distemper (CDV), and rinderpest (Samal, 2008). Recently, newly discovered paramyxoviruses are suspected to be associated with feline kidney disease, such as FeMV-1, FeMV-2, and FPaV (Woo et al., 2012; Sieg et al., 2015; Sieg et al., 2019). Although many evidences have revealed the presence of genomic material of suspicious viruses in clinical samples and tissues (Sieg et al., 2019; Piewbang et al., 2020; De Luca et al., 2021), the pathological alteration on kidney that caused by these viruses remains restricted. Hence, it is worth to perform further investigation.

Feline Morbillivirus (FeMV)

Feline Morbillivirus (FeMV) is a virus belonged to family *Paramyxoviridae*, genus *Morbillivirus*. It is firstly discovered in 2012 in Hongkong, isolated from stray cats, and suspected to be associated with tubulo-interstitial nephritis (TIN) (Woo et al., 2012), with the subsequent presence of eosinophilic intracytoplasmic inclusion bodies (ICIB) (Figure 1) (Chaiyasak et al., 2022). Since then, FeMV is discovered in various countries such as Germany (Sieg et al., 2015), the United Kingdom (McCallum et al., 2018), Italy (Marcacci et al., 2016), Japan (Sakaguchi et al., 2020), Thailand (Chaiyasak et al., 2020a; Piewbang et al., 2020), Malaysia (Mohd Isa et al., 2019), Turkey (Yilmaz et al., 2017), the United states (Sharp et al., 2016), and Brazil (Balbo et al., 2021). The virion organization of FeMV is consisted of six open reading frames (ORFs), which encode six structural proteins and two accessories proteins, and arranged in 16,050 bases of genome length. It indicates the longest genome length among morbilliviruses. The structural proteins of FeMV are consisted of nucleoprotein (N), phosphoprotein (P), matrix protein (M), fusion protein (F),

hemagglutinin protein (H), and polymerase protein (L) (Woo et al., 2012). The compatible host of FeMV is *Felidae* family such as domestic cats and wild *Felidae*. Surprisingly, it is also identified on other non-felidae species such as dog and opossum (Lavorente et al., 2021; Piewbang et al., 2021b). According to genomic characterization, FeMV forms two distinct genotypes. FeMV genotype 1 (FeMV-1) was firstly reported in Hongkong, whereas FeMV genotype 2 (FeMV-2) was initially discovered in Germany. It is notified on in vitro assay that the tissue tropism of FeMV-2 is broad wider than FeMV-1 (Woo et al., 2012; Sieg et al., 2019).

The pathogenesis of FeMV remains unclear. Regarding the presence of H and F envelope proteins, both proteins play a role on attachment, fusion and tissue tropism respectively (De Luca et al., 2021). The prevalence of FeMV is various among continents ranging between 5.4-39.4% in Asia, 0.83-22.8% in Europe, and around 3-23% in America. It is notified that FeMV-1 has higher prevalence compared to FeMV-2. The association of FeMV infection with the development of CKD in cats is still debatable, but among the type of sample the virus is presented, the most sample-type in which the virus mostly detected is kidney and urine (Woo et al., 2012; De Luca et al., 2021).

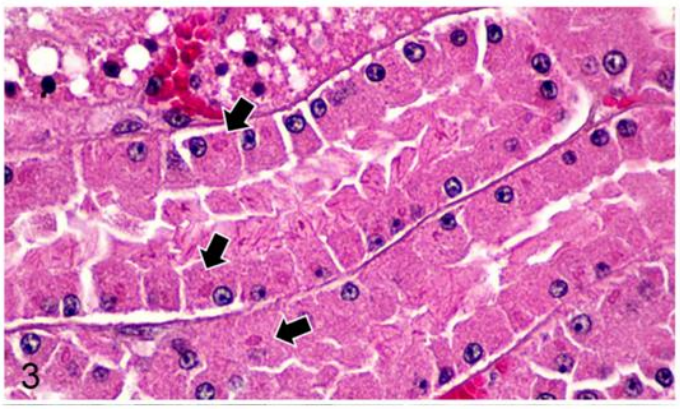

Figure 1 Formation of eosinophilic intracytoplasmic inclusion bodies (ICIB) (arrows) (Chaiyasak et al., 2022).

Despite the genomic material detection on kidney and urine of the cats, previous study revealed the presence of pathognomonic lesion associate with FeMV infection such as eosinophilic ICIB (Chaiyasak et al., 2022). Further, the previous study also reported that FeMV infection generates tubular vacuolation on infected kidney (Woo et al., 2012). However, it still little to know about pathological consequence as well as viral distribution in cat kidneys, given rise by infection of FeMV on cats.

Feline Paramyxovirus (FPaV)

Feline paramyxovirus (FPaV) belongs to family *Paramyxoviridae*. This virus is firstly reported from cats' urine with diagnosed CKD in Germany in 2015 (Sieg et al., 2015). FPaV had been investigated in several countries such as the United Kingdom and Japan using serological and metagenomic-analysis approaches respectively (McCallum et al., 2018; Sakaguchi et al., 2020). The prevalence of FPaV remains restricted. In Germany, out of 206 cat urines, three samples were positive for FPaV genomic material. In Japan, among 51 cat urines, one sample contained FPaV genomic material according to metagenomic analysis targeting FPaV L-gene. Furthermore, a seroprevalence study conducted in the United Kingdom found that out of 72 cat sera, three cats were positive of antibody against FPaV (Sieg et al., 2015; McCallum et al., 2018; Sakaguchi et al., 2020).

To date, the molecular characteristic of FPaV is largely unknown. According to phylogenetic analyses, FPaV, found in Germany, shares 72% homology score with bat paramyxoviruses, and 74% homology score with rodent paramyxoviruses (Sieg et al., 2015). Moreover, FPaV discovered in Japan has a close relationship to *Jeilongvirus* and shares a clade with Mount Mabu Lophuromys Virus 1 (MMLV-1). However, *Jeilongvirus* is a newly discovered member of Paramyxovirus that classified as rodent paramyxovirus. Despite the host origin which *Jeilongvirus* to be

found, *Jeilongvirus* is notified to possess tissue tropism on the rodent's kidney (Vanmechelen et al., 2018).

In addition, the virion organization of FPaV is comprised as nucleoprotein (N), phosphoprotein (P), matrix protein (M), fusion protein (F), TM protein, G protein, polymerase protein (L) (Sakaguchi et al., 2020). Even though FPaV was firstly found from cats suffered from episodic of feline lower urinary tract disease and nephropathy, antibody against FPaV is also discovered in non-azotemic cats as well azotemic cats (Sieg et al., 2015; McCallum et al., 2018). Regarding the host tropism, FPaV-related virus has been discovered in Guignas (*Leopardus guigna*) from Chile. The homology score of FPaV-related viruses were varied. They shared 82-83% similarity with previous FPaV discovered in Germany and Japan (Sakaguchi et al., 2020; Sieg et al., 2020).

Apoptotic activity associates with paramyxovirus infection

Apoptosis is known as type of cell death that physiologically occurs to maintain the cellular homeostasis in both human and animal. Apoptosis is programmed cell death (cellular suicide) aiming to remove aging, impaired and unwanted cells from the body. It is involved in several essential actions such as embryonal development and precaution of cellular metastasis that possibly threatens the body. It is irreversible process requiring energy-dependent reaction and activation of cysteine-aspartic proteases (caspase) (Elmore, 2007; Pfeffer and Singh, 2018; D'Arcy, 2019). In general, apoptosis engages to keep cellular homeostasis. However, it is also a defense mechanism to reveal intracellular antigen; thus, the antigen will be recognized by immune system (Neumann et al., 2015).

In general, apoptosis occurs in two courses that are extrinsic and intrinsic pathways which work independently. However, extrinsic pathway can induce the activation of intrinsic pathway as well (Roy and Nicholson, 2000; Galluzzi et al., 2018).

Extrinsic pathway of apoptosis

Extrinsic pathway of apoptosis (receptor-mediated cell death pathway) is initiated by binding of extracellular cell-death ligands to cell-surface membrane death-receptors (DRs) that belongs to tumor necrosis factor (TNF) receptor superfamily proteins. Cell-death ligands that involves in extrinsic pathway of apoptosis are comprised of TNF, Fas-ligand (FasL), TNF-related weak inducer of apoptosis (TWEAK), TNF-related apoptosis-inducing ligand (TRAIL), and TNF-associated death domain (TRADD). Moreover, the death receptors for the ligands are comprised of tumor necrosis factor receptor-1 (TNF-R1), Fas-transmembrane proteins, TNF-related apoptosis-inducing ligand-1 and -2 (TRAIL-1/-2), and death receptor-6 (DR-6) (Kumar et al., 2005; Elmore, 2007). Once the ligands bind the receptors, the death domain (DD) of the receptor is stimulated to consecutively activate death effector domain (DED). The activated DED will further begin the activation of procaspace-8 and formation of death-inducing signaling complex (DISC). The combination of DISC and activated caspase-8 will immediately promote the cleavage of caspase-3 as executor of apoptosis (Cavalcante et al., 2019).

Intrinsic pathway of apoptosis

Intrinsic pathway of apoptosis (mitochondrial-associated pathway) is triggered by the presence of intracellular-deprivation origin that is capable to lead to the formation of mitochondrial outer membrane permeabilization (MOMP). Although the formation of MOMP is the major subject in intrinsic pathway of apoptosis, endoplasmic reticulum (ER) mediated apoptosis, is possible to occur. The deprivation, that is called damage associated molecular patterns (DAMPS), is found in several forms such as withdrawal of growth factor, DNA damage, reactive oxygen species and the presence of specific viral virulence factors. Apoptosis intrinsic pathway is orchestrated by B cell lymphocyte -2 (BCL-2) superfamily proteins. BCL-2

protein is composed of two types of molecular composition which are BCL-2 homology (BH) domain, which comprised of BH1, BH2, BH3, and BH4, and transmembrane (TM) domain. According to its role in intrinsic pathway, BCL-2 proteins are classified into two families comprised of pro-survival (anti-apoptotic) and pro-apoptotic families. Later, pro-apoptotic family is divided into two sub-families regarding the diversity of the BCL-2 chemical compounds. Pro-survival proteins are consisted of proteins possesses all BH and TM domains, such as BCL-2, myeloid cell leukemia-1 (MCL-1), and BCL-X_L protein. First subfamily of pro-apoptotic proteins possesses three BH domains (BH1, BH2, and BH3) as well as TM domain. Proteins in this sub-family are consisted of BCL-2 associated X protein (BAX), BCL-2 antagonist killer (BAK), and BCL-2 related ovarium killer (BOK). In contrast, another pro-apoptotic sub-family protein possesses only BH3 domain, such as p53-upregulated modulator of apoptosis (PUMA), BH3 interacting domain death agonist (BID), NOXA, and BCL-2 associated agonist of cell death (BAD) (Elmore, 2007; Galluzzi et al., 2018; Cavalcante et al., 2019).

The presence of DAMPS and the intense of cell destroying signals, assign the cell to undergo self-suicide. This couple of initiators induces apoptosis by activating BH3-only protein through three kinds of mechanisms; transcriptional, post transcriptional, and post translational activations. Activated BH3-only proteins assist the apoptosis by hindering activity of BCL-2 pro-survival proteins and/or activate BCL-2 pro-apoptotic (BAX, BAK, BOK) proteins. Activated BAX and BAK begin the pore formation of outer-membrane of mitochondria (OMM) then form mitochondrial apoptosis-induced channel (MAC). Whereas activated BOK that colocalized on ER mediate apoptosis through ER. MAC formation is followed by the release of several apoptogenic factors that normally reside inside the mitochondria intermembrane space, such as cytochrome C, second mitochondrial activator of caspase (SMAC), and Omi/$HtrA_2$. The release of mentioned above apoptotic initiator factors (AIF) inhibit

pro-survival response emitted by the cell, hence apoptosis keeps going. Furthermore, AIF binds to apoptotic protease activating factor (APAF-1) as well as procaspase-9.The activation of caspase-9 leads to execution stage of apoptosis that involves cleaved caspase-3 (Cecconi and D'Amelio, 2010; Bose, 2015; Galluzzi et al., 2018; Cavalcante et al., 2019).

Paramyxoviruses regulating apoptosis

Among RNA virus, paramyxoviruses are notified to regulate apoptotic activity on infected cell. Some paramyxoviruses such as Measles virus (MeV), Feline morbillivirus (FeMV) and Sendai virus (SV) are suggested to induce apoptosis in the infected cell (Esolen et al., 1995; Bitzer et al., 1999; Sutummaporn et al., 2020). In contrast, Mumps virus is reported to inhibit apoptotic activity (Hariya et al., 2000). Among paramyxoviruses that suggested to be associated with kidney disease, only FeMV is reported to elevate apoptotic activity on renal tissue (Sutummaporn et al., 2020). However, the evidence of FeMV inducing caspase-dependent apoptotic activity is remained restricted.

Other viral infections associated to pathological alteration in feline kidneys

Cats are very vulnerable to be infected with infectious agents such as virus, parasite, and bacteria. There are several viruses infecting cat that associated with pathological condition in feline kidney such as feline leukemia virus (FeLV), feline immunodeficiency virus (FIV), feline coronavirus (FCoV), feline calicivirus (FCV), and feline panleukopenia virus (FPLV) (Hartmann et al., 2020; Piewbang et al., 2021a).

Feline leukemia virus (FeLV)

Feline leukemia virus (FeLV) is a virus belonged to family *Retroviridae*, genus *Gammaretrovirus*. The genome of FeLV is made up of two copies of positive

sense single stranded RNA and approximately 8,464 bp in length (Chin et al., 2020). The genome of FeLV is constituted of three genes which are *gag, pol,* and *env* restricted by long terminal repeat (LTR) region on its 3' and 5' prime respectively (Kawamura et al., 2015; Chin et al., 2020). FeLV has the capability to synthesis DNA from its RNA genome by working of reverse transcriptase (RT) enzyme. This potential ability, with contribution of integrase enzyme, facilitates FeLV to integrate its DNA-form genome within host genome, composing provirus (Polani et al., 2010; Hartmann and Hofmann-Lehmann, 2020) (Figure 2).

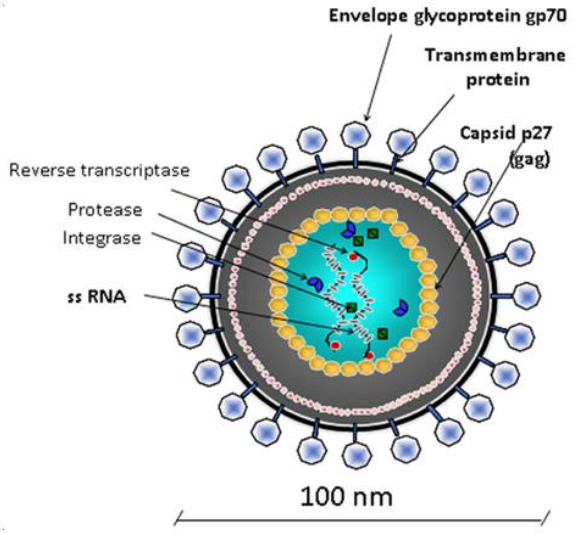

Figure 2 Virion organization of feline leukemia virus (FeLV). The genome of FeLV is comprised of two copies of positive single strand RNA enclosed inside the capsid (Hartmann and Hofmann-Lehmann, 2020).

The prevalence of FeLV infection is varies among countries (Capozza et al., 2021). In South East Asia, studies to investigate the presence of p27 protein by commercial ELISA test-kits reveal the prevalence of FeLV in Malaysia (12.0-12.2%) (Bande et al., 2012) and Thailand (24.5%) (Sukhumavasi et al., 2012). FeLV infection gives rise to several consequence diseases in cats that associates with renal disease such as renal lymphoma, renal neoplasia, and immune-complex glomerulonephritis

(ICGN). Those are the risk factor that leads to CKD (Brown et al., 2016; Rossi et al., 2019; Hartmann and Hofmann-Lehmann, 2020).

Feline immunodeficiency virus (FIV)

Feline immunodeficiency virus (FIV) belongs to family *Retroviridae*, genus *Lentivirus* (Maclachlan et al., 2017). It is firstly described in 1986 in California from cats exhibited immunodeficiency-like syndrome (Pedersen et al., 1987; Sykes, 2014). FIV and FeLV are comorbid pathogens that commonly infect cats (Dunham and Graham, 2008). The virus is transmitted by saliva, biting, and blood transfusion. Previous study in Malaysia reported the prevalence of FIV according to serological assay was around 31.3% (Bande et al., 2012). FIV targets on $CD4^+$ T-lymphocyte which generates continuous immunodeficiency disease. One of the nature of FIV infection is chronic asymptomatic infection, which give rise to chronic inflammatory response (Maclachlan et al., 2017). Previous study notified the higher percentage of proteinuric cats possessed FIV infection compared to uninfected one. Furthermore, several studies also mentioned that FIV infection is associated with ICGN (Baxter et al., 2012; Hartmann et al., 2020).

Feline coronavirus (FCoV)

Feline coronavirus (FCoV) is a virus belonging to genus *Alphacoronavirus* (Maclachlan et al., 2017). It was firstly reported in 1966 (Jaimes and Whittaker, 2018). According to amino acid sequence of spike (S) protein and antibody neutralization, FCoV is classified into two serotypes (type 1 and 2) in which type 1 is more widely distributed than type 2, but type 1 is poorly propagated in tissue culture environment compared to type 2. According to homology analysis on S gene, previous study strongly suggested that FCoV type 2 (FCoV-2) is yielded as the recombination between FCoV type 1 (FCoV-1) and Canine coronavirus (CCoV).

Furthermore, the pathogenicity (virulency) of FCoV can be presented in cats as two distinct pathotypes (biotypes) which antigenically and morphologically undistinguishable. The first pathotype is Feline enteric coronavirus (FECV) that cause mild persistent infection with enterocyte tissue tropism. Furthermore, FECV is transmitted through oral-fecal routes. In contrast, the second pathotype, known as Feline infectious peritonitis virus (FIPV), has more variation in tissue tropism and gives rise to fatal infection (Licitra et al., 2013; Jaimes and Whittaker, 2018).

The notifiable FIPV is brought up by FECV undergoes mutation inside the host, that increase the virulency of the virus and extend its tissue tropism. Moreover, the cats are possibly infected by FIPV from external transmission (Kipar et al., 2010). However, the prevalence of FIPV is lower than FECV. Regarding of the outcome of the infection, FIPV is classified into 2 clinical forms which are non-effusive (dry) and effusive (wet) forms. However, the histopathological findings from both forms are granulomatous inflammatory response, primarily in peritoneal cavity, that might affect kidneys (Drechsler et al., 2011) (Figure 3).

Figure 3 Gross lesion of kidney of cats infected with FIPV. The kidney exhibits severe granulomatous inflammation (courtesy by Department of Pathology, Faculty of Veterinary Science, Chulalongkorn University).

Feline Calicivirus (FCV)

Feline calicivirus (FCV) is a virus belonging to family *Caliciviridae*, genus *Vesivirus*. It is positive-strand non-enveloped RNA virus that is very contagious for *Felidae* family (Maclachlan et al., 2017). FCV is firstly isolated from gastrointestinal tract of cats in New Zealand. FCV infection exhibits two clinical manifestations either acute or chronic. The acute form brings up clinical signs according to the route of infection; aerosol infection generates clinical signs more severe than oral infection. Furthermore, the strain of infecting-FCV also associates with the severity of the clinical signs (Pedersen et al., 2000). While the chronic counterpart causes plasmacytic stomatitis or chronic ulceroproliferative stomatitis (Reubel et al., 1992). Recently, there is an emergence of virulent-systemic feline calicivirus (VS-FCV) in the USA and the UK which causes a high mortality rate and develops severe systemic disease. Meanwhile, non-virulent FCV is commonly contagious but low in mortality rate. To date, it is still unclear the etiology that given rise to VS-FCV, but it is suspected that VS-FCV risen up from particular genotype. Regarding the systemic infection of VS-FCV, the feline junctional adhesion molecule A (JAM-A) and alfa-2,6 sialic acid are suspected to be the receptor for FCV entry. Furthermore, VS-FCV is also detected in endothelial cells, in which systemic distribution in infected cats would occur through bloodstream (Sato et al., 2002; Pesavento et al., 2008). Therefore, the contributing role of VS-FCV in renal diseases should be monitored.

Feline panleukopenia virus (FPLV)

Feline panleukopenia virus (FPLV) is a virus belonging to family *Parvoviridae* that typically causes enteritis and panleukopenia. FPLV was firstly reported in 1928 in France (Sykes, 2014). As known that FPLV is also a member of Carnivore protoparvovirus-1 (CPPV-1), besides canine parvovirus (CPV); both viruses can cause panleukopenic condition in wild and domestic Felidae. FPLV causes feline

panleukopenia disease with the prevalence at 90-95% of cases (Barrs, 2019). FPLV is transmitted through oro-fecal route and indirect contact. The infected cats ingest the feeding or drink the water that contaminated with saliva, urine, feces, or vomitus of infected cats; and the indirect transmission also occurs through the fomites. The virion binds to Transferrin receptor (TfR) that existed on many tissues and undergoes the indirect fusion by endocytosis. The virion collocates in the endosomes to provide the opportunity for the virion to reach the access to nucleus of host cell and undergo genome replication, by hijacking the DNA polymerase of the host (Hueffer et al., 2004).

Regarding the tissue tropism of FPLV, it preferably replicates in active-dividing cell (S-phase of the cycle), such as lymphoid tissue, bone marrow, and cryptal intestinal epithelium (Maclachlan et al., 2017; Barrs, 2019). In addition, FPLV is transmitted from the queen to the fetus during gestation period generates abortion, mummification, stillborn kitten, and nervous system deficiency (Barrs, 2019). Notably, a recent study reported the localization of FPLV in kidney of wild fishing cat (*Prionailurus viverrinus*) with pathological alteration such as renal tubular vacuolation and interstitial hemorrhage (Piewbang et al., 2021a).

Diagnostic approaches of viral infection in the kidney

There are several approaches to detect the presence of virus in animals, such as virus isolation, observation using electron microscopy, serological detection and molecular detection (Maclachlan et al., 2017). Beforehand, viral detection is mostly carried out by virus isolation or serological detection. Although both methods are frequently used, they have some drawbacks such as time consuming and laboratorial-based practice, hence they are not suitable to be applied in veterinary primary care that needs immediate response. To overcome this burden, the application of Polymerase Chain Reaction (PCR) in viral detection is acceptable for diagnosis. PCR is an *in vitro* enzymatic reaction

to amplify specific region of whole genetic material, mimicking DNA replication in the cell. PCR is a specified method which aims to amplify DNA-based target pathogens such as viruses from family *Parvoviridae*. Moreover, Reverse-Transcription PCR (RT-PCR) is a method to amplify RNA-based target pathogens such as *Flaviridae*, *Bunyaviridae*, *Paramyxoviridae*, and *Coronaviridae* viruses (Belak, 2007; Hoelzer et al., 2008; Tekes et al., 2008; Tong et al., 2008; Artika et al., 2020). Further, the advancement of technologies leads the development of real quantification of amplification rate of PCR/RT-PCR that is called real-time PCR/real-time RT-PCR (Emery et al., 2004).

The application of both PCR and RT-PCR in clinical field bring up many benefits. Those methods are time saving and applicable to various spectrums of target pathogens. Thus, the decision of treatment can be administered to the patient as soon as the result comes out (Yang and Rothman, 2004). In human medicine, the application of PCR/RT-PCR in detection of viral disease are purposed to detect several virus infections such as Human Immunodeficiency Virus type 1 (HIV-1), Hepatitis B Virus, and Human Cytomegalovirus (Valones et al., 2009). In veterinary medicine, the applications of PCR/RT-PCR are commonly used to detect the presence of viral disease in livestock and small animal (Belak, 2007; Daniels, 2013). RT-PCR and PCR can be employed for various type of samples such as blood (Jeanes et al., 2022), urine (Woo et al., 2012), cerebrospinal fluid (Frisk et al., 1999) and homogenized tissue (Wardhani et al., 2021).

Regarding the pathologic kidney in cats, PCR are commonly to be used to detect the presence of dominant karyotype that give rise to Feline Polycystic Kidney Disease (FPKD) (Scalon et al., 2014). Moreover, in viral diagnostic method associated to pathological condition in kidney, RT-PCR and PCR are applied to confirm several viral diseases such as FeMV (Woo et al., 2012), FPaV (Sieg et al., 2015) and FPLV (Piewbang et al., 2021a). Despite molecular detection target on viral genomic material, other method such as Immunohistochemistry (IHC) and *in situ* hybridization (ISH) can be carried out to localize the presence of viral

protein and partial of genomic material of virus, respectively. IHC and ISH are both methods that mostly carried out to localize the tissue tropism of virus infection (Piewbang et al., 2020; Piewbang et al., 2021a).

CHAPTER 3

MATERIALS AND METHODS

Sample collection and clinical information

The sample in this study was collected from carcass submitted for routine necropsy in Department of Pathology, Faculty of Veterinary Science, Chulalongkorn University. The sample collection had been approved by Institutional Animal Care and Use Committee (IACUC) (Approval no. 2231023) and Institutional Biosafety Committee (IBC) (Approval No. 2231030). The inclusion criteria from the collected samples; the carcass was fresh to mild autolysis and included all ages, breeds and sex. The age of collected cats were classified according to the guidelines of American Animal Hospital Association (AAHA) and Association of Feline Practitioners (AAFP): kitten (<1 year old); young adult cat (1-6 years old); mature adult cat (7-10 years old); senior cat (>10 years old) (Quimby et al., 2021). The samples contained both left and right sides of the kidney.

The samples were collected for one year period (April 2021-April 2022). This study comprised of kidney-pairs from one-hundred and fifty (n=150) cat carcass. The collected samples were grouped according to histopathology examination. Normal kidney group were classified as kidney that histologically normal, whereas pathologic kidney group were classified as the kidney that exhibit any of microscopic lesions such as inflammatory cell infiltration or tubular degeneration. Macroscopic appearance of the collected kidney was vary, ranging from kidney with normal appearance, contracted or decreased in size, swollen, fibrosis, hemorrhage, infarction, difficulties to be decapsulated, mass, cyst, amyloidosis, granuloma, and congestion (Newman, 2012; Brown et al., 2016). The kidney samples were collected for molecular investigation and histopathological investigation. Before collecting the samples, both left and right kidneys were cut on midsagittal line. Each halves of right

and left kidneys were collected for further study. One-third of upper, middle, and lower parts of both kidneys were subjected for fresh tissue collection (Figure 4). Each part was chopped and mixed. The chopped-tissue was kept randomly in 1.5 ml centrifuge tube, then it was stored in -80°C for molecular investigation. The remaining of middle-part of the kidney (containing cortical, medullar, and pelvis areas) were preserved in 10% neutral buffer formalin for histopathological evaluation, special staining determination, as well as *in situ* hybridization (ISH), immunohistochemical (IHC) and apoptotic assays (Figure 4). Essential clinical information including Blood Urea Nitrogen (BUN), serum creatinine, serum Symmetric dimethylarginine (SDMA) (if available) and the latest medical record of each carcass were retrieved (at least one month prior the death) (Rossi et al., 2019).

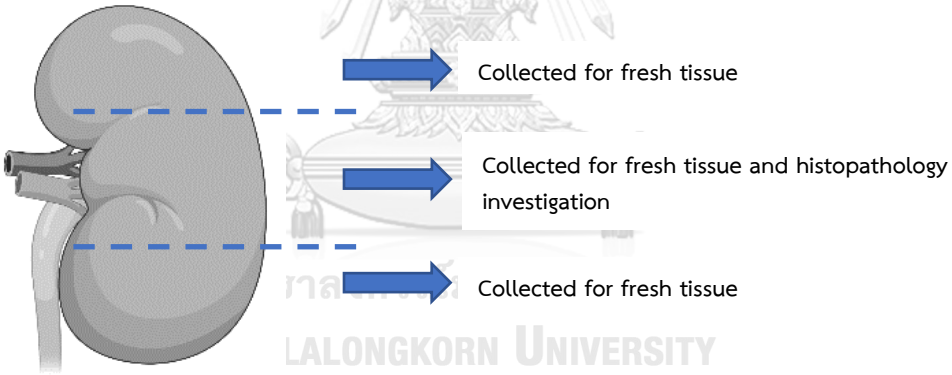

Figure 4 The scheme of sample collection of feline kidney for molecular and histopathological study (created in BioRender.com).

Molecular investigation of paramyxoviruses (FeMV-1, FeMV-2, FPaV)

Tissue homogenization

The collected samples were individually homogenized to make 10% suspended tissue solution. Approximately 5 g of the tissue were homogenized in 500 µl of 1x sterile phosphate buffer saline (PBS). The tissue was minced on petri dish

using surgical blade and needle. Then, it was transferred into a single-use plastic tube containing 500 µl of PBS. After that, the homogenization was performed using Tissue Rupture (Qiagen, Germany). The homogenized tissue solution was stored in -80°C freezer until genomic extraction.

Genomic material extraction

Genomic material extraction was performed using Viral Nucleic Acid Extraction Kit II (Geneaid, Taiwan). The homogenized tissue was thawed and then centrifuged prior the extraction to separate the supernatant from the pellet. Two hundred microliters of each sample were employed for the extraction. The genomic material extraction was done according to manufacturer protocol. The obtained nucleic acid was quantified and qualified using spectrophotometer analysis (NanoDrop, Thermo Scientific™, USA), then the concentration and purity of DNA/RNA was recorded. It was stored in -80°C prior to molecular screening.

Reverse transcription-polymerase chain reaction (RT-PCR) / PCR

The molecular investigation was performed to screen the paramyxoviruses which are feline morbillivirus genotype 1 (FeMV-1), feline morbillivirus genotype 2 (FeMV-2), and feline paramyxovirus (FPaV). Further, the positive cases from respective virus was employed for selective virus screening to rule out the virus that may associates with pathological condition in kidney including feline leukemia virus (FeLV), feline immunodeficiency virus (FIV), feline coronavirus (FCoV), feline calicivirus (FCV), and feline panleukopenia virus (FPLV) (Hartmann et al., 2020).

Either conventional one-step RT-PCR (cRT-PCR) or conventional PCR (cPCR) was employed using QIAGEN OneStep RT-PCR Kit (Qiagen, Germany) and GoTaq® Green Master Mix (Promega, USA), respectively. The sequence of forward and reverse primers, target gene, and product size (Table 1), as well as thermocycling arrangement (Table 2) were listed below.

In regard to ensure that the reaction is performed appropriately, the positive control of sequenced known template or vaccine of respective viruses was used. The non-

template control containing distillated water was used as negative control. The PCR products was analyzed using QIAxcel advance capillary electrophoresis machine or was visualized in 1.5-2% agarose gel electrophoresis containing 5% of ethidium bromide, then observed under UV light. Those samples showing the band was compared to respective positive controls. The sample representing the band on expected position was further purified using Macherey-Nagel™ NucleoSpin™ Gel and PCR Clean-up Kit (Macherey-Nagel, Germany) according to manufacturer protocol. The purified PCR product was sent for bi-directional sequencing. The sequencing result was analyzed and confirmed using BioEdit alignment editor and Basic Local Alignment Search Tool (BLAST) from National Center for Biotechnology Information (USA).

Table 1 List of primer sets for virus detection in this study.

Virus	Target gene[8]	Direction	Primer sequence 5'-3'	Product size (bp)
Feline leukemia virus[1]	LTR	Forward	AAACAGCAGAAGTTTCAAGGCCGCTACCAG	145
		Reverse	CTGATGGCTCGTTTTATAGCAGAAAGCGCGCG	
		Forward	AAATTTCAAGGCCGCTACCAGCAGTCTCCAGG	101
		Reverse	AGAAGCGAGAGGCGTGGGGATTGGTTAGTTAA	
Feline immunodeficiency virus[2]	gag	Forward	AGGGAGAAGTTTGGATTAGCA	391
		Reverse	TCCTTATCTGCTGCACAACCT	
		Forward	AGGTAGAGGAGCCTCCACAG	134
		Reverse	GTTGGACCTCCTCTCCTCCT	
Feline paramyxovirus[3]	L	Forward	GCCATATTTTGTGGAATAATHATHAAYGG	~500
		Reverse	CTCATTTTGTAIGTCATYTTNGCRAA	
Feline morbillivirus[4]	L	Forward	CAGAGACTTAATGAAATTTATGG	155
		Reverse	CCACCCATCGGGTACTT	
Feline coronavirus[5]	ORF1b	Forward	GGGTTGGGACTATCCTAAGTGTGA	405
		Reverse	TAACACACAACICCATCATCA	
Feline calicivirus[6]	ORF1	Forward	GAACTACCCGCCAATCA	120
		Reverse	AGCACRYCATATGCGGC	
Feline panleukopenia virus[7]	VP	Forward	ATGGCACCTCCGGCAAAGA	±2246
		Reverse	TTTCTAGGTGCTAGTTGAG	

[1](Lacharoje et al., 2021); [2](Techakriengkrai et al., 2018); [3](Tong et al., 2008); [4](Woo et al., 2012); [5](Ksiazek et al., 2003; Wardhani et al., 2021); [6](Piewbang et al., 2019; Wardhani et al., 2021); [7](Mochizuki et al., 1996; Wardhani et al., 2021).

[8]Abbreviation of target gene : LTR (long terminal repeat); gag (gag gene); L (polymerase gene); ORF (open reading frame); VP (Viral protein).

Table 2 Thermocycling arrangement of viral screening that used in this study.

Thermocycler arrangement	Virus								
	FeLV[1]		FIV[2]		FPaV[3]	FeMV[4]	FCoV[5]	FCV[6]	FPLV[7]
	1st round	2nd round	1st round	2nd round					
RNA denaturation					60˚C, 1 m				
Reverse Transcriptase					50˚C, 30 m	50˚C, 30 m	50˚C, 30 m	50˚C, 30 m	
Initial denaturation	94˚C, 5 m	94˚C, 5 m	94˚C, 3 m	94˚C, 3 m	94˚C, 15 m	94˚C, 15 m	95˚C, 15 m	95˚C, 15 m	95˚C, 5 m
Denaturation	94˚C, 45 s	94˚C, 30 s	94˚C, 30 s	94˚C, 30 s	94˚C, 30 s	94˚C, 30 s	94˚C, 1 m	95˚C, 30 s	94˚C, 30 s
Annealing	65˚C, 1 m	65˚C, 45 s	55˚C, 30 s	55˚C, 30 s	49.7˚C, 30 s	55˚C, 30 s	54˚C, 1 m	60˚C, 30 s	55˚C, 2 m
Extension	73˚C, 1 m	73˚C, 45 s	72˚C, 1 m	72˚C, 1 m	72˚C, 1 m	72˚C, 1 m	72˚C, 1 m	72˚C, 30 s	72˚C, 2 m
Final extension	73˚C, 5 m	73˚C, 5 m	72˚C, 10 m	72˚C, 10 m	72˚C, 10 m	72˚C, 10 m	72˚C, 10 m	72˚C, 10 m	72˚C, 10 m
Cycle	40x	45x	35x	35x	40x	40x	45x	40x	30x

[1](Lacharoje et al., 2021); [2](Techakriengkrai et al., 2018); [3](Tong et al., 2008); [4](Woo et al., 2012); [5](Ksiazek et al., 2003; Wardhani et al., 2021); [6](Piewbang et al., 2019; Wardhani et al., 2021); [7](Mochizuki et al., 1996; Wardhani et al., 2021).

Histopathology examination

Tissue processing on formalin-fixed paraffin embedded tissue (FFPE)

The formalin-fixed kidney tissues (containing cortical, medullar and pelvis areas) were incubated in 60°C for 48 hours before embedding it into Formalin-fixed paraffin embedded tissue (FFPE). After the incubation, the tissue was trimmed into 2 mm thickness then kept in tissue cassette. Then, it was employed to pre-embedding step consisted of dehydration and clearing steps. The tissue was dehydrated into graded series of ethanol to remove the water containment from the tissue completely. After dehydration step, the tissue was subjected into clearing step in series of xylene. After pre-embedding step, the tissue was embedded into paraffin wax (58-60°C) and transferred onto cold plate to make it harden. Embedded tissue was cut in 5-µm thickness using microtome, then the paraffin ribbon was placed on warm water bath followed by transferring the ribbon on a clean glass slide before further staining process.

Hematoxylin and eosin (H&E) staining

For staining process, the sections were employed for deparaffinization and rehydration steps, staining step, followed by dehydration, clearing steps, and mounting. For deparaffinization, sections were soaked into two xylene solutions for 10 minutes respectively, followed by rehydration step in graded series of ethanol for 5 minutes. Further, the slides were stained using Mayer hematoxylin and eosin Y solutions. Finally, the stained sections were dehydrated using graded series of ethanol followed by clearing steps using xylene, then mounting. Sections were examined under a light microscope.

Special staining determination

To further investigate the pathological alteration of renal tissue, special staining was performed on paramyxoviruses RT-PCR-positive cases by using Masson trichrome and Periodic acid-schiff's (PAS). Masson trichrome staining was used to evaluate the infiltration of fibrotic tissue on interstitial of associated renal tissue, whereas PAS staining was used to evaluate the condition of tubular basement membrane of respective tissue kidney.

Masson trichrome (MT) staining

The sections were incubated in 60°C incubator for 15 minutes followed by cooling down the sections in room temperature. Then, they were employed for deparaffinization in series of xylene followed by rehydration steps in series of alcohol. Following the steps, the sections were washed in the water flow and distillated water for 5 minutes respectively. After deparaffinization, rehydration and washing steps, the slides were fixed in Bouin's solution at room temperature overnight. Followed the incubation, the sections were washed in running water for 10 minutes. Firstly, the slides were stained using Weigert's iron Hematoxylin for 10 minutes to stain the nucleic acid. The iron containment in Weigert's iron Hematoxylin prevented the decolorization of the nucleic acid caused by acidic stains that used in further steps. Then the slides were washed in running water for 10 minutes. Secondly, the slides were stained in Biebrich scarlett-acid fuchsin solution for 1 hour to coloring both muscle and collagen material in respective tissue (because its molecule is small, hence it will bind to all components of tissue). Then, the slides were rinsed on distillated water (dip the section quickly). After that, the slides were soaked in Phosphomolybdic-Phosphotungstic acid for 15 minutes to discolor Biebrich scarlett-acid fuchsin from stained-collagen and leaved the muscle in red color. Moreover, Phosphomolybdic-Phosphotungstic acid was the mordant fixative agent for

Aniline Blue. Thirdly, the slides were stained using Aniline Blue, for 40 minutes in room temperature, to stain the collagen in blue color. This step was followed by rinsing the slides in distillated water, then soaking the slides in 1% Glacial Acetic Acid for 3 minutes to remove excessive stain of Aniline Blue. Finally, the slides were employed for dehydration in series alcohol, clearing in series of xylene and mounted. Masson trichrome staining was objected to evaluate the degree of fibrosis in tissue. Fibrosis is an event when the fibrous connective tissues such as collagen excessively accumulate on interstitial area of renal tissue and observed as blue color (Figure 5).

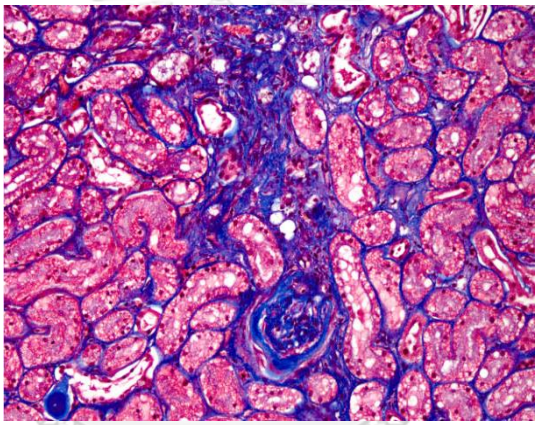

Figure 5 The infiltration of fibrous connective tissue in renal tissue is marked by blue color, located on interstitial of renal tissue (McLeland et al., 2015).

Periodic acid-schiff's (PAS) staining

The slides were incubated in 60°C incubator for 15 minutes followed by cooling down the sections in room temperature for 5 minutes. The sections were employed for deparaffinization in series of xylene followed by rehydration in series of alcohol and washing in running water as well as distillated water. After deparaffinization, the slides were subjected for oxidation in 0.5% Periodic acid for 5 minutes. Periodic acid reagent oxidized the carbon compound in the renal tissue. Following the oxidation, the sections were rinsed in running tap water for 5 minutes.

The oxidized-carbon compound in the tissue was further subjected for incubation in Schiff's reagent for 40 minutes. Then, the slides were soaked in 0.5% Sodium metabisulfite for 5 minutes. The slides were rinsed in running tap water for 5 minutes and distillated water for 15 seconds. After this step, the slides were counterstained using Mayer's Hematoxylin. This step was followed by dehydration step and mounting. PAS staining will stain the tissue containing polysaccharides. It is reported that tubular basement membrane of kidney is composed by glycoprotein. Hence, by performing PAS staining, we can evaluate the condition of the tubular basement membrane (Figure 6).

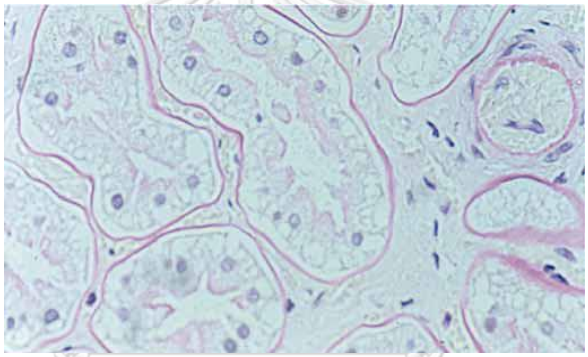

Figure 6 PAS staining on tubular basement membrane of renal tissue is marked by magenta color (arrows) (Thomsen et al., 2006).

Apoptotic activity assays

To date, it was remained unknown that paramyxovirus such as FeMV would increase caspase-dependent apoptotic activity on renal tissue. Thus, apoptotic activity assay was aimed to detect the activity of activated (cleaved) caspase-3 on nucleus of tubular epithelial cells. The immunohistochemistry was conducted according to manufacturer protocol of SignalStain® Proliferation/Apoptosis IHC Sampler Kit (Cell Signaling TECHNOLOGY, United States). To begin the procedure, the positive charged slides of each positive case were incubated in 60°C incubator for 45 minutes. Following the incubation, the slides were preceded for deparaffinization and rehydration. The antigen retrieval was performed by using citrate buffer pH 6.0 in

95°C water bath, for 20 minutes. After antigen retrieval, the endogenous peroxide digestion was performed in 0.3% hydrogen peroxide for 30 minutes. Further, non-specific binding was blocked using 2.5% bovine serum albumin (BSA) incubated in room temperature for 1.5 hours. The primary antibody was diluted using Antibody diluent (Cell Signaling TECHNOLOGY, United States) with concentration 1:400. Primary antibody was incubated in 4°C overnight. After triple wash using 1X PBS, the slides were incubated with secondary antibody (anti-rabbit Dako REAL Envision Detection System, Dako) in room temperature for 1 hour. The colour was developed using DAB (1:50) generated brown colour on nucleus tubular epithelial cells that undergone apoptotic activity. The slides were counterstained using haematoxylin. After dehydration, the slides were mounted.

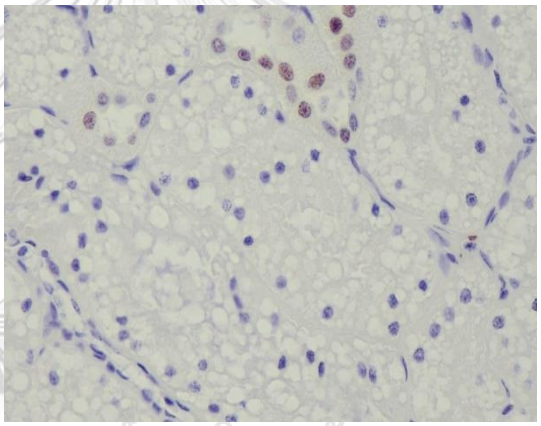

Figure 7 Apoptotic activity was marked by brown colour exhibited by nucleus of tubular epithelial cells.

Histopathological evaluation

The histopathology evaluation was blindly performed by three investigators (AZ, CP, ST). The result of H&E staining, special staining, and apoptotic assay were analyzed by using semi-quantitative histopathology scoring. The renal tissues of positive paramyxovirus cases were evaluated against normal histologic renal tissue using low-power magnification (40x) on 5 fields area, as well as higher power magnification (100X and 400X). The semi-quantitative histopathological scoring was performed according to previous study with necessary modification (McLeland et

al., 2015). The histopathologic variables and the score are mentioned below (Table 3).

Table 3 Guidance of semiquantitative scoring for histopathology evaluation.

Histopathologic variables	Score	Further description
Percentage of interstitial inflammation[1]		
- No inflammation	0	- Pattern of inflammation: focal, multifocal, extensive, diffuse - Type of inflammatory cell infiltrate - The most affected area: cortical area, medullar area, and pelvis area
- <25% inflammatory cell infiltrate the renal interstitial area	1	
- 25-50%	2	
- 51-75%	3	
- >75%	4	
Percentage of intact tubular basement membrane		
- <25% tubular basement membrane of renal tissue intact	1	The most affected area: cortical area, medullar area, and pelvis area
- 25-50%	2	
- 51-75%	3	
- >75%	4	
Degree of fibrosis[1]		
- No fibrosis	0	
- <25% renal tissue is affected with fibrosis	1	The most affected area: cortical area, medullar area, and pelvis area
- 25-50%	2	
- 51-75%	3	
- >75%	4	
Apoptotic activity		
- No apoptotic activity	0	
- <25% apoptotic activity occurs in renal tissue	1	The most affected area: cortical area, medullar area, and pelvis area
- 25-50%	2	
- 51-75%	3	
- >75%	4	

[1](McLeland et al., 2015)

The score of each examiner were summarized then the mean was retrieved. Further, it was analyzed using non-parametric statistical analysis two-tailed Spearman coefficient correlation (Landmann et al., 2021).

Viral localization and distribution

The study of viral localization and cellular tropism was carried out by performing Immunohistochemistry (IHC) and *In situ* hybridization (ISH). IHC and ISH were performed on positive cRT-PCR samples. Moreover, IHC and ISH were employed for semiquantitative scoring according to intensity of signal that exhibited by cytoplasm of renal tubules and ICIB. The scoring was blindly conducted by three examiners as mentioned above. The score of each examiner was summarized, the mean value was retrieved, then it used for statistical analysis. The obtained score value was used as variable to determine the association between paramyxovirus infection and severity of histopathologic variables.

Immunohistochemistry (IHC)

The IHC was performed according to previous study (Piewbang et al., 2020). The FFPE kidney tissue was cut at 4 µm thick, then placed in positive-charged slide. The slides were incubated in 60°C then employed for deparaffinization and hydration, followed by antigen retrieval step in citrate buffer pH 6.0 by autoclaving at 121°C for 5 minutes. The endogenous peroxide digestion was carried out by incubating the slides in 3% hydrogen peroxide in room temperature for 15 minutes. Later, they were subjected to block non-specific reaction using 5% skimmed milk solution at 37°C for 30 minutes. Then, the slides were incubated with primary antibody at 37°C for one hour (rabbit polyclonal antibody against His-rFeMV-M), using dilution 1:250. After the primary antibody incubation, the slides were employed for series of rinsing, following by incubation in secondary antibody (Horseradish peroxidase conjugated secondary antibody) in room temperature for 1 hour (anti-rabbit Dako REAL Envision Detection System, Dako). The staining signal was visualized

by adding 3,3'-diaminobenzidine (DAB) (1:100) to allow the expression of antibody-antigen reaction. Finally, the slides were counterstained using Mayer's Haematoxylin. The positive signal was observed as brown colour (Figure 7).

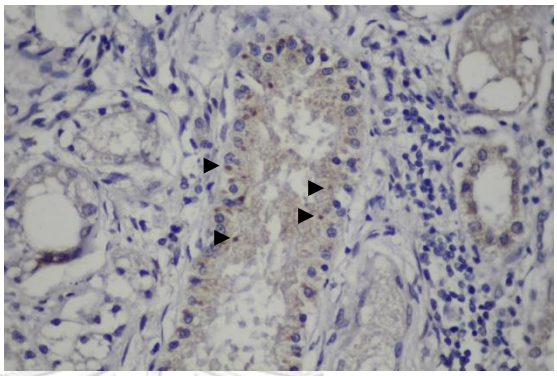

Figure 8 Positive immunostaining signal of IHC against Feline morbillivirus M gene (arrows).

***In situ* hybridization (ISH)**

ISH was performed to detect the presence of specific genetic material of paramyxovirus on feline renal tissue. Non-radioactive digoxigenin (DIG) labelled nucleotides was used in this study and was employed based on the specific gene target of each paramyxovirus (partial of L-gene). The assay was comprised of two steps which were probe construction and hybridization step.

Probe construction

Probe for ISH was constructed from gel purified RT-PCR product of positive paramyxoviruses cases. DIG-labelling was carried out according to manufacturer protocol of PCR DIG Probe Synthesis Kit (Roche, Germany). The labelled-probe was visualized on 1% of agarose gel to assure that the probe had been successfully constructed (Appendix; Supplementary Figure 1).

Hybridization step

Briefly the slides were subjected to deparaffinize, rehydrate, and rinse in PBS. Prior to hybridization step, the slides were employed for antigen unmasking step. The slides were incubated in citrate buffer pH 6.0, autoclaved at 121℃ for 5 minutes following the antigen unmasking step, the slides were then washed in 1X Tris-NaCl-EDTA (TNE) buffer for 5 minutes. Then, the slides was employed for endogenous peroxidase digestion in 3% hydrogen peroxidase for 15 minutes and non-specific reaction blocking in 0.5% bovine serum albumin in 37℃ for 1 hour. Hereinafter, the hybridization buffer was applied on the slides followed by incubation in light-protected-humidified-chamber containing deionized-formamide at 37℃ for 1 hour. After the hybridization step, the slides were employed for washing in series of saline sodium citrate (SSC) buffer for 5 minutes respectively following the steps, HRP-labelled anti-DIG (1:200) was applied to each respective slide. The probe binding was visualized using ImmPACT®VIP Substrate Kit, Peroxidase (Vector Laboratories, USA) according to manufacturer protocol. Finally, the slides were counterstained with methyl green then mounting. Evaluation of detected signal was observed under light microscope by presenting purple color at particular infected cell. The distribution of positive hybridized signal expressed on the tissue was counted on 3 areas of kidney; cortical area, medullar area, and pelvis area.

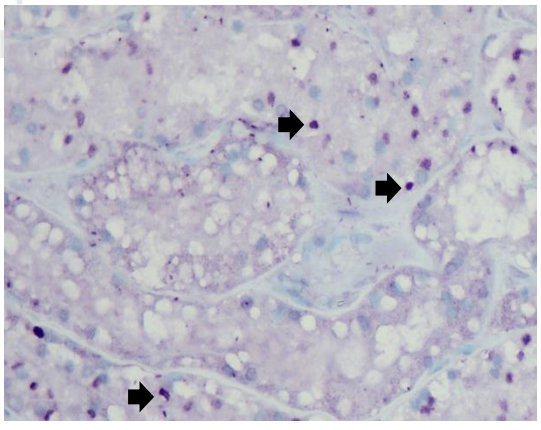

Figure 9 Positive ISH signals were exhibited by ICIB that marked with purple colour (Arrows).

Data analysis

The result of molecular screening was elucidated accordingly. The obtained data of semi-quantitative scoring were employed for quantile-quantile (Q-Q) plot using Microsoft Excel to confirm the normality of the distribution. The correlation of paramyxovirus infection (that examined by IHC and ISH) with histopathological variables was examined using two-tailed Spearman correlation method with confidence interval 95% and *p-value <0.05* to find the association of the paramyxovirus infection and the pathological alteration in the kidney (Landmann et al., 2021). The statistical correlation was employed using GraphPad Prism version 9.0. The obtained Spearman correlation coefficient (r) was interpreted according to guidance in Correlation coefficients : Appropriate use and interpretation (Schober et al., 2018).

CHAPTER 4
RESULTS

Clinical background of collected samples

One-hundred fifty kidney samples were collected during April 2021-April 2022. The collected samples were comprised of various cat breeds such as Domestic short hair (DSH) (n=92), Persian cat (n=16), Scottish fold (n=14), American shorthair (n=4), Serval cat (n=3), British shorthair (n=3), Exotic shorthair (n=2), Maine coon (n=2), Siamese cat (n=2), Tonkinese (n=1), Caracal cat (n=1), British longhair (n=1), Sphynx (n=1), Devon Rex (n=1), Burmese cat (n=1), Ragdoll (n=1) and unknown (n=5) (Figure 10).

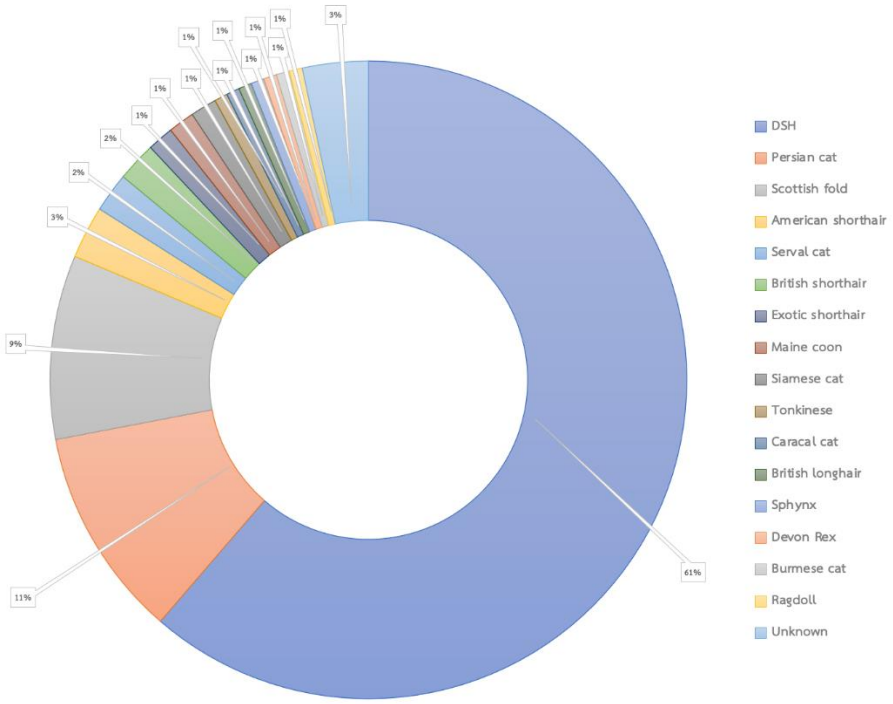

Figure 10 Pie chart of breed diversity of collected samples.

The samples were collected from various age of cats; kitten (21.33%; n=32), young adult (53.33%; n=80), mature adults (10%; n=15), and senior cats (9.33%; n=14) and unknown (6%; n=9). The background of lifestyle of each sample was

various; ninety-seven (64.67%) of the samples were recorded as household cats (raised indoor, outdoor, or both), eleven (7.33%) cats were stray cats, two cats (1.33%) were raised in breeding farm, one cat (0.67%) was raised in shelter, and thirty-nine cats (26%) were unknown. Further, collected samples were histopathologically classified into histopathologic kidney group and normal kidney group.

Among 150 kidneys, 115 kidneys (76.67%) were assigned as histopathologic kidney (pathologic group), which comprised of normal appearance to various gross lesion such as irregular surface, mild to moderate contracted kidney, patchy hemorrhage, renal infarction, and formation of multifocal cyst (polycystic kidney disease (PKD) (Figure 11). Moreover, 35 kidneys (23.33%) were assigned as normal kidneys (normal group).

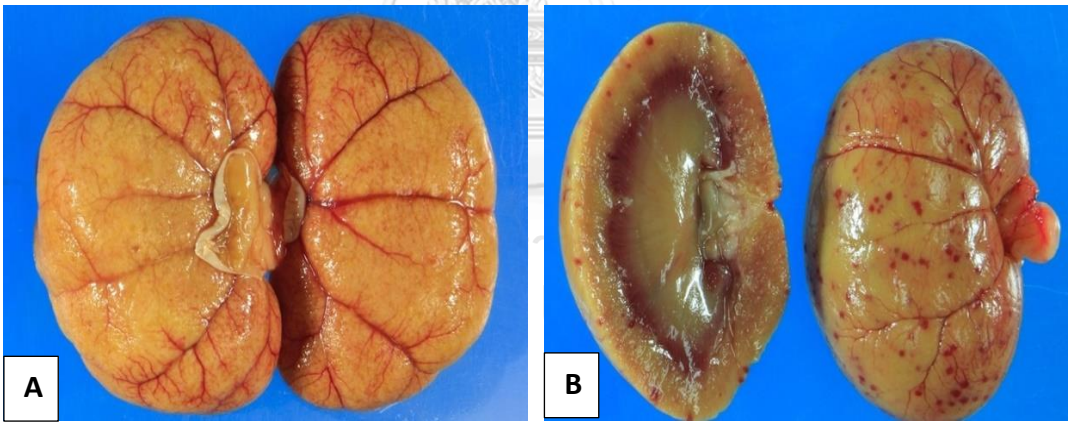

Figure 11 Kidney, cat. Gross lesions of histopathologic kidney group; (A) contracted kidney. (B) patchy hemorrhage.

Molecular screening of paramyxoviruses in feline kidneys

Molecular screening of paramyxoviruses were initially carried out using degenerated pan-primer-pairs that amplify specific region of polymerase protein gene (L-gene) of Respirovirus-Morbillivirus-Henipavirus (Res-Mor-Hen) from previous study

(Tong et al., 2008). The positive control that used was sequence-known template of FeMV genotype 1 (FeMV-1) strain Lapön from Germany (courtesy by Dr. Michael Sieg). However, the result of the screening was not capable to detect any genomic material of FeMV-1, FeMV-2, and FPaV from collected samples. Concerning the lack of fulfillment in detecting the genomic material of the respective viruses from the samples, a minor investigation was carried out to confirm the sensitivity of Res-Mor-Hen primer pairs with FeMV-1 strain Thailand from previous study (Chaiyasak et al., 2020b).

Herein after, second attempt to detect the presence of paramyxoviruses in feline kidney was carried out using specific primer to detect partial of L-gene of FeMV-1 from previous study (Woo et al., 2012). The result of the screening revealed that nine (6%) out of 150 samples were exhibited bands accordance to positive control (Figure 12). Bi-directional sequencing of the samples confirmed that the respective samples were FeMV-1 (Table 3). Moreover, all positive cases were considered as DSH breed cat (Table 3) and included in pathologic kidney group.

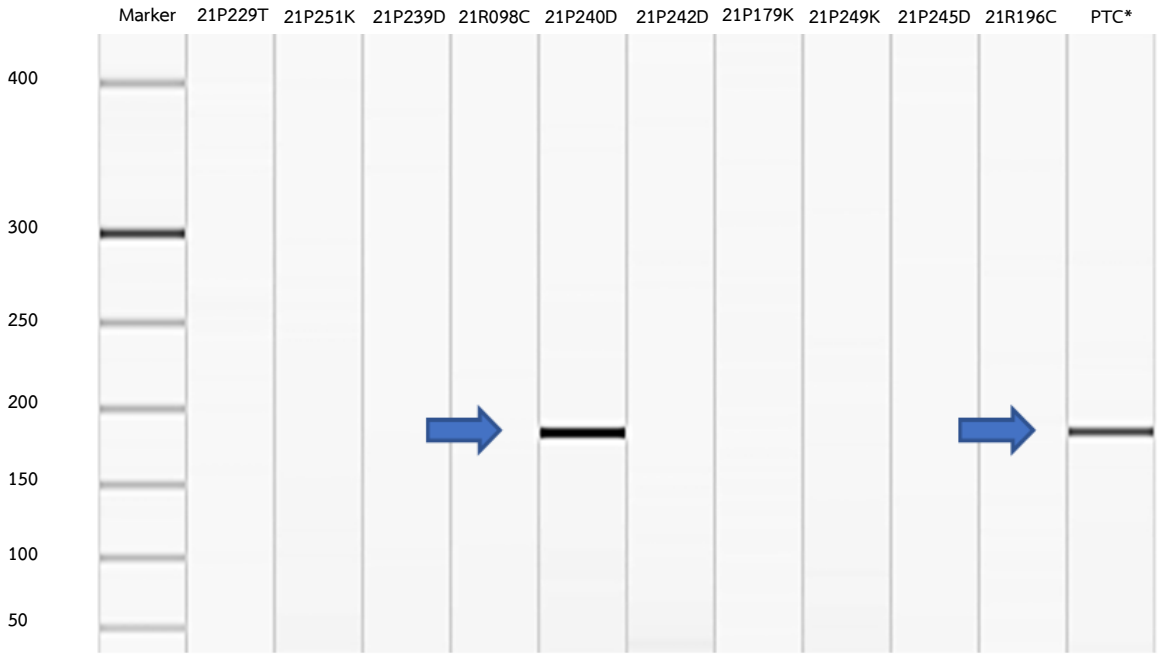

Figure 12 QIAxcel advance capillary electrophoresis of positive cases of FeMV-1 (arrows). The expected product size according to the primer is ~155 bp.

*PTC= Positive template control

Furthermore, selective viral screening to detect viruses associated with kidney disease such as FeLV, FIV, FPV, FCoV and FCV were carried out. Among those selected viruses, FeLV pro-viral was detected on four FeMV-1-positive cases (Table 4).

Table 4 List of FeMV-1 positive cases confirmed by bi-directional sequencing and selective screening of other feline viruses

Case	Age (years)	Breed	FeLV	FIV	FPV	FCoV	FCV
21P240D	3	DSH	-	-	-	-	-
21P276C	1	DSH	+	-	-	-	-
21P346Y	10	DSH	-	-	-	-	-
21P413W	16	DSH	-	-	-	-	-
21P603Y	1	DSH	-	-	-	-	-
22P060Y	3	DSH	+	-	-	-	-
22P118R	2	DSH	+	-	-	-	-
22P119R	3	DSH	+	-	-	-	-
22P126C	1	DSH	-	-	-	-	-

Histopathological finding and viral localization of FeMV-1 positive cases

21P240D/Domestic shorthair/3 years old

In gross lesion, there was no remarkable lesion to be observed from the kidney (Figure 13). In H.E staining, the interstitial area of renal tissue was infiltrated with lymphoplasmacytic inflammatory cells mainly in cortical area. The tubular epithelial cells possessed the formation of eosinophilic ICIB (Figure 14).

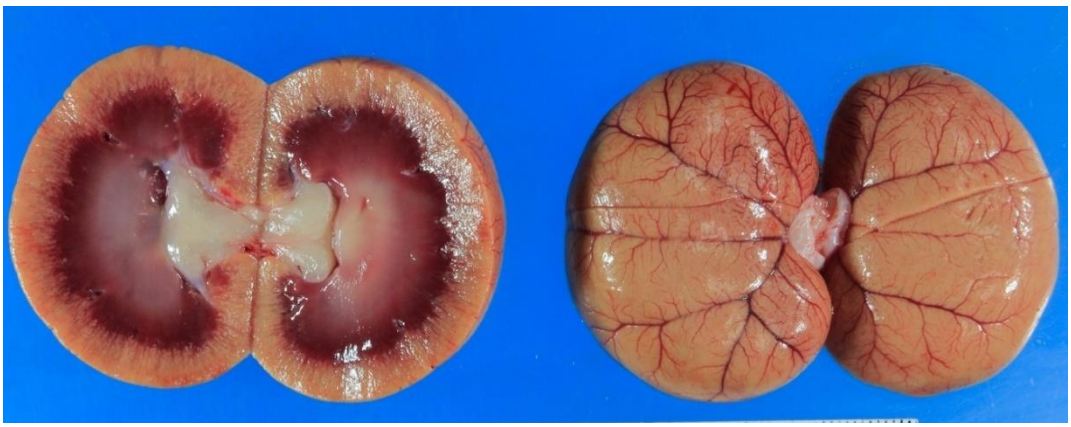

Figure 13 Kidney, cat, 21P240D. No remarkable lesion was observed on the kidney.

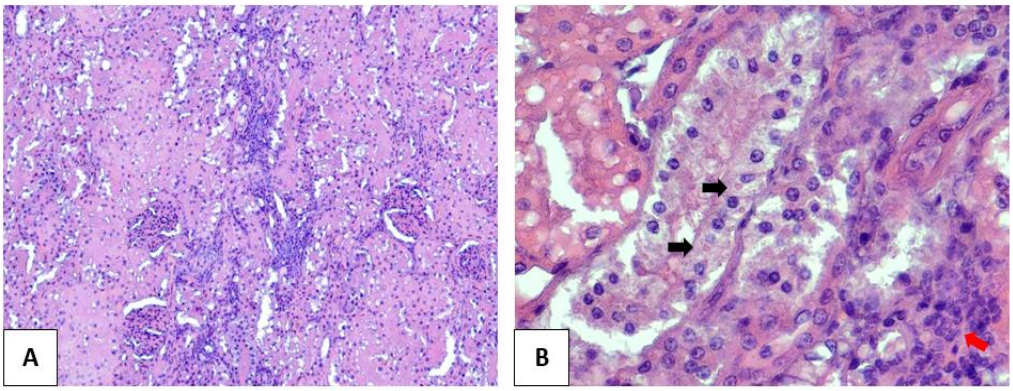

Figure 14 Kidney, cat, 21P240D. (A) Renal interstitial was infiltrated with inflammatory cell (HE, 100x). (B) Lymphoplasmacytic inflammatory cells (red arrow) and eosinophilic ICIB in the tubular epithelial cells were presented (black arrow) (HE, 400x).

PAS staining revealed that the tubular basement membrane was ruptured. In consequence, it was difficult to distinguish the basement membrane of one tubule to another. Hereinafter, the detachment of tubular epithelial cells to the lumen (sloughing) was observed. Moreover, mild membranoproliferative glomerulonephritis (MPGN) that marked by thickening of bowman capsule and glomerular basement membrane (GBM) was observed as well (Figure 15). MT staining showing that interstitial scaring (fibrosis) was not able to be observed (Figure 15). In this case, apoptotic activity was not able to be observed.

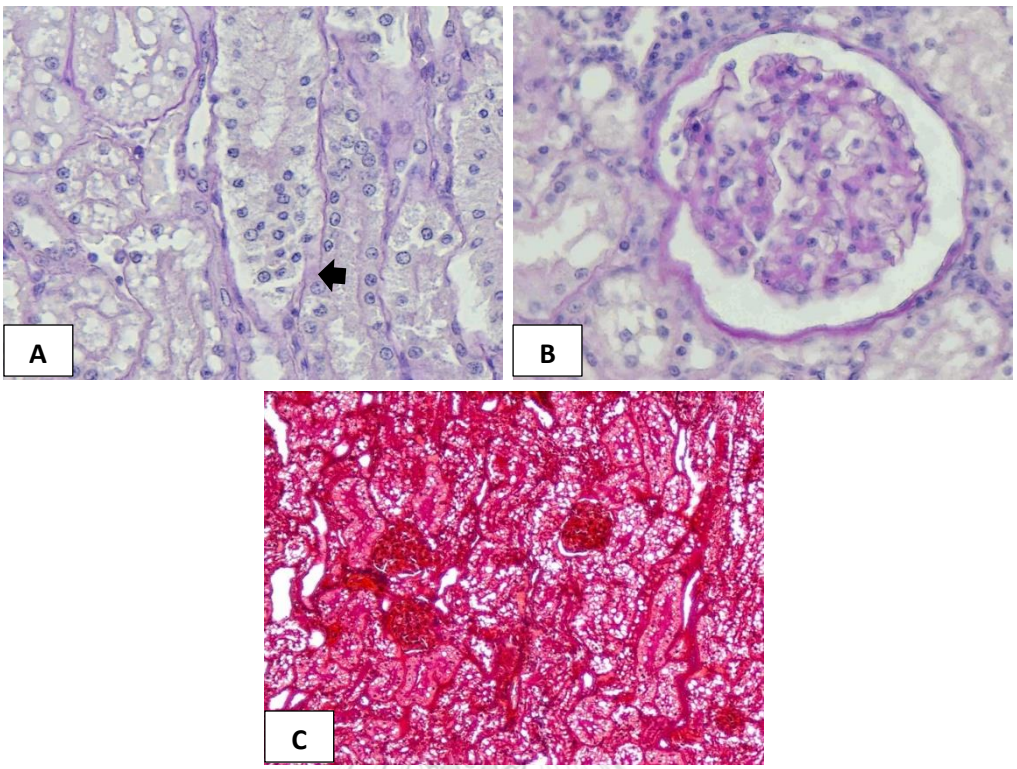

Figure 15 Kidney, cat, 21P240D. (A) Tubular basement membrane of the renal tissue was ruptured, and tubular epithelial cells sloughed into tubular lumen (black arrow) (PAS, 400x). (B) Mild membranoproliferative glomerulonephritis (MPGN) was observed (PAS, 400x). (C) Fibrosis was not observed to infiltrate interstitial renal tissue (no blue color) (MT, 100x).

According to IHC assay against matrix protein of FeMV, the tissue did not exhibit the immunostaining signals. However, ISH assay revealed that *in-situ* signals was only exhibited on cortical area of renal tissue. *In-situ* signal was expressed by cytoplasm of tubular epithelial cells. Interestingly, *in-situ* signal was also expressed by the nucleus of tubular epithelial cells in which the cytoplasm did not exhibit *in-situ* signal (Figure 16).

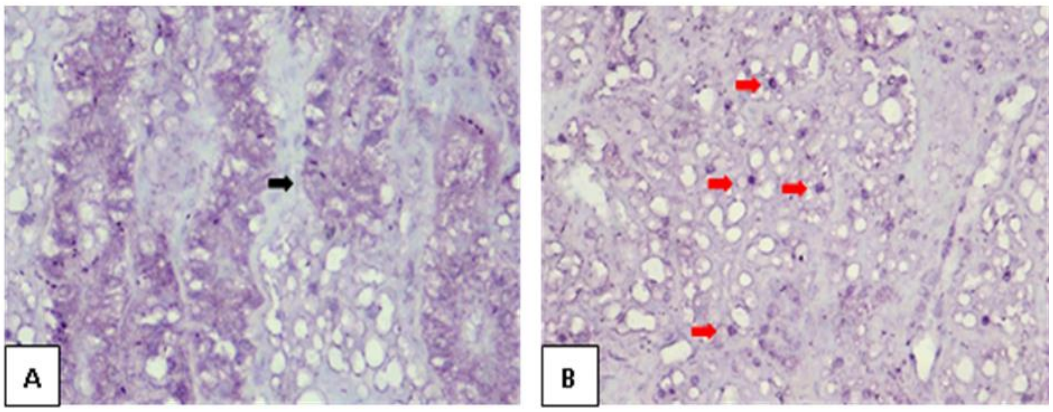

Figure 16 Kidney, cat, 21P240D. (A) The renal tubular epithelial cells exhibited positive ISH signal (black arrow) (ISH, 400x). (B) Nucleus of tubular epithelial cells expressed ISH signal, hallmark the presence of genomic material of FeMV-1 occupied the nucleus (red arrow) (ISH, 400x).

21P276C/Domestic shorthair/1 year old

In gross examination, there was no remarkable lesion was observed. In H.E staining, renal tissue exhibited infiltration of lymphoplasmacytic inflammatory cell mainly in cortical area (Figure 17). The tubular epithelial cells exhibited the formation of pale eosinophilic ICIB particularly in proximal tubules (Figure 17). PAS staining showing that tubular basement membrane was intact with slightly tubular epithelial cells detachment (Figure 18A). Furthermore, MT staining showed mild infiltration of fibrous tissue on cortical area of renal tissue (Figure 18B). Apoptotic activity was expressed by nucleus of tubular epithelial cells (Figure 19).

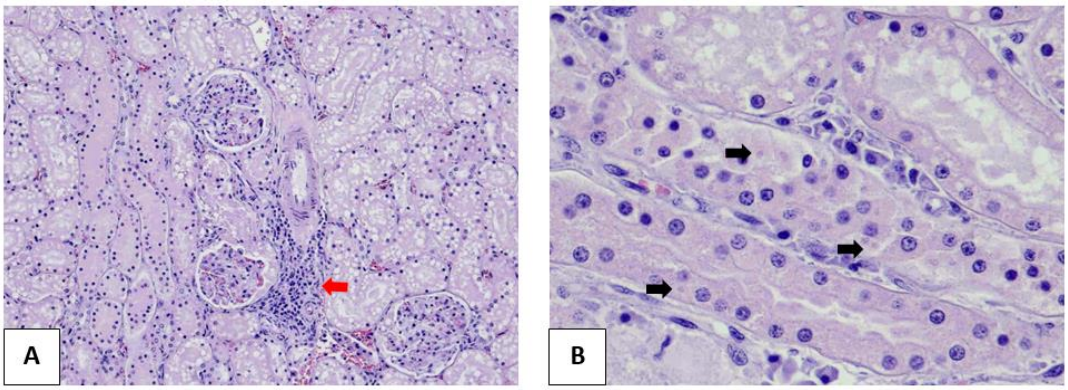

Figure 17 Kidney, cat, 21P276C. (A) Lymphoplasmacytic inflammatory cells infiltrate renal interstitial tissue (red arrow) (HE, 100x). (B) The tubular epithelial cells exhibited formation of eosinophilic ICIB (black arrow) (HE, 400x).

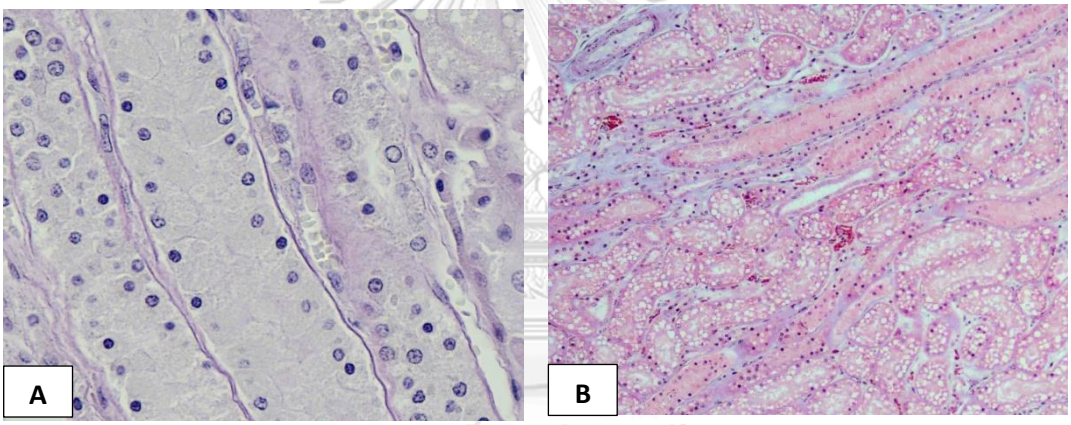

Figure 18 Kidney, cat, 21P276C. (A) The tubular basement membrane was intact with detachment of tubular epithelial to lumen of the tubules (PAS, 400x). (B) The interstitial of renal tissue was infiltrated with fibrous tissue marked by the accumulation of collagenous matter-stained blue (MT, 100x).

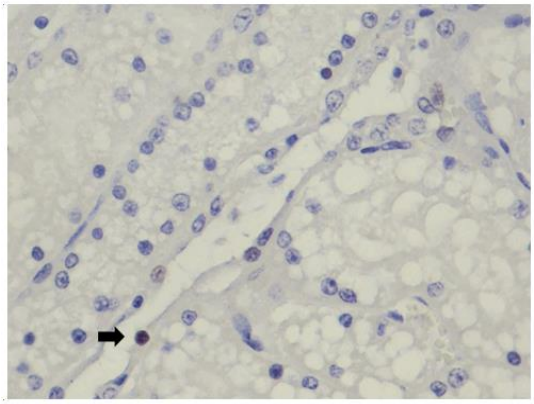

Figure 19 Kidney, cat, 21P276C. Immunosignal of cleaved caspase-3 was exhibited by nucleus of the tubules that marked by brown color (black arrow) (Apoptotic activity, 400x).

IHC assay against M-protein indicated that positive immunostaining signal was exhibited on cortical, medullar, and pelvis areas. The formation of eosinophilic ICIB exhibited positive immunostaining signal as well (Figure 20). Furthermore, the immunostaining signal was exhibited by the cytoplasm of tubular epithelial cells (Figure 20). It was also observed that immunostaining signal was exhibited by nucleus of epithelial cells on proximal tubule in which the formation of eosinophilic ICIB was absence (Figure 20). In accordance with the findings in IHC assay, ISH assay revealed that *in-situ* positive-signal was exhibited on cortical, medullar, and pelvis area of renal tissue. Moreover, the formation of eosinophilic ICIB expressed *in-situ* signal. *In-situ* signal was expressed by cytoplasm of epithelia of distal tubule, collecting tubule, and proximal tubule (absence of formation of eosinophilic ICIB). Interestingly, nucleus of proximal tubule, in which the formation of ICIB was absence, expressed *in-situ* signal as well (Figure 21).

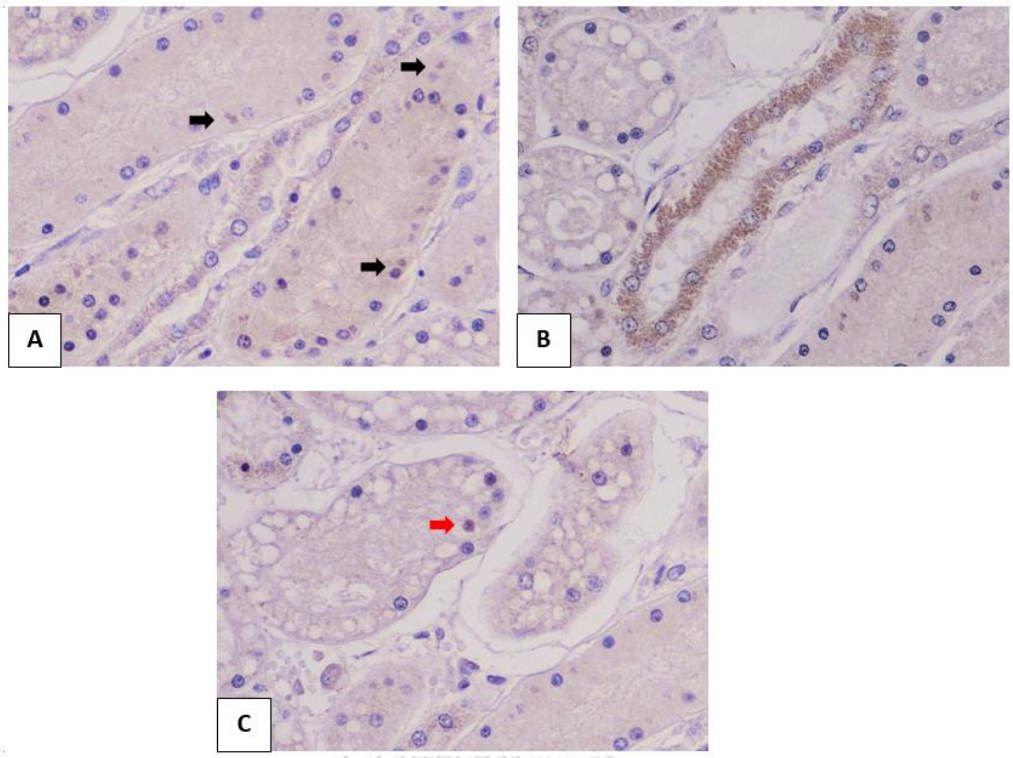

Figure 20 Kidney, cat, 21P276C. (A) Formation of eosinophilic ICIB expressed immunostaining signal marked by brown color (black arrow) (IHC, 400x). (B) Strong immunosignal was emitted by cytoplasm of tubular epithelial cells (IHC, 400x). (C) The immunostaining signal was expressed by nucleus of proximal tubule (red arrow) (IHC ,400x).

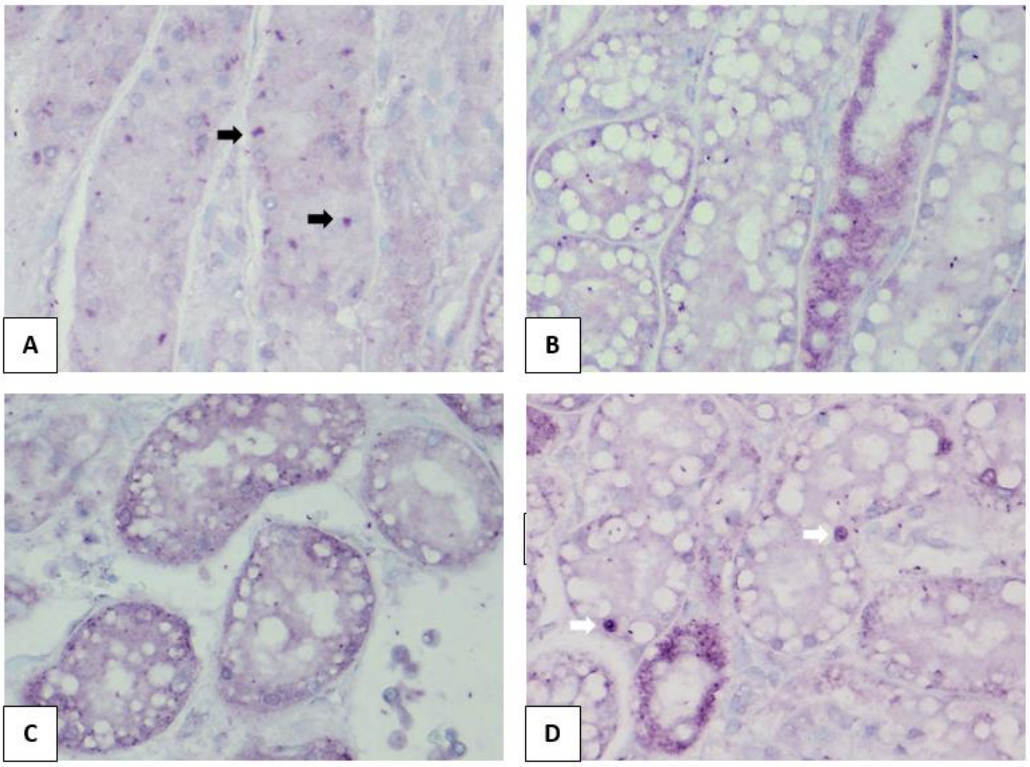

Figure 21 Kidney, cat, 21P276C. (A) ICIB formation of the tubules exhibited ISH signal (black arrow) (ISH, 400x). (B) Cytoplasm of tubular epithelial cells of collecting tubule expressed *in-situ* signal (ISH, 400x). (C) In-situ signal was exhibited by cytoplasm of epithelia of proximal tubules (ISH, 400x) and (D) nucleus of proximal tubule (white arrow) (ISH, 400x).

21P346Y/Domestic shorthair/10 years old

Gross lesion of the kidney showed pale-mild contracted kidney with dilatation of renal pelvis area and presence of renal calculi (Figure 22). According to H.E slide examination, the tissue exhibited infiltration of lymphoplasmacytic inflammatory cell mainly on cortical area. The inflammatory cell scattered to medullar area as well. The tubular epithelial of proximal tubules presented the formation of pale eosinophilic ICIB (Figure 23).

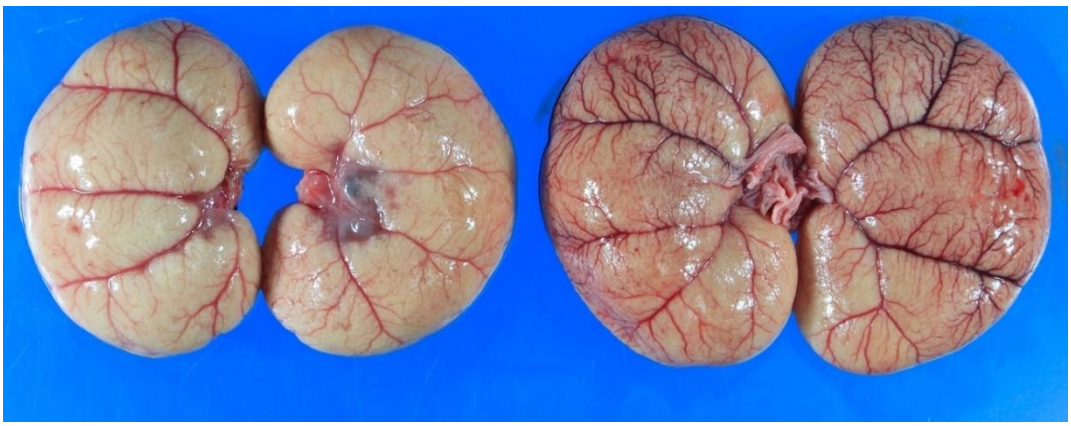

Figure 22 Kidney, cat, 21P346Y. The kidney was mild contracted with pale appearance.

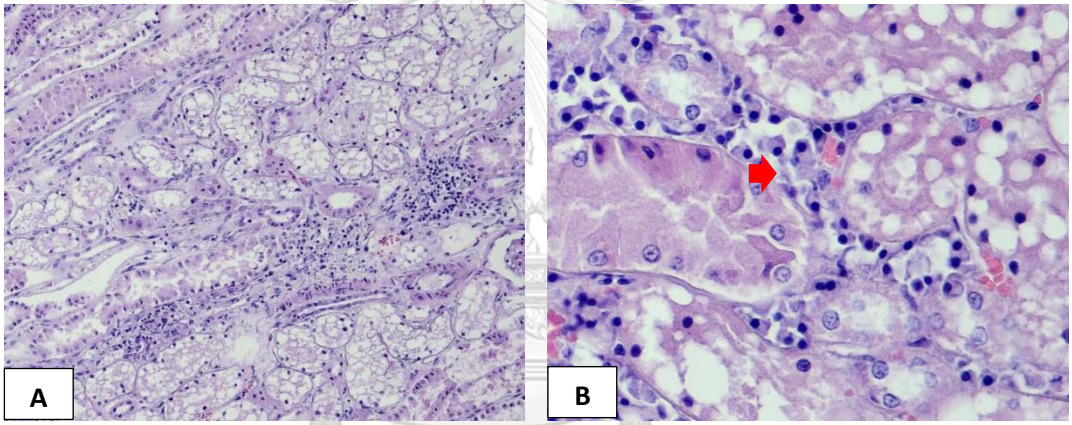

Figure 23 Kidney, cat, 21P346Y. (A) The inflammatory cell infiltrates the interstitial area of the renal tissue (HE, 100x). (B) Type of inflammatory cell infiltrated the interstitial area is lymphoplasmacytic inflammatory cell (red arrow). The tubular epithelial cell exhibited pale eosinophilic ICIB (HE, 400x).

PAS staining revealed that tubular basement membrane was ruptured followed by the detachment of tubular epithelial into lumen (Figure 24). MT staining indicated that fibrous tissue was observed to infiltrate renal interstitial, particularly cortical and medullar area (Figure 24). The apoptotic activity that marked by the presence of cleaved caspase 3 immunostaining signal was unable to be observed in this case.

Immunostaining signal against M-protein was observed on cortical, medullar and pelvis areas of renal tissue. ICIB of proximal tubule expressed pale immunostaining signal. However, cytoplasm of collecting tubules expressed strong immunostaining signal (Figure 25). Accordance with the expression of immunostaining signal through all areas of renal tissue, ISH signal was observed on cortical, medullar and pelvis area of renal tissue. In contrast with the intensity of immunostaining signal, ISH signal was observed to be stronger. The in-situ signal was exhibited on ICIB, cytoplasm of distal tubule and collecting duct (Figure 26).

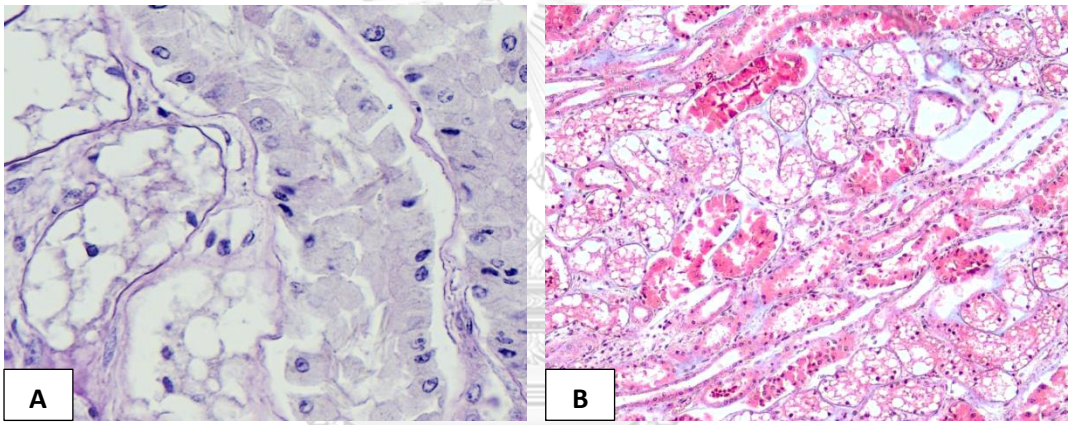

Figure 24 Kidney, cat, 21P346Y. (A) The tubular basement membrane was ruptured followed with sloughing of tubular epithelial cells into lumen (PAS, 400x). (B) Interstitial of renal tissue was exhibited infiltration of fibrous tissue (MT, 100x).

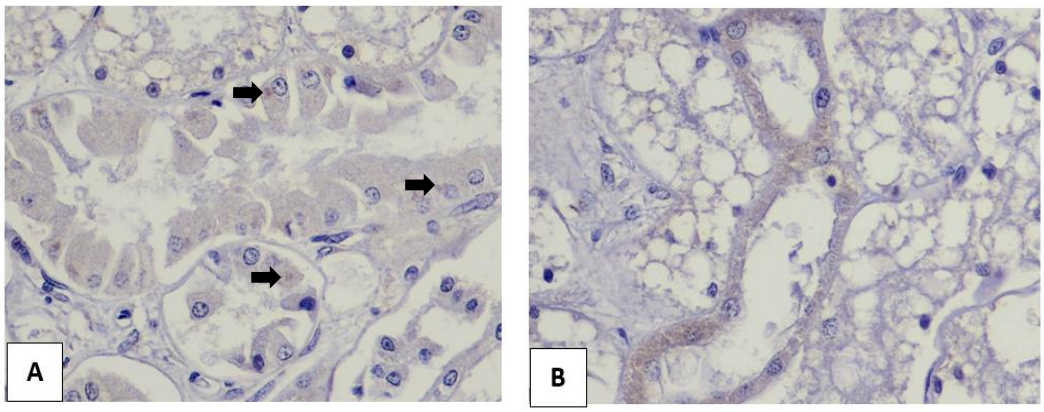

Figure 25 Kidney, cat, 21P346Y. (A) Pale immunostaining signal was exhibited by ICIB (IHC, 400x). The cytoplasm of collecting tubule exhibited immunostaining signal (IHC, 400x).

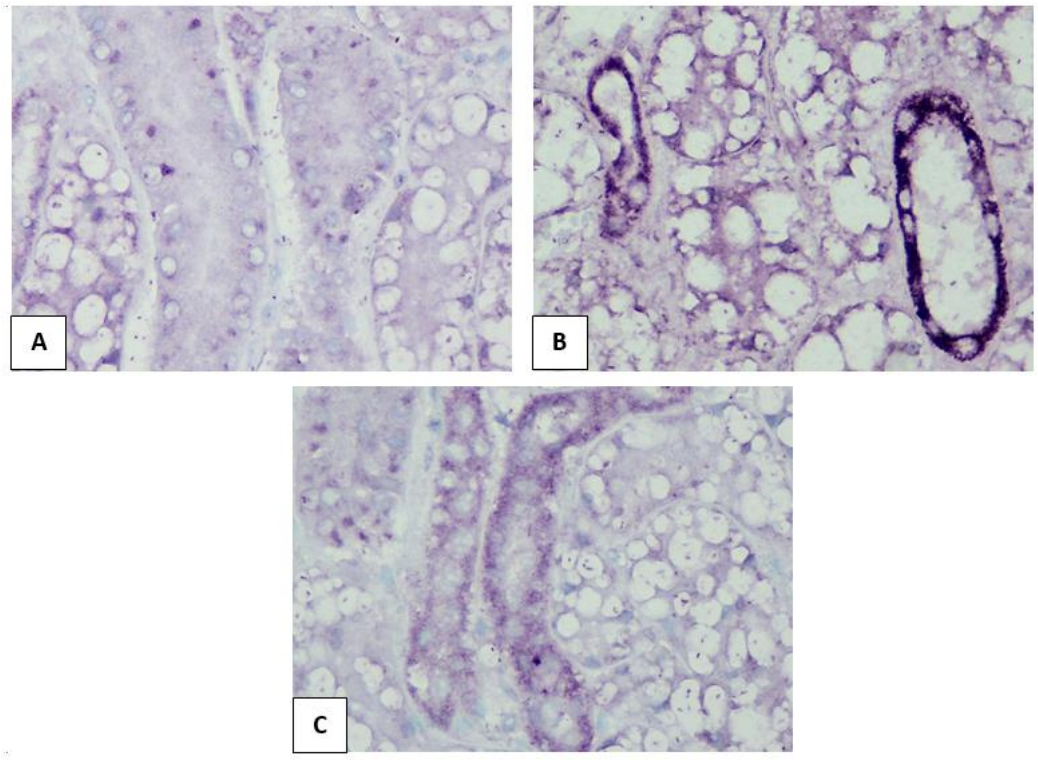

Figure 26 Kidney, cat, 21P346Y. (A) Formation of ICIB exhibited ISH signal (ISH, 400x). (B) Cytoplasm of collecting tubule exhibited strong ISH signal (ISH, 400x). (C) Cytoplasm of distal tubules exhibited ISH signal (ISH, 400x).

21P413W/DSH/16 years old

Macroscopic lesion of the kidney showed mild irregular surface (Figure 27). HE staining showing that lymphoplasmacytic inflammatory cell was observed in the interstitial area of the renal tissue prominently in cortical area. The inflammatory cell was observed in medullar area as well. Proximal tubular epithelial cells exhibited pale eosinophilic ICIB formation (Figure 28). The basement membrane of tubules was ruptured with sloughing of the epithelial cells into tubular lumen. Moreover, moderate membranoproliferative glomerulonephritis was observed (Figure 29). Moderate infiltration of fibrous tissue was observed (Figure 29). Low apoptotic activity was observed on nucleus of tubular epithelial (Figure 30).

Figure 27 Kidney, cat, 21P413Y. The kidney showed mild-irregular surface.

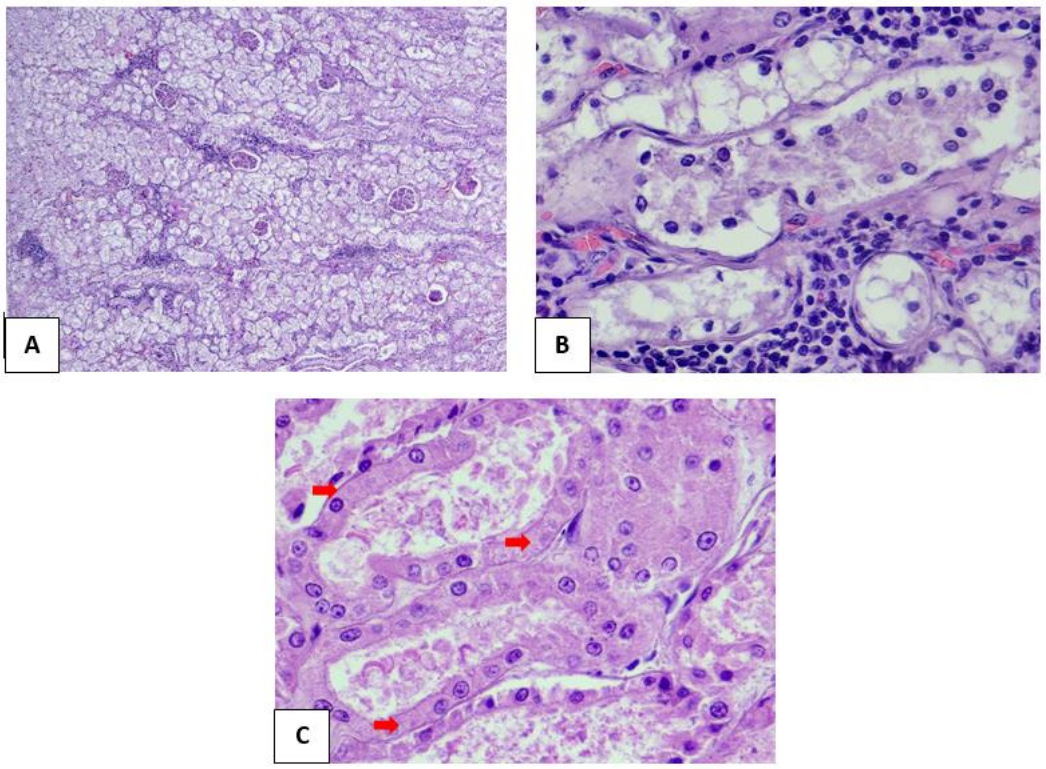

Figure 28 Kidney, cat, 21P413Y. (A) The inflammatory cell infiltrated the interstitial area of the renal tissue (HE, 100x). (B) Type of inflammatory cell is lymphoplasmacytic (HE, 400x). (C) Tubular epithelial cells exhibited pale eosinophilic ICIB (red arrow) (HE, 400x).

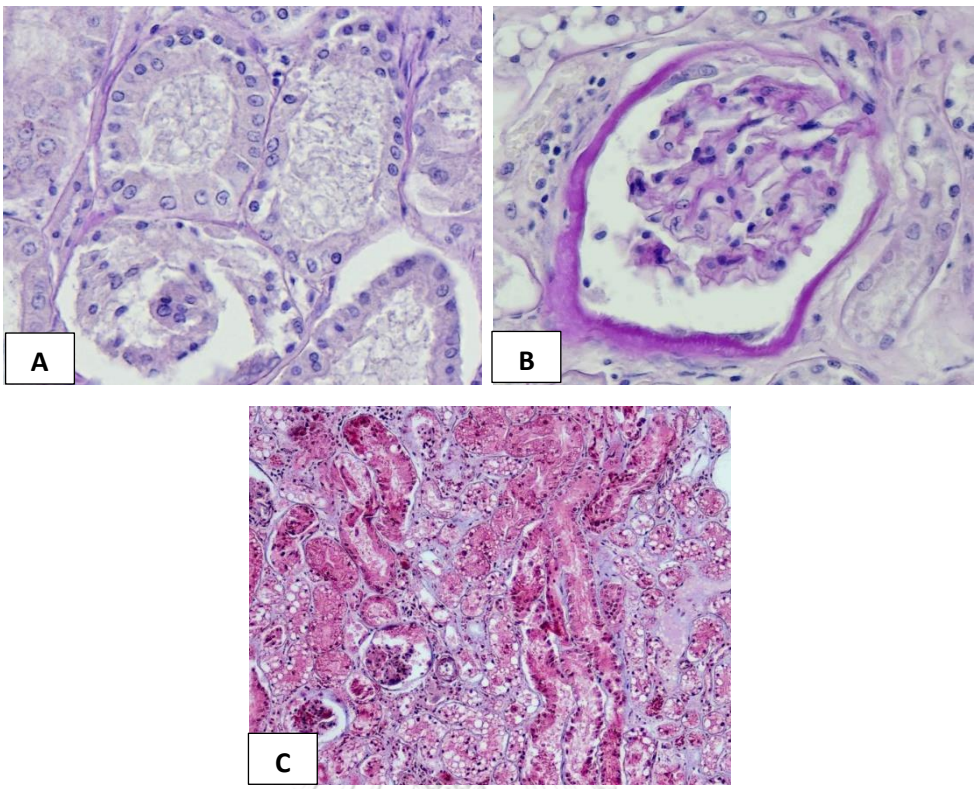

Figure 29 Kidney, cat, 21P413Y. (A) Tubular basement membrane was ruptured with accumulation of epithelial cells into tubular lumen (PAS, 400x). (B) Glomerulus suffered from MPGN (PAS, 400x). (C) Fibrous tissue was infiltrated the renal interstitial area (MT, 100x).

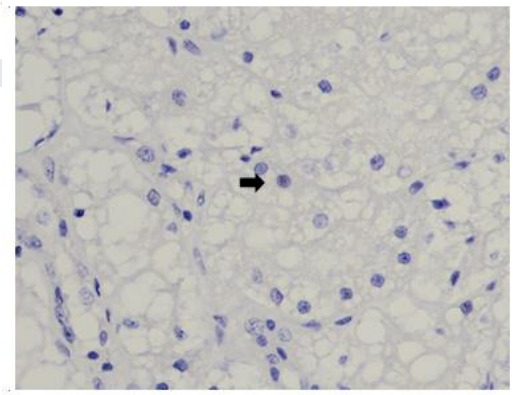

Figure 30 Kidney, cat, 21P413Y. Apoptotic activity of cleaved caspase-3. Brown color on nucleus of tubular epithelial cells marked the immunostaining signal of apoptotic activity (400x).

The immunostaining signal against M protein of FeMV disclosed that the immunostaining signal was expressed on cortical and medullar area of renal tissue. Pale immunostaining signal was exhibited by ICIB formation that been observed on proximal tubule. Cytoplasm of distal tubule and collecting duct were expressed immunostaining signal (Figure 31). In contrast to immunostaining signal, ISH signal was to be observed more intense and expressed on broader area such as cortical, medullar, and pelvis area of renal tissue. Furthermore, the *in-situ* signal was exhibited by ICIB of epithelial and cytoplasm of tubules such as distal tubule. Surprisingly, the inflammatory cell and nucleus of Henle loop also exhibited *in-situ* signal (Figure 32).

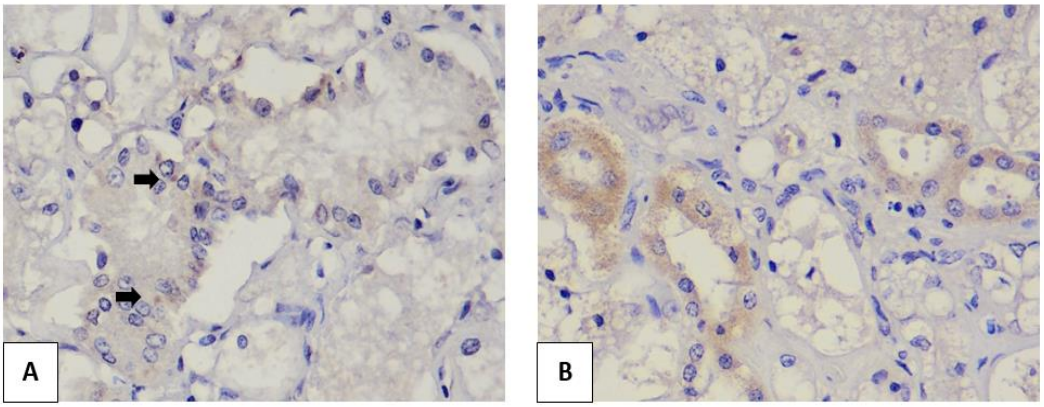

Figure 31 Kidney, cat, 21P413Y. (A) The immunostaining signal was exhibited by ICIB (black arrow) (IHC, 400x). (B) The immunostaining signal was exhibited by cytoplasm of epithelial cells of distal tubule and collecting duct (IHC, 400x).

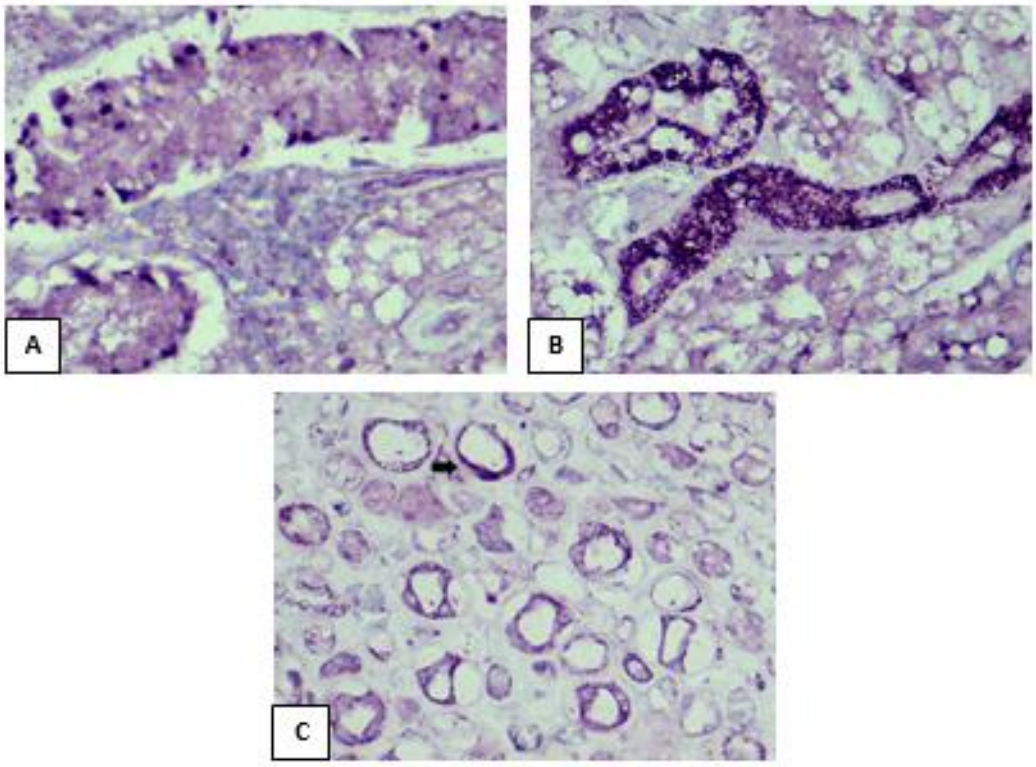

Figure 32 Kidney, cat, 21P413Y. (A) The *in-situ* signal was exhibited by ICIB (ISH, 400x). (B) Cytoplasm of distal tubules was exhibited strong *in-situ* signal (ISH, 400x). (C) The nucleus of Henle loop exhibited *in-situ* signal (ISH, 400x).

21P603Y/Domestic shorthair/1 year old

There was no remarkable gross lesion was observed on the infected kidney. H.E staining revealed that the interstitial area of renal tissue was infiltrated with lymphoplasmacytic inflammatory cell mainly in cortical area. Further, the inflammatory cell infiltrates the medullar area of the renal tissue. Eosinophilic ICIB formation was observed in proximal tubule (Figure 33). PAS staining showing that tubular basement membrane was intact with the detachment of tubular epithelial cells. Moreover, severe membranoproliferative glomerulonephritis was observed (Figure 34). MT staining showing that the interstitial area of the renal tissue was infiltrated with moderate degree of fibrous tissue (Figure 34). The tissue also exhibited cleaved caspase-3 immunosignal (Figure 35).

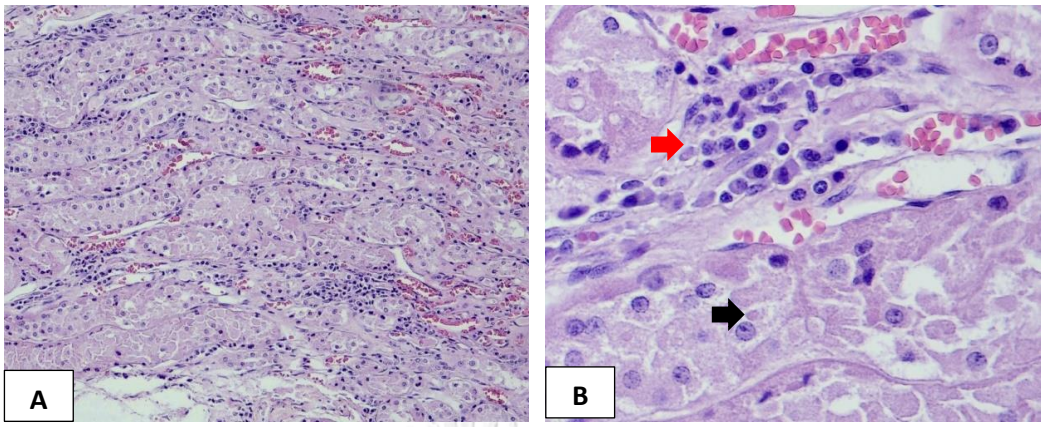

Figure 33 Kidney, cat, 21P603Y. (A) The inflammatory cell infiltrate interstitial of the renal tubules (HE, 100x). (B) Interstitial of renal tubule was infiltrated with lymphoplasmacytic inflammatory cell (red arrow). The tubules exhibited formation of eosinophilic ICIB (black arrow) (HE, 400x).

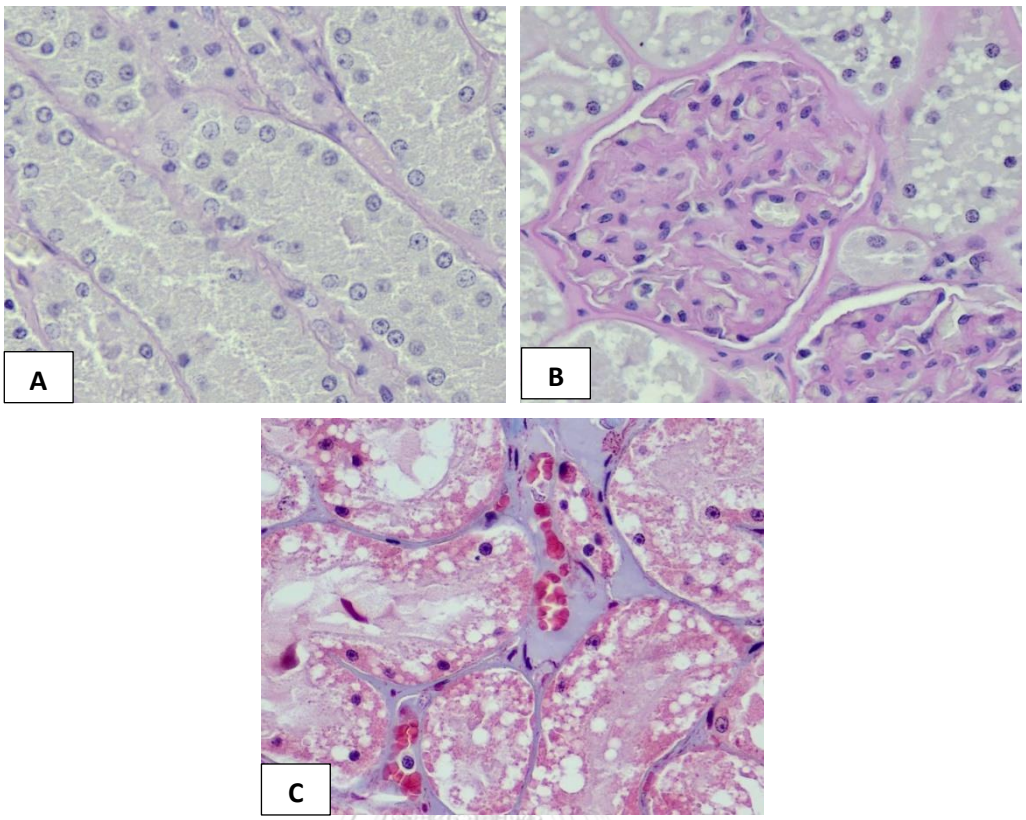

Figure 34 Kidney, cat, 21P603Y. (A) The tubular basement membrane was intact. However, the tubular epithelial was observed to be detached (PAS, 400x). (B) Severe membranoproliferative glomerulonephritis was observed on the glomerulus (400x). (C) Fibrous tissue was observed to infiltrate interstitial area of renal tissue (MT, 400x).

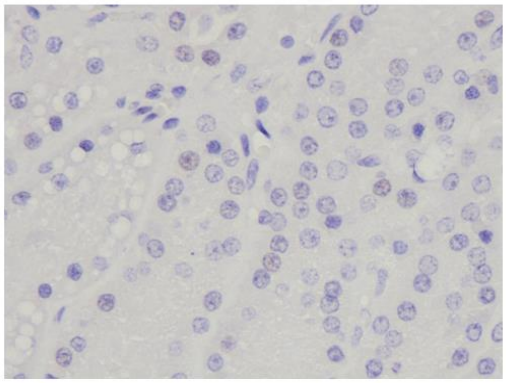

Figure 35 Kidney, cat, 21P603Y. Nucleus of epithelial cells exhibited apoptotic activity (Apoptotic activity, 400x).

Immunostaining signal against M-protein was expressed on cortical, medullar, and pelvis of the renal tissue. Immunostaining signal was exhibited by ICIB in proximal tubule. Moreover, the immunostaining signal was exhibited by cytoplasm of collecting and distal tubules. An appealing finding showing that immunostaining signal was exhibited by nucleus of proximal tubule in which the eosinophilic ICIB formation was not presented (Figure 36). Accordance with the immunostaining expression through all area of kidney, viral localization using ISH assay supported the finding. ISH signal was exhibited on cortical, medullar, and pelvis of the kidney. ISH signal was exhibited by ICIB of proximal tubule. Interestingly, cytoplasm of proximal tubule, in which ICIB was not presented, expressed ISH signal. Furthermore, nucleus of proximal tubule and nucleus of Henle loop were expressed *in-situ* signal as well (Figure 37).

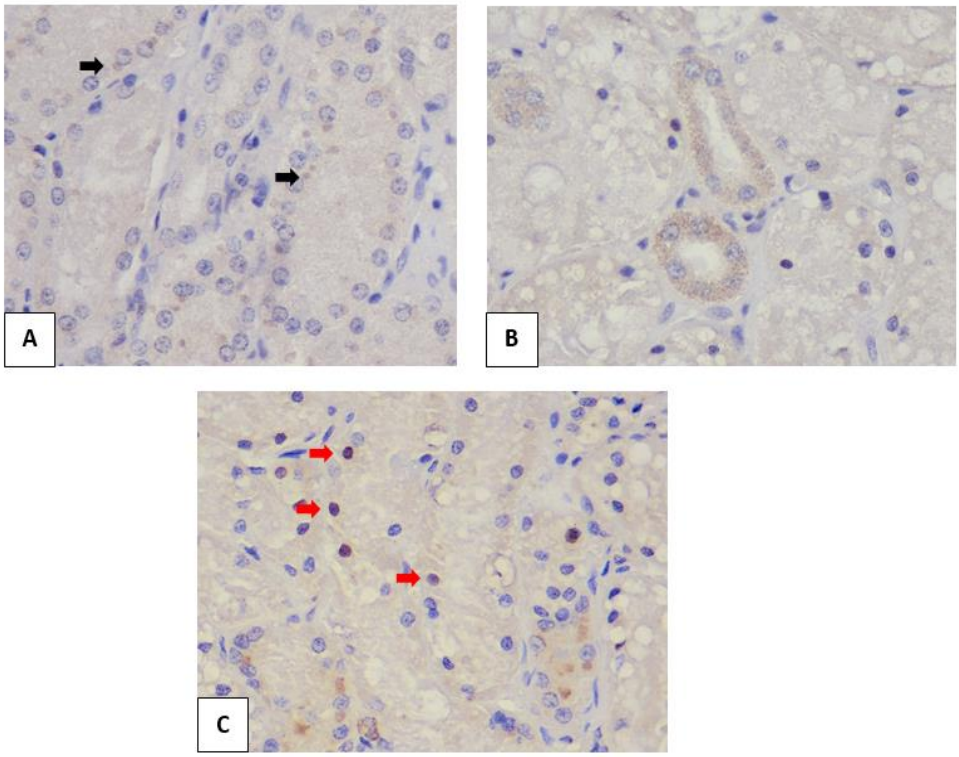

Figure 36 Kidney, cat, 21P603Y. (A) Formation of ICIB in epithelial cells of proximal tubule expressed immunostaining signal (black arrow) (IHC, 400x). (B) Cytoplasm of epithelial cells of distal tubule and collecting tubule exhibited immunostaining signal (IHC, 400x). (C) Nucleus of proximal tubule exhibited immunostaining signal (red arrow) (IHC, 400x).

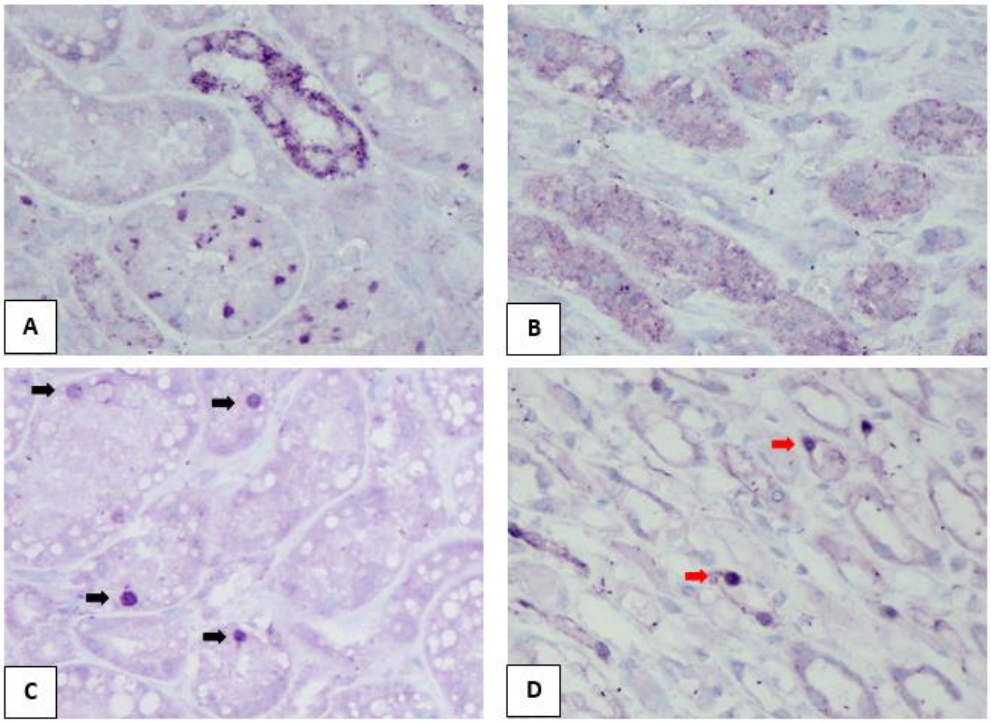

Figure 37 Kidney, cat, 21P603Y. (A) ICIB of proximal tubule exhibited *in-situ* signal (400x). (B) Cytoplasm of proximal tubules exhibited *in-situ* signal (400x). (C) Nucleus of proximal tubule exhibited *in-situ* signal (black arrow) (400x). (D) The nucleus of Henle loop exhibited *in-situ* signal (red arrow) (400x).

22P060Y/Domestic shorthair/3 years old

In macroscopic examination, there was no remarkable gross lesion was observed. Histopathologically, the interstitial renal tissue was infiltrated with lymphoplasmacytic inflammatory cell. Furthermore, the tubular epithelial cells exhibited the formation of eosinophilic ICIB (Figure 38). PAS staining revealed that the tubular basement membrane was intact; however the detachment of tubular epithelial cell was observed. The PAS staining also revealed that mild membranoproliferative glomerulonephritis was observed (Figure 39). MT staining revealed that interstitial area of renal tissue exhibited infiltration of fibrous tissue (Figure 39).

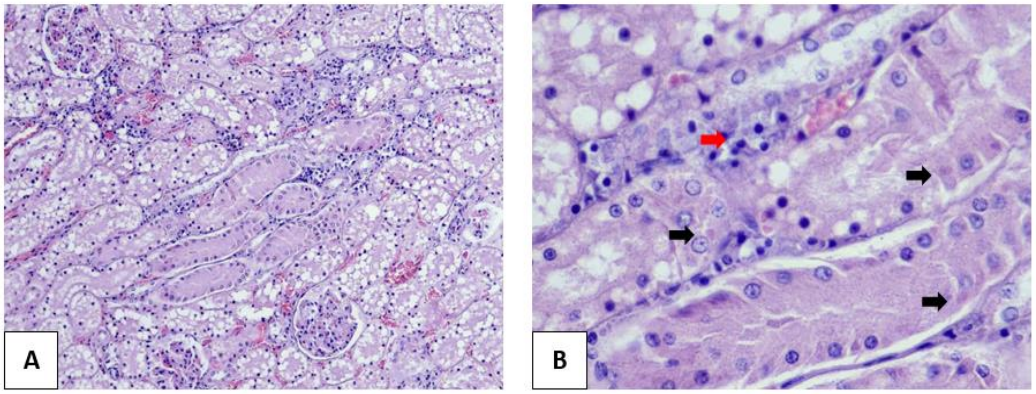

Figure 38 Kidney, cat, 22P060Y. (A) Inflammatory cell infiltrate interstitial of renal tissue (HE, 100x). (B) Interstitial inflammatory cell was comprised of lymphocytes and plasma cells (red arrow). The tubular epithelial cells exhibited eosinophilic ICIB (black arrow) in cytoplasm (HE, 400x).

Tubular epithelial cells exhibited immunostaining signal of cleaved caspase-3 (Figure 40). Immunostaining signal against Matrix protein of FeMV was expressed on cortical, medullar, and pelvis area of kidney. The immunostaining signal was expressed by ICIB of proximal tubule. Furthermore, immunostaining signal was expressed on nucleus of proximal tubule in which the formation of ICIB was absence. The cytoplasm of distal tubule expressed immunostaining signal as well (Figure 41). In accordance with IHC assay, ISH assay revealed that partial of genomic material of FeMV-1 was detected on cortical, medullar, and pelvis area of the tissue. Moreover, *in-situ* signal was exhibited by the ICIB on proximal tubule. It was observed that *in-situ* signal was expressed by the nucleus and cytoplasm of proximal tubule in which eosinophilic ICIB formation was absent. Nucleus of Henle loop expressed *in-situ* signal as well (Figure 42).

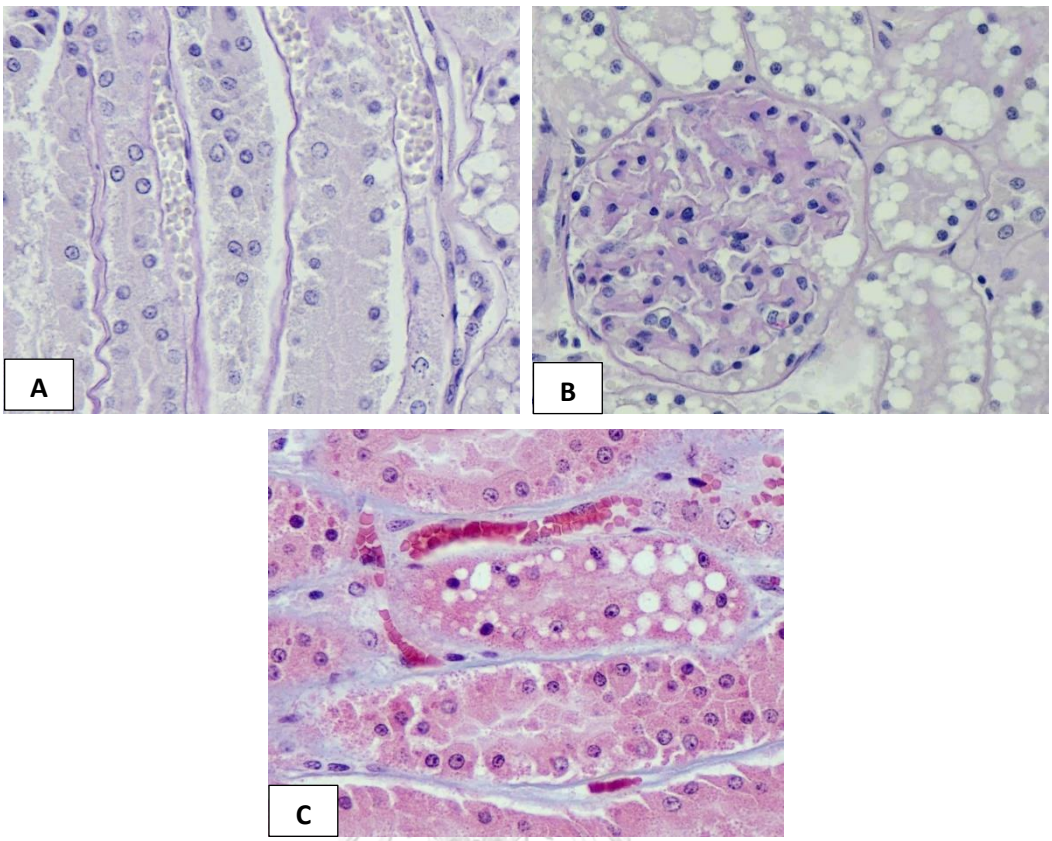

Figure 39 Kidney, cat, 22P060Y. (A) Tubular basement membrane was intact with detachment of epithelial cells (PAS, 400x). (B) Membranoproliferative glomerulonephritis was observed (PAS, 400x). (C) The fibrous tissue was observed infiltrated interstitial of renal tissue marked by the presence of blue color (MT, 400x).

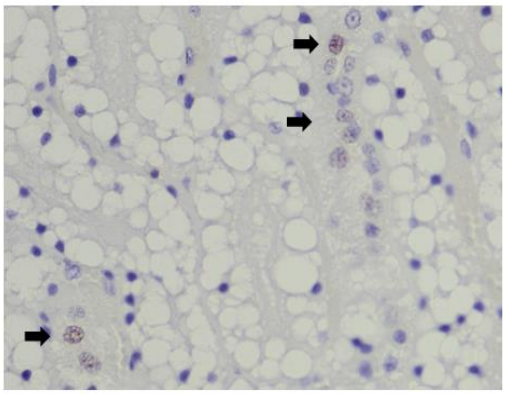

Figure 40 Kidney, cat, 22P060Y. Expression of cleaved caspase-3 was observed in nucleus of renal tubule (Apoptotic activity, 400x).

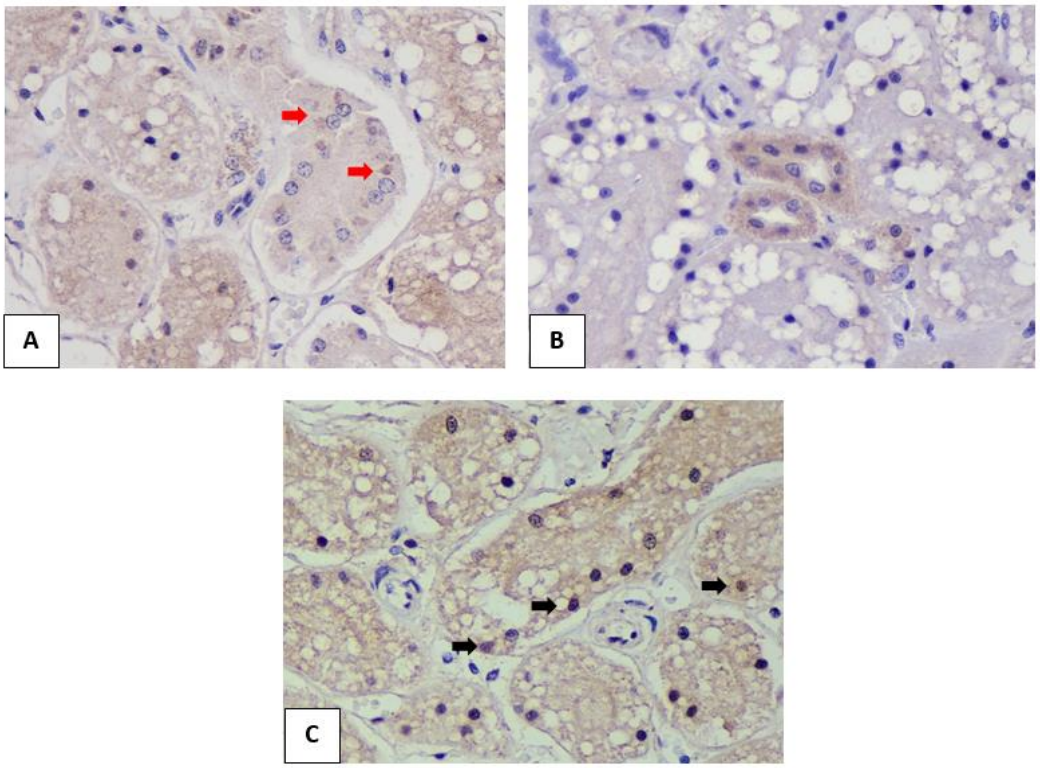

Figure 41 Kidney, cat, 22P060Y. (A) Immunostaining signal was exhibited by ICIB located on proximal tubule (red arrow) (IHC, 400x). (B) Cytoplasm of distal tubules exhibited immunosignal (IHC, 400x). (C) The nucleus of proximal tubule exhibited immunostaining signal (black arrow) (IHC, 400x).

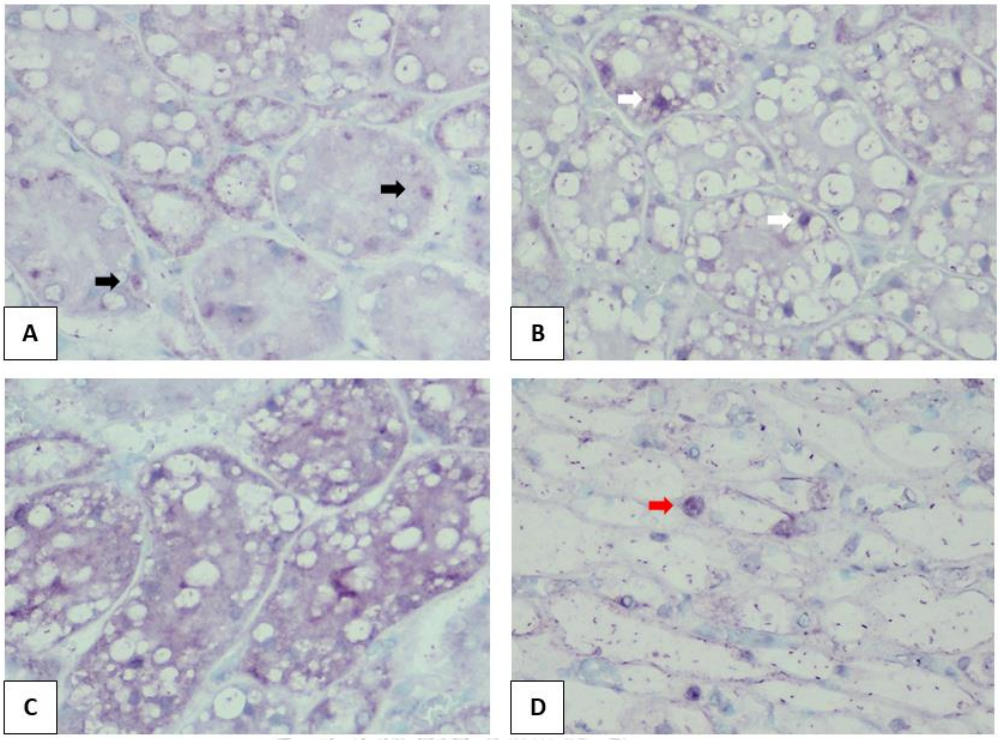

Figure 42 Kidney, cat, 22P060Y. (A) *In-situ* signal was expressed on ICIB of proximal tubule (black arrow) (ISH, 400x). (B) The nucleus of proximal tubule expressed *in-situ* signal (white arrow) (ISH, 400x). (C) Cytoplasm of proximal tubule expressed *in-situ* signal (400x). (D) Nucleus of Henle loop exhibited *in-situ* signal (red arrow) (ISH, 400x).

22P118R/Domestic shorthair/2 years old

There was no remarkable gross lesion on the kidney. Histologically, very mild infiltration of lymphoplasmacytic inflammatory cell was observed on renal interstitial area. Moreover, the tubular epithelial cells exhibited the formation of eosinophilic ICIB (Figure 43). PAS staining revealed that the basement membrane was intact; however the detachment of tubular epithelial was observed. The renal tissue exhibited cleaved caspase 3 immunosignal (Figure 44). Furthermore, the renal tissue exhibited the presence of mild membranoproliferative glomerulonephritis (Figure 44). Renal scarring was mildly observed (Figure 45).

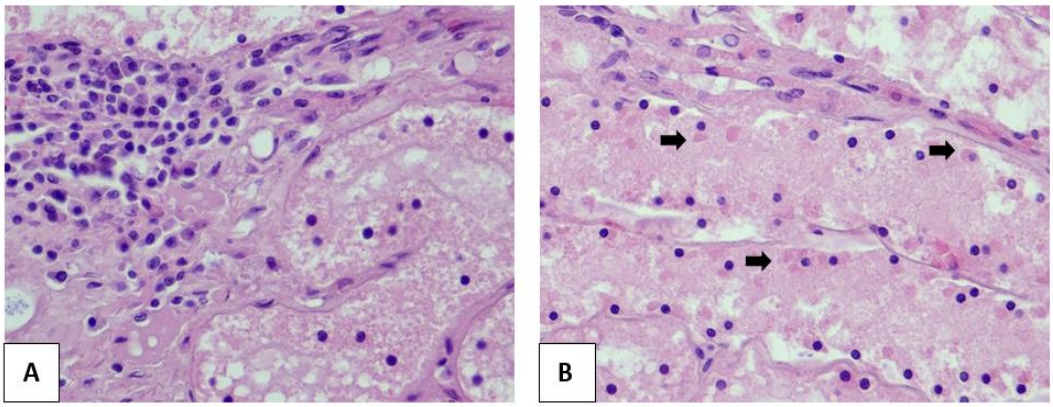

Figure 43 Kidney, cat, 22P118R. (A) Lymphoplasmacytic inflammatory cell infiltrate interstitial of renal tissue (HE, 400x). (B) Tubular epithelial exhibited formation of eosinophilic ICIB (black arrow) (HE, 400x).

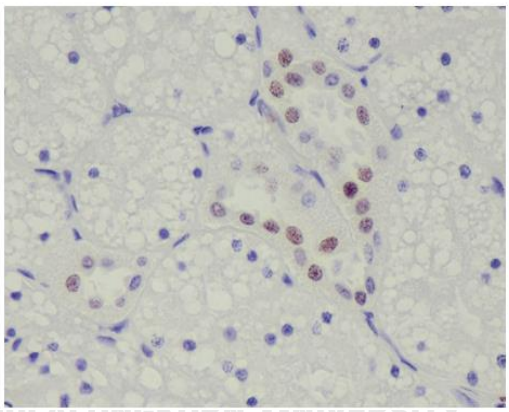

Figure 44 Kidney, cat, 22P118R. Apoptotic activity marked by the presence of cleaved caspase 3 was expressed on nucleus of tubular epithelial cell (Apoptotic activity, 400x).

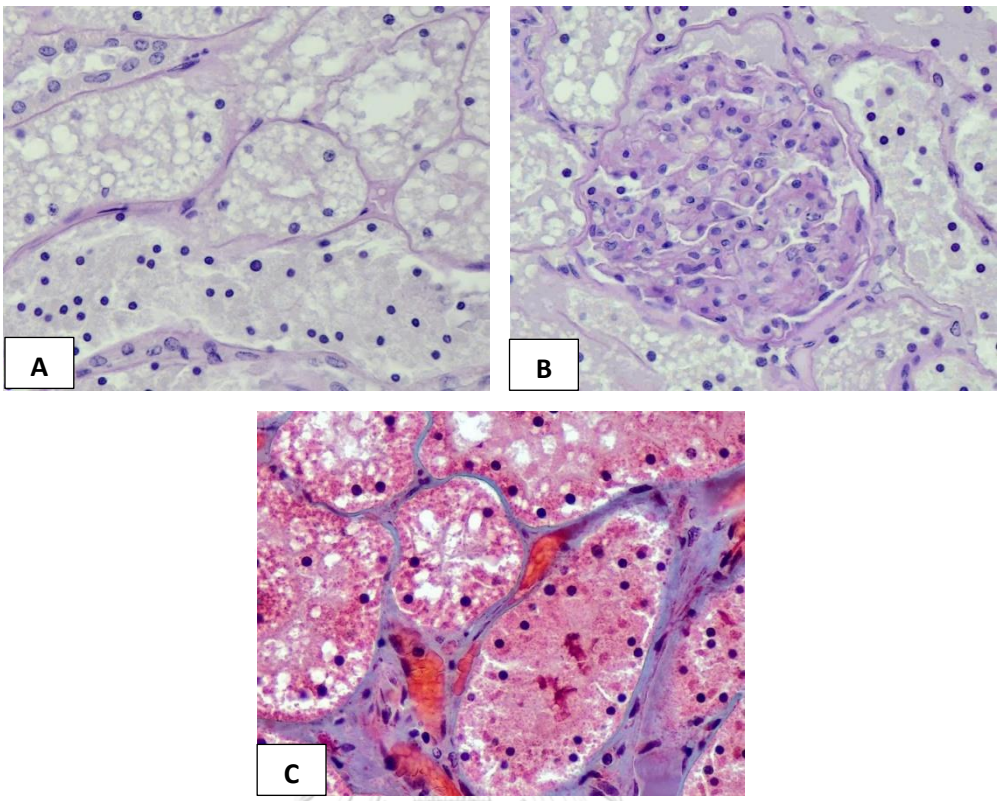

Figure 45 Kidney, cat, 22P118R. (A) Tubular epithelial cell was observed to be detached from basement membrane (PAS, 400x). (B) Mild thickening of Bowman capsule was observed (PAS, 400x). Fibrous tissue was observed to be infiltrated the renal interstitial (MT, 400x).

IHC assay against M-protein revealed that the areas of renal tissue such as cortical, medullar, and pelvis area. Moreover, immunosignal was exhibited by ICIB and cytoplasm of collecting tubule (Figure 46). Accordance with immunostaining signal, *in-situ* signals were exhibited on cortical, medullar, and pelvis area of the tissue. *In-situ* signal was expressed by ICIB and cytoplasm of distal tubule epithelial cell (Figure 47).

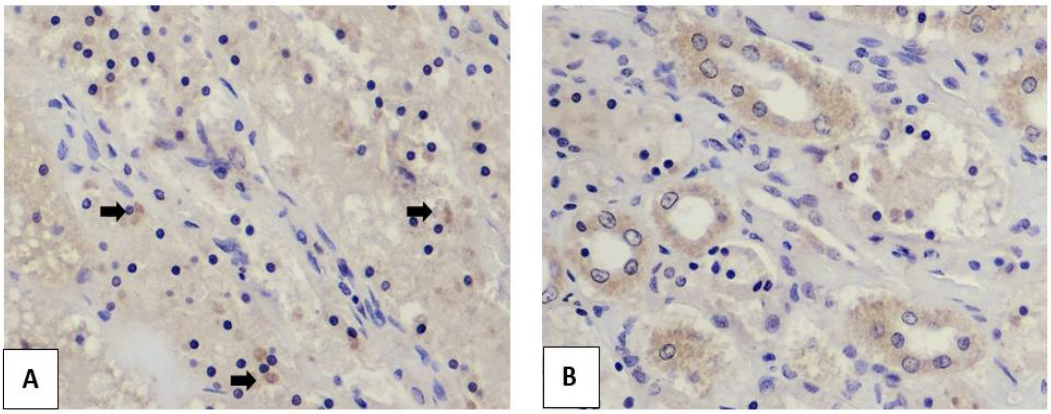

Figure 46 Kidney, cat, 22P118R. (A) Immunosignal was expressed by ICIB of proximal tubule (black arrow) (IHC, 400x). (B) Cytoplasm of collecting tubule exhibited immunosignal (IHC, 400x).

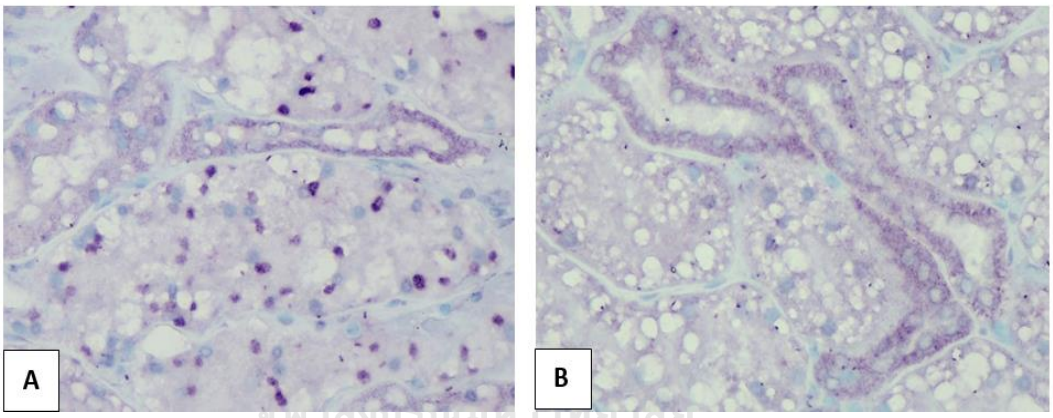

Figure 47 Kidney, cat, 22P118R. (A) Formation of ICIB exhibited ISH signal (ISH, 400x). (B) Cytoplasm of distal tubules exhibited *in-situ* signal (ISH, 400x).

22P119R/Domestic shorthair/3 years old

Macroscopic examination of the kidney showing there was no remarkable lesion found on the kidney. HE staining revealed that interstitial of the renal tissue was infiltrated with lymphoplasmacytic inflammatory cell, mainly in cortical area. The tubular epithelial cells exhibited with the formation of eosinophilic ICIB (Figure 48).

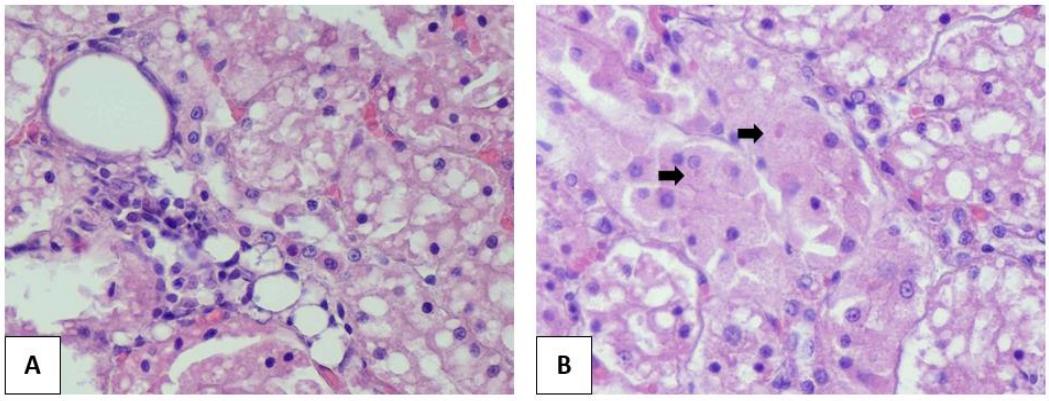

Figure 48 Kidney, cat, 22P119R. (A) Lymphoplasmacytic inflammatory cell infiltrate interstitial of renal tissue (HE, 400x). (B) Tubular epithelial exhibited formation of eosinophilic ICIB black arrow (HE, 400x).

PAS staining revealed that tubular basement membrane was ruptured. Tubular epithelial cells were detached and sloughing into tubular lumen (Figure 49). Fibrous tissue was observed infiltrating the interstitial of renal tissue (Figure 49). The tissue exhibited immunostaining signal against cleaved caspase 3 (Figure 50). The immunostaining signal was exhibited on cortical, medullar, and pelvis of the renal tissue. Immunostaining signal was exhibited by ICIB as well as cytoplasm collecting tubule (Figure 51). In accordance with immunostaining signal, ISH signal was exhibited in cortical, medullar, and pelvis area of renal tissue. Furthermore, *in-situ* signal was exhibited by ICIB and cytoplasm of collecting tubule (Figure 52).

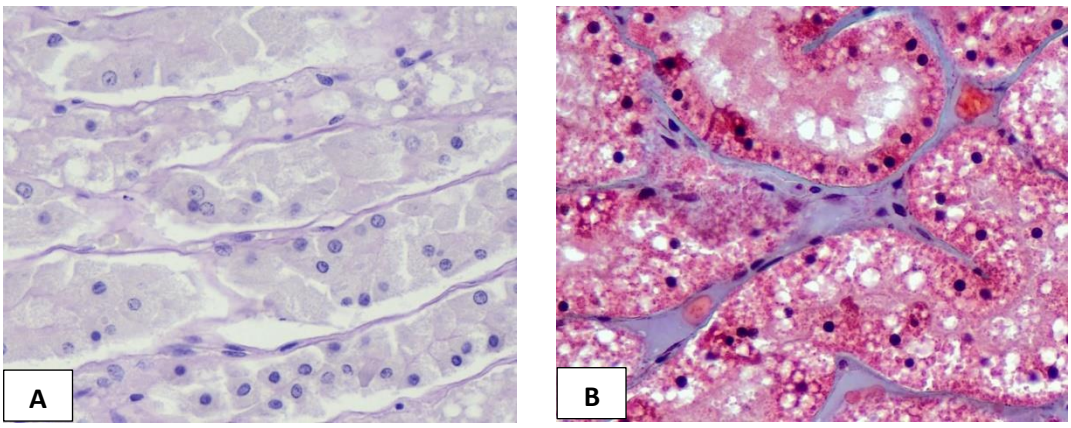

Figure 49 Kidney, cat, 22P119R. (A) Tubular basement membrane was ruptured and the tubular epithelial cell sloughing into tubular lumen (PAS, 400x). (B) Fibrous tissue infiltrated renal interstitial area (MT, 400x).

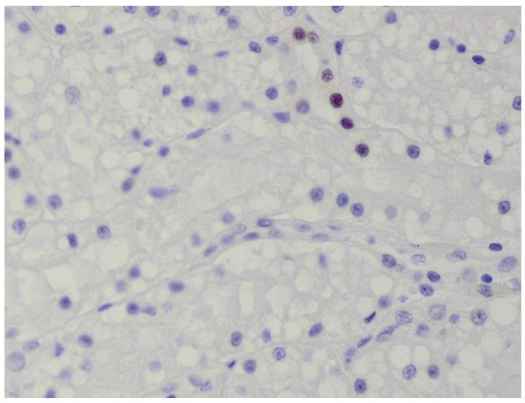

Figure 50 Kidney, cat, 22P119R. Nucleus of epithelial cells exhibited apoptotic activity marked by brown color (Apoptotic activity, 400x).

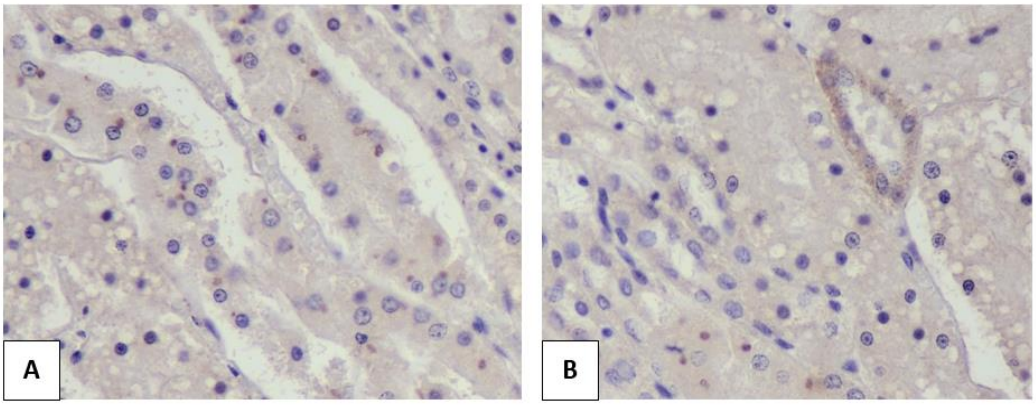

Figure 51 Kidney, cat, 22P119R. (A) Formation of ICIB exhibited immunostaining signal marked by brown color (IHC, 400x). (B) Cytoplasm of collecting tubule exhibited immunosignal (IHC, 400x).

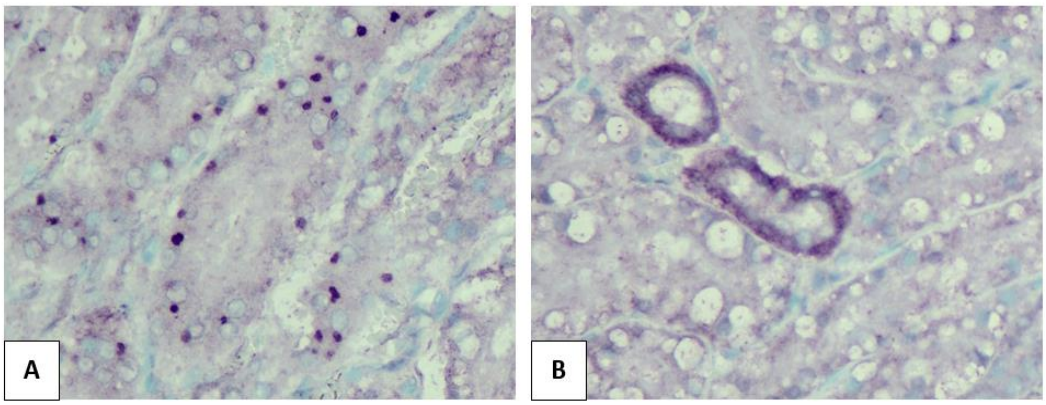

Figure 52 Kidney, cat, 22P119R. (A) Formation of ICIB expressed *in-situ* signal (ISH, 400x). (B) Cytoplasm of collecting tubule exhibited *in-situ* signal (ISH, 400x).

22P126C/Domestic shorthair/1 years old

There was no remarkable gross lesion on the kidney. HE staining showing the tissue was infiltrated with lymphoplasmacytic inflammatory cells. The tubular epithelial cells exhibited formation of eosinophilic ICIB (Figure 53). PAS staining showing that tubular basement membrane and tubular epithelial cells were intact. However, basement membranes of some tubules were erupted followed by

sloughing of tubular epithelial cells into lumen (Figure 54). Infiltration of fibrous tissue was observed (Figure 54). The tissue exhibited immunosignal of cleaved caspase 3 (Figure 55).

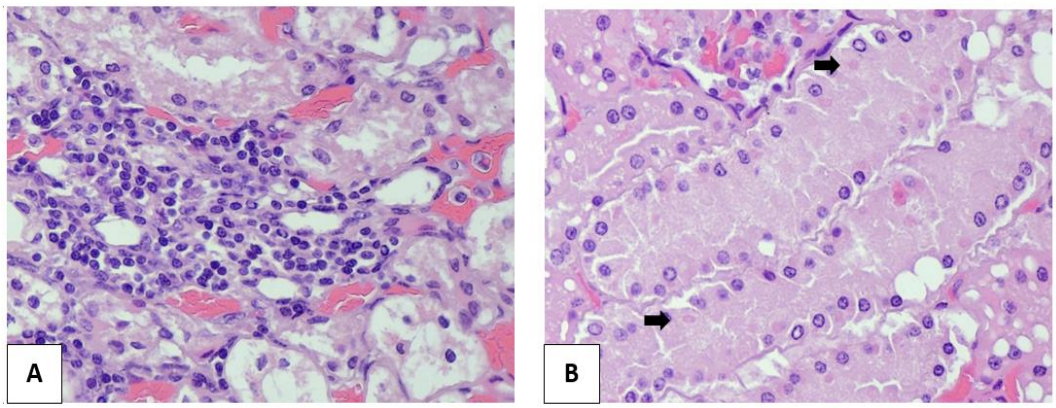

Figure 53 Kidney, cat, 22P126C. (A) Lymphoplasmacytic inflammatory cell was observed infiltrating interstitial area of renal tissue (HE, 400x). (B) Tubular epithelial cell exhibited eosinophilic ICIB (arrows) (HE, 400x).

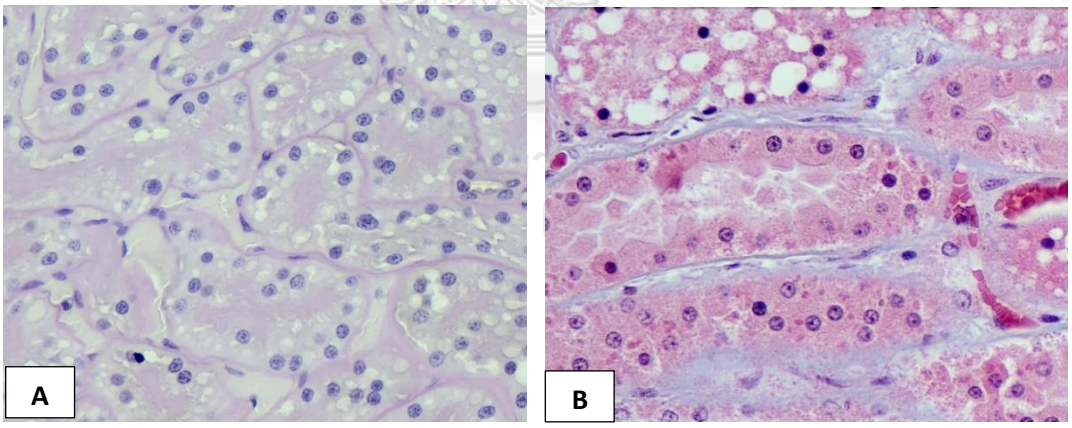

Figure 54 Kidney, cat, 22P126C. (A) Basement membranes of the tubules were intact. However, tubular epithelial cell of some tubules were detached (PAS, 400x). (B) Fibrous tissue was observe to infiltrate the renal interstitial area (MT, 400x).

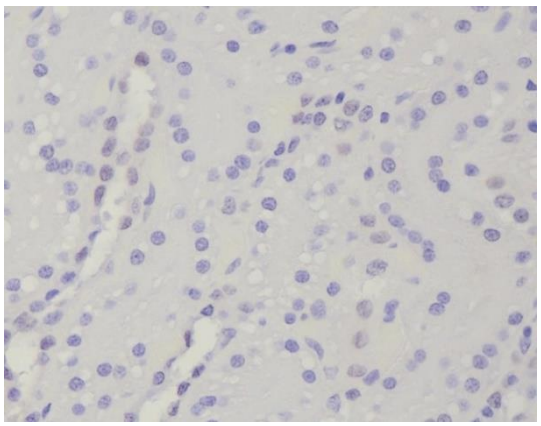

Figure 55 Kidney, cat, 22P126C. Nucleus of tubules exhibited immunostaining signal of apoptotic activity (Apoptotic activity, 400x).

IHC assay against M-protein of FeMV revealed that there was no immunostaining signal observed. However, the *in-situ* signal is exhibited on cortical, medullar, and pelvis area of the renal tissue. Surprisingly, nucleus of the tubules expressed ISH signal (Figure 56).

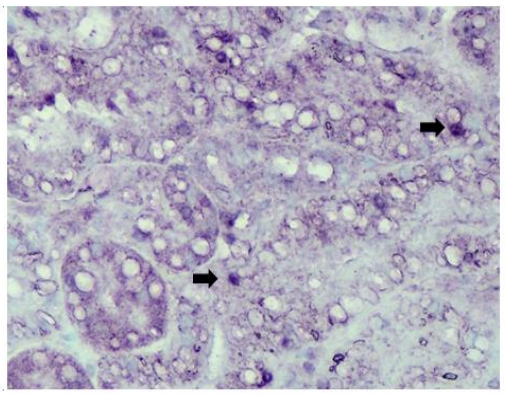

Figure 56 Kidney, cat, 22P126C. ISH signal was exhibited by nucleus of the tubules (ISH, 400x).

Table 5 Summary of histopathological finding of FeMV-1 positive cases.

Case	Gross lesion	ICIB-like formation	Interstitial inflammation	PAS	MT	Apoptotic activity	IHC		ISH	
							Signal	Area***	Signal	Area***
21P240D	NRL*	+	+	MPGN**	-	-	-	-	+	C
21P276C	NRL	+	+	-	+	+	+	C, M, P	+	C, M, P
21P346Y	Renal calculi; mild irregular surface; dilatation of renal pelvis	+	+	-	+	-	+	C, M, P	+	C, M, P
21P413W	Mild irregular surface	+	+	MPGN	+	+	+	C, M	+	C, M, P
21P603Y	NRL	+	+	MPGN	+	+	+	C, M, P	+	C, M, P
22P060Y	NRL	+	+	MPGN	+	+	+	C, M, P	+	C, M, P
22P118R	NRL	+	+	MPGN	+	+	+	C, M, P	+	C, M, P
22P119R	NRL	+	+	-	+	+	+	C, M, P	+	C, M, P
22P126C	NRL	+	+	-	+	+	-	-	+	C, M, P

*NRL : No remarkable lesion

**MPGN : Membranoproliferative glomerulonephritis

***C: Cortical area; M: Medullar area; P: Pelvis area

Semiquantitative scoring

Semiquantitative scoring was carried out by three examiners. The scores for histopathological variable from each examiner were accumulated then the mean value was obtained. Moreover, the scores of ISH and IHC were preceded in the same manner (Table 5).

Table 6 Summary of semi-quantitative scoring (means) of signals exhibited by ISH, IHC and parameters of pathological alteration.

Case	ISH	IHC	Degree of inflammation	Intact of tubular basement membrane	Fibrosis	Caspase 3
21P240D	0.7	0	2	1.5	0	0
21P276C	2	2.85	1	2	1	2.3
21P346Y	0.5	0.85	2	2	2	0
21P413W	1.8	1.2	2	1.5	3	1.3
21P603Y	2.65	2	1	3.5	2	2.3
22P060Y	1	2.35	1	2	1	1
22P118R	1	2.65	1	2	1.5	1
22P119R	2.65	2.65	1	1.5	1.5	3.7
22P126C	0.7	0.5	1	3	1	0

According to Q-Q plot evaluation, the obtained data was not normally distributed; hence Spearman correlation test was carried out to define the correlation of FeMV-1 infection and pathological consequence in kidney.

Spearman correlation test

In the beginning, the correlation test was carried out on ISH and IHC score against histopathological variables. The summary of the correlation was presented below (Table 7-8).

Table 7 Summary of Spearman coefficient correlation of ISH against histopathologic variables.

Histopathologic variables	**Spearman coefficient correlation**	**Interpretation**[1]	**Significancy (*p<0.05*)**
Inflammation degree	-0.5085	Moderate negative correlation	Not significant (*p=0.1786*)
Tubular basement intact	-0.01796	Negligible correlation	Not significant (*p=0.9651*)
Fibrosis	0.2814	Weak positive correlation	Not significant (*p=0.4562*)
Caspase 3	0.9741	Very strong positive correlation	Significant (*p=0.0003*)

[1](Schober et al., 2018)

Table 8 Summary of Spearman coefficient correlation of IHC against histopathologic variables.

Histopathologic variables	**Spearman coefficient correlation**	**Interpretation**[1]	**Significancy (*p<0.05*)**
Inflammation degree	-0.6417	Moderate negative correlation	Not significant (*p=0.0833*)
Tubular basement intact	-0.02226	Negligible correlation	Not significant (*p=0.4778*)
Fibrosis	0.09444	Negligible correlation	Not significant (*p=0.403*)
Caspase 3	0.7500	Strong positive correlation	Significant (*p=0.0130*)

[1](Schober et al., 2018)

CHAPTER 5
DISCUSSION AND CONCLUSION

Prevalence of FeMV-1 infection in cat kidneys

Paramyxoviruses such as FeMV-1, FeMV-2, and FPaV had been suggested to be associated with kidney disease in cats (Woo et al., 2012; Sieg et al., 2015; Sieg et al., 2019). Investigation of the presence of paramyxovirus genomic material had been carried out on various types of clinical sample such as blood, oral swab, rectal swab, feces, and urine (Woo et al., 2012; Furuya et al., 2014; Sieg et al., 2015). Moreover, it also had been carried out in several tissues such as kidney, lymph node, spleen, lung, intestine, liver, brain, and urinary bladder (Yilmaz et al., 2017; De Luca et al., 2020; Sieg et al., 2020; Chaiyasak et al., 2022). Among those samples, paramyxoviruses was detected more frequent in kidney and urine (De Luca et al., 2021).

In this study, paramyxoviruses screening was carried out in renal tissue of cats submitted for routine necropsy. Among paramyxovirus-associated with kidney disease, FeMV-1 was detected on 9 samples (6%) using FeMV-1 specific primers (Woo et al., 2012), instead of pan-primer pairs (Tong et al., 2008). This study did not investigate further the underlying reason of the inability of the pan-primer to detect genomic material of FeMV-1. However, it might be suggested that L-gene of feline morbillivirus, particularly FeMV-1, possessed genetic heterogenicity which affecting the compatibility of the pan-primer. Previous study had categorized FeMV-1 into three distinguished clusters which was FeMV-1 cluster A, B, and C (Park et al., 2016; Chaiyasak et al., 2020b). In this study, genomic material of FeMV-2 and FPaV were not detected. Regarding the prevalence of FeMV-2 and FPaV from previous study, both FeMV-2 and FPaV had lower prevalence rate compared to FeMV-1. To date, FeMV-2 was firstly and only discovered in Germany (Sieg et al., 2019). Moreover, FPaV was discovered in Germany (Sieg et al., 2015), Japan (Sakaguchi et al., 2020), and Chile (Sieg et al., 2020).

In this study, FeMV-1 positive cases were comprised of seven young cats with age range 1-3 years old (77.8%), and two senior cats with age range 10-16 years old (22.2%). This finding revealed that genomic material of FeMV-1 was prone to be

found in young adult cats (1-6 years old) compared to senior cats (>10 years old). However, this study was not aimed to investigate the association of FeMV infection and life stage of cats, as the collected samples were consisted of cats from various life stages that predominant by young adult cats (1-6 years old) (53.33%). The association of FeMV infection and life stage of cats was investigated on previous study conducted in Italy; they showed that the genomic material of FeMV-1 was profoundly detected in blood, urine, and kidney of young and middle aged cats (~2-7 years old), whereas antibody of FeMV was prominently detected on serum of older cats (>8 years old) (De Luca et al., 2020).

Pattern of FeMV-1 infection was suggested to be classified into three patterns; pattern 1 portrayed by the presence of viral RNA and antibody (RNA+/Ab+); pattern 2 portrayed the presence of viral RNA and the absence of antibody (RNA+/Ab-); pattern 3 portrayed the absence of viral RNA and the presence of antibody (RNA-/Ab+). Moreover, it reported that young and middled age cats were profoundly to express pattern 1 and 2. In contrast, pattern 3 was only expressed by senior cats (De Luca et al., 2020). One of the consequences of FeMV-1 infection was the presence of persistent infection, approximately more than two months after the initial infection. During persistency, the virus was shed to environment through urine excretion. Hereinafter, it was notified that antibody against FeMV was detected on day 5 and 7 after initial infection (Nikolin et al., 2022).

Unfortunately, the antibody against FeMV was not investigated in this study. However, 77.8% of FeMV-positive cases were considered as young adult cats, which of the respective cats had longer lifespan; they would likely to possess all FeMV-infection-patterns that had been described before (De Luca et al., 2020).

Regarding the breed association, all cases were considered as DSH. High prevalence of positive FeMV-1 cases occurred in DSH might be associated with the number of DSH breed that collected which constituted 53.33% of all samples. This finding was in line with latest study that carried out in Italy (2021), in which prevalence of FeMV-1 was higher in DSH compared to other breeds, as DSH constituted 84.3% of the overall collected sample (Donato et al., 2021).

Seven positive cases of FeMV-1 were raised in household as a family-pet. Case 21P240D was considered as stray cat. However, environmental lifestyle, in which case 22P126C was raised, was not able to be retrieved. To date, FeMV-1 had been discovered from cats raised in various environments such as household cats (indoor or outdoor), colony cats, and stray cats (Mohd Isa et al., 2019; Chaiyasak et al., 2020b; Donato et al., 2021). Among the positive FeMV-1 cases, it was remained unknown how would they got infected with FeMV-1. Case 21P240D was recorded as stray cat, which FeMV-1 was firstly discovered in Hongkong in 2012 (Woo et al., 2012). Moreover, case 21P276 was recorded to be missing then returned with feverish condition and followed by sudden death. This finding notified that FeMV circulated in environment and capable to infect the susceptible host (cat). In addition, case 21P346Y and 21P603Y were recorded living in household with multiple cats and dogs. Regarding this co-living circumstances, interspecies transmission between cat and dog were possible. Previous study in Thailand had revealed that FeMV-1 was detected from lung of dogs that possessed respiratory disease (Piewbang et al., 2021b). Up to now, FeMV was suspected to be transmitted through urine excretion. However, *in vivo* study from the group in Germany marked that FeMV was also shed through nasal (nasal swab), although the amount was lower than viral RNA that excreted in urine (Nikolin et al., 2022), that this remained debatable whether progeny virus excreted through nasal would likely to cause the infection on other susceptible cats.

Among these positive cases, four cases (21P276C, 22P060Y, 22P118R, and 22P119R) were marked to be co-infected with FeLV. In contrast, other viruses such as FIV, FCoV, FCV, and FPV were not detected on all cases. In this study, FeLV screening was carried out by detecting the presence of pro-virus on the renal tissue. Regarding the latest medical record of those FeLV co-infected cases and the current finding, it would likely to be suggested that 22P060Y and 22P119R were showing progressive

and regressive infection, respectively. Previous study had investigated that infection of FeLV generates several consequences on kidney such as renal neoplasia and formation of immune-complex glomerulonephritis (ICGN) (Rossi et al., 2019; Hartmann et al., 2020) that contributed to cause chronic kidney disease (CKD) in cats (Brown et al., 2016). Regarding this finding, it would likely to be suggested that co-infection of FeMV-FeLV might contribute on kidney impairment. Unfortunately, the clinical data such as BUN, SDMA, and creatinine values from each cases were not capable to be retrieved to prove this suggestion.

Pathological findings and viral localization of FeMV-1

Gross lesion of FeMV-1 positive kidney

Gross findings of kidneys of all positive cases were varies from non-remarkable lesion to mild irregular surface. The obvious gross lesion was found on case 21P346Y and 21P413W which considered as senior cats with age range 10-16 years old. In contrast, other positive cases that was considered as young cats, did not exhibited any gross lesion on their kidney. According to the length of the course, kidney disease in cats was classified into acute kidney injury (AKI) and chronic kidney disease (CKD) (Monaghan et al., 2012; Brown et al., 2016). The occurrence of AKI was usually investigated by considering the clinical examination data such as BUN, creatinine, and SDMA. In contrast, for the occurrence of CKD, other than confirming it using such clinical examinations, post-mortem examination was able to use to suspect that the kidney suffered from CKD (Bartges, 2012; McLeland et al., 2015). Considering the gross lesion on cases 21P346Y and 21P413W, those cases might suffer from CKD. The remarkable gross findings of CKD is renal fibrosis which characterized by irregular surface, contracted kidney, and difficulty to detach the renal capsule (Bartges, 2012; Reynolds and Lefebvre, 2013; Brown et al., 2016). Unfortunately, the latest medical record such as BUN, creatinine, and SDMA of all

cases were not able to be retrieved to confirm this suggestion. Furthermore, CKD was prone to be found on aging cats, although the occurrence of CKD on young cats was also notified (Bartges, 2012).

There were several gross lesions might associate with the FeMV-infection such as pale appearance, congestion on corticomedullary junction, contracted kidney, and granuloma formation. However, in previous study, no-remarkable lesion was also observed on FeMV-infected kidney (Yilmaz et al., 2017; Muratore et al., 2020; Piewbang et al., 2020; Chaiyasak et al., 2022; Nikolin et al., 2022).

Histopathological findings of FeMV-1 positive kidney

HE examination

HE staining examination showed that all positive cases exhibited lymphoplasmacytic tubulointerstitial nephritis (TIN) and profoundly found on cortical area of renal tissue. The first report of FeMV (formerly named as FmoPV) mentioned that FeMV infection might associated with the occurrence of tubulointerstitial nephritis (TIN) (Woo et al., 2012) which also one of hallmark of chronic kidney disease (CKD) in cats (McLeland et al., 2015; Rayhel et al., 2020). Previous studies had reported that FeMV infection might associated with the infiltration of lymphoplasmacytic inflammatory cell on renal interstitium (Crisi et al., 2020; De Luca et al., 2020; Piewbang et al., 2020). Demonstration of TIN became the hallmark of FeMV infection (both FeMV-1 and FeMV-2). Particularly, this pattern was not only observed on FeMV that infect domestic cat but also wild Felidae from previous study (Woo et al., 2012; Piewbang et al., 2020; Nikolin et al., 2022). In regards of immunity response of kidney, infection that occurs in kidney might trigger several inflammatory cells such as dendritic cells, macrophages, neutrophils, mast cells, natural killer cells (NK) and lymphocytes (Soos et al., 2006; Kurts et al., 2013; Abraham and Miao, 2015). The infiltration of lymphocyte and plasma cell in the interstitial area of kidney might

associate with pathogenicity of FeMV which previous study suggested being in line with other morbillivirus such as Measles virus (MeV). The underlying of this suggestion that was lymphocyte and plasma cell expressed signaling lymphocytic activation molecule (SLAM) or CD150, which was considered as the receptor of morbillivirus including FeMV (De Salort et al., 2011; De Luca et al., 2020; Nambulli et al., 2022; Nikolin et al., 2022).

Another histopathological finding from HE slide evaluation is the presence of eosinophilic-ICIB formation on tubular epithelial cells of proximal tubules. The presence of eosinophilic-ICIB-like formation on renal epithelial cells, particularly on proximal tubules, was considered as pathognomonic lesion that might associate with FeMV infection, particularly FeMV-1 (Chaiyasak et al., 2022). Other than FeMV infection, the formation of eosinophilic-ICIB would likely associate with hyaline droplet in kidney (Decker et al., 2012).

Special staining determination

Special staining using PAS and MT revealed several histopathological findings. In PAS staining, the tubular basement membrane of each case had various conditions. The lesion comprised from intact renal-tubules to ruptured-tubular basement membrane followed by detachment of tubular epithelial cells. In association of FeMV infection, it was remained debatable whether FeMV-infection could rupture the tubular basement membrane of infected kidneys. However, it had been confirmed that cats infected with FeMV had showed the declining of amount of uromodulin and cauxin in the urine. The declining of both proteomes marked the damage of kidney tubules as both proteins were produced by tubules (Woo et al., 2012; Crisi et al., 2020). Unfortunately, in this study both proteomes (uromodulin and cauxin) were not measured. Furthermore, other histopathological finding of PAS staining was the occurrence of membranoproliferative-glomerulonephritis (MPGN) on

five cases (21P240D, 21P413W, 21P603Y, 22P060Y, 22P118R), range from mild to severe level. MPGN was one of hallmark of the occurrence of Immune-complex glomerulonephritis (ICGN). Previous study conducted in Japan had reported the occurrence of immune-complex formation of FeMV infection by localized the presence of feline IgG on glomerulus (Sutummaporn et al., 2019). However, in this study the sub-localization assay of feline-IgG was not carried out to confirm the accumulation of feline-IgG on the glomerulus. Regarding selective viral screening, two cases of MPGN-cats (22P060Y and 22P118R) were co-infected with FeLV. Hence, it would likely that FeLV infection might contributed on formation of MPGN formation as previous study had reported (Inoue et al., 2001). Regardless the severity of MPGN, it had been reported that MPGN could be found on cats as young as 9 months old (Asano et al., 2008). ICGN on kidneys occurred in two ways; it was the consequence of immune-complex accumulation on glomerulus or the inability of immune system to completely neutralize the antigen that run-in blood circulation. Occurrence of MPGN would likely to contribute as initiator to induce CKD on cats (Rossi et al., 2019). However, according to viral localization assays, there was no immunostaining signal and ISH signal of FeMV were exhibited by the glomerulus.

MT special staining revealed that FeMV-infected kidney suffer from interstitial fibrosis, except case 21P240D. According to semiquantitative scoring, the most severe fibrosis was observed on case 21P413 (score 3) that was considered as senior cat (16 years old) and also possessed gross lesion of irregular surface. Furthermore, the prominent interstitial fibrosis was also observed on 21P346Y (score 2) that considered as senior cat (10 years old). In contrast, case 21P603Y (score 2) was also exhibited fibrosis although it was considered as young cats (1 year old), which also exhibited severe-MPGN. Previous study that carried out in Japan suggested the significant association of FeMV and formation of interstitial fibrosis (Sutummaporn et al., 2019). However, on that study, positive-FeMV-antigen-cases were consisted of cats with age

range 2-18 years old (n=14), that was dominated by senior cats (n=9) (Sutummaporn et al., 2019). Hence, the occurrence of interstitial fibrosis would likely to be obvious which accordance with the aging of the cats. In contrast, in this study seven out of nine cases were considered as young cats (1-3 years old) which were obviously different compared to that study. However, the interstitial fibrosis did occur on six cases that considered as young cats. Hereinafter, if those cats had longer life span, FeMV infection might contribute on early involvement of CKD. The presence of interstitial fibrosis on most cases could be the hallmark of chronic response on injury that occurred in renal tissue. The degree of fibrosis might have reverse correlation with the rate of self-repairment carried out by kidney, to counterattack the consequence of the insult (Lawson et al., 2015). However, in this study, proliferative activity was not investigated.

Caspase-dependent apoptotic activity

Paramyxoviridae was one of virus family that had been reported to be associated with regulation of apoptosis (Sun et al., 2004; Del Puerto et al., 2011). Previous study had investigated apoptotic activity associated with FeMV infection. However, apoptotic assay was carried out by using TUNEL assay, which could not confirm whether the apoptotic activity was undergone caspase-dependent or not (Sutummaporn et al., 2020). In this study, apoptotic assay was carried out by detecting immunostaining signal of activated (cleavaged) caspase-3, as the executor of caspase-dependent apoptotic activity, to confirm that FeMV infection might induce caspase-dependent apoptotic activity. Among nine cases, seven cases exhibited apoptotic activity. The apoptotic activity was exhibited by nucleus of tubular epithelial cells. It was still remained unknown the underlaying process of how FeMV induced caspase-dependent apoptosis. However, apoptosis is one of mechanism that kidney undergone as the response to injury (Cowgill et al., 2016;

Chen et al., 2020). Moreover, apoptosis was other mechanism to eliminate the virus from infected cell (Bruggeman, 2019) and a viral strategy to spread to adjacent cells without inducing inflammatory response which is the extension of immune response (Roulston et al., 1999). Furthermore, the continuing of apoptotic activity on renal cells was capable to induce interstitial fibrosis that the hallmark of CKD (Jang and Padanilam, 2015). One of counterattack that kidney used to compensate apoptotic activity on renal tissue is by performing proliferation activity. However, in this study proliferation activity was not investigated further. It was remained unknown what pathway that FeMV uses to induce apoptosis. However, another morbillivirus such as *Peste des petits ruminants* induce apoptosis through extrinsic pathway had been reported (Sahoo et al., 2020).

Viral localization assays

Viral localization assay was conducted by performing IHC against M-protein of FeMV and ISH to detect partial L-gene. The result of IHC showed that seven cases exhibited immunostaining signal. The cases which did not exhibit any immunostaining signal were 21P240D and 21P126R. Immunostaining signal was exhibited on all areas of renal tissue (cortical, medullar, and pelvis). However, one case 21P413W did not exhibit immunostaining signal on pelvis area. In details, immunostaining signal was exhibited by eosinophilic-ICIB formation and cytoplasm of tubular epithelial cells. Interestingly, in some cases such as 21P603C, the immunostaining signal was exhibited by nucleus of tubular epithelial cells. IHC assay was aimed to detect the presence of M-protein of FeMV. The presence of M-protein that meant that FeMV had produced the protein then might already assemble the progeny virus (active virus). Previous study reported that immunostaining signal was exhibited by eosinophilic-ICIB formation (Chaiyasak et al., 2022) and cytoplasm of tubular epithelial cells (Crisi et al., 2020). Regarding the findings in this study, it would likely

reveal that FeMV undergo replication and viral assembly not only on cytoplasm but also on nucleus. However, glomerulus of the renal tissue did not exhibit immunostaining signals. ISH assay showing that *in-situ* signals was exhibited by all FeMV-1 positive cases including cases that did not exhibit immunostaining signal (21P240D and 22P126C). ISH signal was exhibited on all renal tissue areas (cortical, medullar, and pelvis). Accordance with immunostaining signals, ISH signals was exhibited by eosinophilic-ICIB formation and cytoplasm of tubular epithelial cells. Nucleus of some FeMV-cases exhibited ISH signals (21P240D and 22P126C).

Regarding the result of IHC and ISH assay, it would likely to be notified that although immunostaining signal against M-protein did not exhibit, the partial of L-gene was remained to be detected. Although all cases demonstrated eosinophilic-ICIB-like formation, not all ICIB-cases exhibit immunostaining signal or ISH signals. The presence of eosinophilic-ICIB-like formation in cats kidney might associate with hyalin-droplets formation (Decker et al., 2012). However, in this study the presence of hyalin-droplets was not investigated further. Moreover, the IHC and ISH assay detect different target of FeMV. Between M-protein or L-protein of FeMV, L-protein was notified to be the most conserve gene/protein in FeMV. Similar approach was conducted from previous study by detecting P and N protein which generated different outcomes (Sutummaporn et al., 2019). Other than the difference of tools in detecting the viral localization of FeMV, it was likely possible that the difference in outcome of IHC and ISH assay might associate with stage of replication of FeMV, in which for cases that only exhibit immunostaining signals would likely represent the active progeny virus. In contrast, the case that only exhibited ISH signal would likely on subclinical stage.

Association of FeMV-1 and histopathological consequence of renal tissue

Spearman correlation statistical analysis revealed the correlation between intensity of ISH and IHC signal compared to histopathological parameters in this study; degree of inflammation, tubular basement membrane integrity, fibrosis, and amount of expression of cleavage caspase 3. The Spearman coefficient comprised of various correlations. However, the significancy was observed on ISH-IHC signal intensity compared with the degree of apoptosis. Moreover, the correlation revealed to be strong positive correlation that means apoptotic proportion might be increasing as the intensity of ISH-IHC signal increasing. This finding was accordance with previous study that suggests FeMV-1 infection increased proportion of apoptosis (Sutummaporn et al., 2020).

In this study, apoptotic activity assay was conducted by detecting the activity of cleavage caspase 3 which works as executor of apoptosis. Apoptosis occurred through two pathways that are extrinsic and intrinsic pathway. However, it was suggested to investigate further to clarify which pathway FeMV would likely to induce apoptosis.

Although in this study correlation of ISH-IHC signals and interstitial fibrosis was negligible and not significance, interstitial fibrosis in kidney was hallmark that chronic infection might occur as the result of severe injury (Brown et al., 2016).

CONCLUSION

In this study, among paramyxoviruses, FeMV-1 partial genomic material was detected on nine cases. In contrast, FeMV-2 and FPaV were not detected. It was suggested that FeMV-1 had higher prevalence compared to other paramyxovirus-associated kidney diseases. The ISH and IHC signals that was exhibited by the nucleus of tubules would likely gave rise an understanding that subcellular localization of FeMV was not only on cytoplasm but also in nucleus which might suggest FeMV used nucleus to carry genomic replication and virion assemble. Moreover, it was also proved that FeMV infection might contribute to increase apoptotic activity of renal tubules. However, in this study the association of FeMV infection and histopathological consequences was carried out by comparing ISH-IHC signals to histopathological scoring. In the future study, real-time RT-PCR for FeMV quantification might be needed to be carried out to confirm this finding.

REFERENCES

Abraham SN and Miao Y. 2015. The nature of immune responses to urinary tract infections. Nat Rev Immunol. 15(10): 655-663.

Artika IM, Wiyatno A and Ma'roef CN. 2020. Pathogenic viruses: Molecular detection and characterization. Infect Genet Evol. 81: 104215.

Asano T, Tsukamoto A, Ohno K, Ogihara K, Kamiie J and Shirota K. 2008. Membranoproliferative glomerulonephritis in a young cat. J Vet Med Sci. 70(12): 1373-1375.

AVMA. 2018. "Subject: Pet Ownership and Demographics Sourcebook. Total Pet ownership and Pet Populations 2017-2018." (online). Available: https://www.avma.org/sites/default/files/resources/AVMA-Pet-Demographics-Executive-Summary.pdf.

Balbo LC, Fritzen JTT, Lorenzetti E, Medeiros TNS, Jardim AM, Alfieri AA and Alfieri AF. 2021. Molecular characterization of Feline paramyxovirus and Feline morbillivirus in cats from Brazil. Braz J Microbiol.

Bande F, Arshad SS, Hassan L, Zakaria Z, Sapian NA, Rahman NA and Alazawy A. 2012. Prevalence and risk factors of feline leukaemia virus and feline immunodeficiency virus in peninsular Malaysia. BMC Vet Res. 8: 33.

Barrs VR. 2019. Feline Panleukopenia: A Re-emergent Disease. Vet Clin North Am Small Anim Pract. 49(4): 651-670.

Bartges JW. 2012. Chronic kidney disease in dogs and cats. Vet Clin North Am Small Anim Pract. 42(4): 669-692, vi.

Bascands JL and Schanstra JP. 2005. Obstructive nephropathy: insights from genetically engineered animals. Kidney International. 68(3): 925-937.

Baxter KJ, Levy JK, Edinboro CH, Vaden SL and Tompkins MB. 2012. Renal disease in cats infected with feline immunodeficiency virus. J Vet Intern Med. 26(2): 238-243.

Beatty JA and Hartmann K. 2021. Advances in Feline Viruses and Viral Diseases. In: Viruses. 2021/06/03 ed. (ed.).

Belak S. 2007. Molecular diagnosis of viral diseases, present trends and future aspects A view from the OIE Collaborating Centre for the Application of Polymerase Chain Reaction Methods for Diagnosis of Viral Diseases in Veterinary Medicine. Vaccine. 25(30): 5444-5452.

Bitzer M, Prinz F, Bauer M, Spiegel M, Neubert WJ, Gregor M, Schulze-Osthoff K and Lauer U. 1999. Sendai Virus Infection Induces Apoptosis through Activation of Caspase-8 (FLICE) and Caspase-3 (CPP32). Journal of Virology. 73(1): 702-708.

Black LM, Lever JM and Agarwal A. 2019. Renal Inflammation and Fibrosis: A Double-edged Sword. J Histochem Cytochem. 67(9): 663-681.

Bonelli P, Masu G, Dei Giudici S, Pintus D, Peruzzu A, Piseddu T, Santucciu C, Cossu A, Demurtas N and Masala G. 2018. Cystic echinococcosis in a domestic cat (Felis catus) in Italy. Parasite. 25: 25.

Bose K. 2015. Proteases in Apoptosis: Pathways, Protocols and Translational Advances. Anticancer research. 36 1: 482.

Bouljihad M, Lindeman CJ and Hayden DW. 2002. Pyogranulomatous meningoencephalitis associated with dematiaceous fungal (Cladophialophora bantiana) infection in a domestic cat. J Vet Diagn Invest. 14(1): 70-72.

Brown CA, Elliott J, Schmiedt CW and Brown SA. 2016. Chronic Kidney Disease in Aged Cats: Clinical Features, Morphology, and Proposed Pathogeneses. Vet Pathol. 53(2): 309-326.

Bruggeman LA. 2007. Viral subversion mechanisms in chronic kidney disease pathogenesis. Clin J Am Soc Nephrol. 2 Suppl 1: S13-19.

Bruggeman LA. 2019. Common Mechanisms of Viral Injury to the Kidney. Adv Chronic Kidney Dis. 26(3): 164-170.

Capozza P, Lorusso E, Colella V, Thibault JC, Tan DY, Tronel JP, Halos L, Beugnet F, Elia G, Nguyen VL, Occhiogrosso L, Martella V, Otranto D and Decaro N. 2021. Feline leukemia virus in owned cats in Southeast Asia and Taiwan. Vet Microbiol. 254: 109008.

Cavalcante GC, Schaan AP, Cabral GF, Santana-da-Silva MN, Pinto P, Vidal AF and Ribeiro-Dos-Santos A. 2019. A Cell's Fate: An Overview of the Molecular Biology and Genetics of Apoptosis. Int J Mol Sci. 20(17).

Cecconi F and D'Amelio M. 2010. Apoptosome: An up-and-coming therapeutical tool. In: Apoptosome: An Up-and-coming Therapeutical Tool. Springer Netherlands. 1-322.

Chaiyasak S, Piewbang C, Rungsipipat A and Techangamsuwan S. 2020a. Molecular epidemiology and genome analysis of feline morbillivirus in household and shelter cats in Thailand. BMC Vet Res. 16(1): 240.

Chaiyasak S, Piewbang C, Rungsipipat A and Techangamsuwan S. 2020b. Molecular epidemiology and genome analysis of feline morbillivirus in household and shelter cats in Thailand. BMC Veterinary Research. 16(1): 240.

Chaiyasak S, Piewbang C, Yostawonkul J, Boonrungsiman S, Kasantikul T, Rungsipipat A and Techangamsuwan S. 2022. Renal epitheliotropism of feline morbillivirus in two cats. Vet Pathol. 59(1): 127-131.

Chen H, Dunaevich A, Apfelbaum N, Kuzi S, Mazaki-Tovi M, Aroch I and Segev G. 2020. Acute on chronic kidney disease in cats: Etiology, clinical and clinicopathologic findings, prognostic markers, and outcome. J Vet Intern Med. 34(4): 1496-1506.

Chen L, Han X, Li Y, Zhang C and Xing X. 2021. The Clinical Characteristics and Outcomes of Adult Patients With Pneumonia Related to Three Paramyxoviruses. Frontiers in Medicine. 7.

Chin PJ, La Neve F, Zanda V and Khan AS. 2020. Complete Genome Sequence of Feline Leukemia Virus Kawakami-Theilen Strain KT-FeLV-UCD-1. Microbiol Resour Announc. 9(20).

Cowgill LD, Polzin DJ, Elliott J, Nabity MB, Segev G, Grauer GF, Brown S, Langston C and van Dongen AM. 2016. Is Progressive Chronic Kidney Disease a Slow Acute Kidney Injury? Vet Clin North Am Small Anim Pract. 46(6): 995-1013.

Crisi PE, Dondi F, De Luca E, Di Tommaso M, Vasylyeva K, Ferlizza E, Savini G, Luciani A, Malatesta D, Lorusso A and Boari A. 2020. Early Renal Involvement in Cats with Natural Feline Morbillivirus Infection. Animals (Basel). 10(5).

D'Arcy MS. 2019. Cell death: a review of the major forms of apoptosis, necrosis and autophagy. Cell Biol Int. 43(6): 582-592.

Daniels JB. 2013. Molecular diagnostics for infectious disease in small animal medicine: an overview from the laboratory. Vet Clin North Am Small Anim Pract. 43(6):

1373-1384, vii.

De Luca E, Crisi PE, Marcacci M, Malatesta D, Di Sabatino D, Cito F, D'Alterio N, Puglia I, Berjaoui S, Colaianni ML, Tinelli A, Ripà P, Vincifori G, Di Teodoro G, Dondi F, Savini G, Boari A and Lorusso A. 2020. Epidemiology, pathological aspects and genome heterogeneity of feline morbillivirus in Italy. Vet Microbiol. 240: 108484.

De Luca E, Sautto GA, Crisi PE and Lorusso A. 2021. Feline Morbillivirus Infection in Domestic Cats: What Have We Learned So Far? Viruses. 13(4).

De Salort J, Sintes J, Llinas L, Matesanz-Isabel J and Engel P. 2011. Expression of SLAM (CD150) cell-surface receptors on human B-cell subsets: from pro-B to plasma cells. Immunology Letters. 134(2): 129-136.

Decker JH, Dochterman LW, Niquette AL and Brej M. 2012. Association of renal tubular hyaline droplets with lymphoma in CD-1 mice. Toxicol Pathol. 40(4): 651-655.

Del Puerto HL, Martins AS, Milsted A, Souza-Fagundes EM, Braz GF, Hissa B, Andrade LO, Alves F, Rajao DS, Leite RC and Vasconcelos AC. 2011. Canine distemper virus induces apoptosis in cervical tumor derived cell lines. Virol J. 8: 334.

Donato G, Masucci M, De Luca E, Alibrandi A, De Majo M, Berjaoui S, Martino C, Mangano C, Lorusso A and Pennisi MG. 2021. Feline Morbillivirus in Southern Italy: Epidemiology, Clinico-Pathological Features and Phylogenetic Analysis in Cats. Viruses. 13(8).

Drechsler Y, Alcaraz A, Bossong FJ, Collisson EW and Diniz PP. 2011. Feline coronavirus in multicat environments. Vet Clin North Am Small Anim Pract. 41(6): 1133-1169.

Dunham SP and Graham E. 2008. Retroviral infections of small animals. Vet Clin North Am Small Anim Pract. 38(4): 879-901, ix.

Elmore S. 2007. Apoptosis: a review of programmed cell death. Toxicol Pathol. 35(4): 495-516.

Emery SL, Erdman DD, Bowen MD, Newton BR, Winchell JM, Meyer RF, Tong S, Cook BT, Holloway BP, McCaustland KA, Rota PA, Bankamp B, Lowe LE, Ksiazek TG, Bellini WJ and Anderson LJ. 2004. Real-time reverse transcription-polymerase chain reaction assay for SARS-associated coronavirus. Emerg Infect Dis. 10(2): 311-316.

Esolen LM, Park SW, Hardwick JM and Griffin DE. 1995. Apoptosis as a cause of death in measles virus-infected cells. J Virol. 69(6): 3955-3958.

FEDIAF. 2020. "Subject: FEDIAF FACTS & FIGURES 2020 European Overview" (online). Available: https://drive.google.com/file/d/1ER8F1E3gwX2g3Tl5aGpxPziCuyOj-1p_/view.

Finch NC, Syme HM and Elliott J. 2016. Risk Factors for Development of Chronic Kidney Disease in Cats. J Vet Intern Med. 30(2): 602-610.

Frisk AL, Konig M, Moritz A and Baumgartner W. 1999. Detection of canine distemper virus nucleoprotein RNA by reverse transcription-PCR using serum, whole blood, and cerebrospinal fluid from dogs with distemper. J Clin Microbiol. 37(11): 3634-3643.

Furuya T, Sassa Y, Omatsu T, Nagai M, Fukushima R, Shibutani M, Yamaguchi T, Uematsu Y, Shirota K and Mizutani T. 2014. Existence of feline morbillivirus infection in Japanese cat populations. Arch Virol. 159(2): 371-373.

Galluzzi L and Vitale I and Aaronson SA and Abrams JM and Adam D and Agostinis P and Alnemri ES and Altucci L and Amelio I and Andrews DW and Annicchiarico-Petruzzelli M and Antonov AV and Arama E and Baehrecke EH and Barlev NA and Bazan NG and Bernassola F and Bertrand MJM and Bianchi K and Blagosklonny MV and Blomgren K and Borner C and Boya P and Brenner C and Campanella M and Candi E and Carmona-Gutierrez D and Cecconi F and Chan FK and Chandel NS and Cheng EH and Chipuk JE and Cidlowski JA and Ciechanover A and Cohen GM and Conrad M and Cubillos-Ruiz JR and Czabotar PE and D'Angiolella V and Dawson TM and Dawson VL and De Laurenzi V and De Maria R and Debatin KM and DeBerardinis RJ and Deshmukh M and Di Daniele N and Di Virgilio F and Dixit VM and Dixon SJ and Duckett CS and Dynlacht BD and El-Deiry WS and Elrod JW and Fimia GM and Fulda S and Garcia-Saez AJ and Garg AD and Garrido C and Gavathiotis E and Golstein P and Gottlieb E and Green DR and Greene LA and Gronemeyer H and Gross A and Hajnoczky G and Hardwick JM and Harris IS and Hengartner MO and Hetz C and Ichijo H and Jaattela M and Joseph B and Jost PJ and Juin PP and Kaiser WJ and Karin M and Kaufmann T and Kepp O and Kimchi A and Kitsis RN and Klionsky DJ and Knight RA and Kumar S and Lee SW and Lemasters JJ and Levine B and

Linkermann A and Lipton SA and Lockshin RA and Lopez-Otin C and Lowe SW and Luedde T and Lugli E and MacFarlane M and Madeo F and Malewicz M and Malorni W and Manic G and Marine JC and Martin SJ and Martinou JC and Medema JP and Mehlen P and Meier P and Melino S and Miao EA and Molkentin JD and Moll UM and Munoz-Pinedo C and Nagata S and Nunez G and Oberst A and Oren M and Overholtzer M and Pagano M and Panaretakis T and Pasparakis M and Penninger JM and Pereira DM and Pervaiz S and Peter ME and Piacentini M and Pinton P and Prehn JHM and Puthalakath H and Rabinovich GA and Rehm M and Rizzuto R and Rodrigues CMP and Rubinsztein DC and Rudel T and Ryan KM and Sayan E and Scorrano L and Shao F and Shi Y and Silke J and Simon HU and Sistigu A and Stockwell BR and Strasser A and Szabadkai G and Tait SWG and Tang D and Tavernarakis N and Thorburn A and Tsujimoto Y and Turk B and Vanden Berghe T and Vandenabeele P and Vander Heiden MG and Villunger A and Virgin HW and Vousden KH and Vucic D and Wagner EF and Walczak H and Wallach D and Wang Y and Wells JA and Wood W and Yuan J and Zakeri Z and Zhivotovsky B and Zitvogel L and Melino G and Kroemer G. 2018. Molecular mechanisms of cell death: recommendations of the Nomenclature Committee on Cell Death 2018. Cell Death Differ. 25(3): 486-541.

Hariya Y, Yokosawa N, Yonekura N, Kohama G and Fuji N. 2000. Mumps virus can suppress the effective augmentation of HPC-induced apoptosis by IFN-gamma through disruption of IFN signaling in U937 cells. Microbiol Immunol. 44(6): 537-541.

Hartmann K and Hofmann-Lehmann R. 2020. What's New in Feline Leukemia Virus Infection. Vet Clin North Am Small Anim Pract. 50(5): 1013-1036.

Hartmann K, Pennisi MG and Dorsch R. 2020. Infectious Agents in Feline Chronic Kidney Disease: What Is the Evidence? Advances in Small Animal Care. 1: 189-206.

Hoelzer K, Shackelton LA, Parrish CR and Holmes EC. 2008. Phylogenetic analysis reveals the emergence, evolution and dispersal of carnivore parvoviruses. J Gen Virol. 89(Pt 9): 2280-2289.

Hsu RK and Hsu CY. 2016. The Role of Acute Kidney Injury in Chronic Kidney Disease. Semin Nephrol. 36(4): 283-292.

Hueffer K, Palermo LM and Parrish CR. 2004. Parvovirus infection of cells by using variants of the feline transferrin receptor altering clathrin-mediated endocytosis, membrane domain localization, and capsid-binding domains. J Virol. 78(11): 5601-5611.

Inoue K, Kami-ie J, Ohtake S, Wakui S, Machida S and Shirota K. 2001. Atypical membranoproliferative glomerulonephritis in a cat. Vet Pathol. 38(4): 468-470.

Jaimes JA and Whittaker GR. 2018. Feline coronavirus: Insights into viral pathogenesis based on the spike protein structure and function. Virology. 517: 108-121.

Jang H-S and Padanilam BJ. 2015. Simultaneous deletion of Bax and Bak is required to prevent apoptosis and interstitial fibrosis in obstructive nephropathy. American Journal of Physiology-Renal Physiology. 309(6): F540-F550.

Jeanes EC, Wegg ML, Mitchell JA, Priestnall SL, Fleming L and Dawson C. 2022. Comparison of the prevalence of Domestic Cat Hepadnavirus in a population of cats with uveitis and in a healthy blood donor cat population in the United Kingdom. Vet Ophthalmol. 25(2): 165-172.

Kawamura M, Watanabe S, Odahara Y, Nakagawa S, Endo Y, Tsujimoto H and Nishigaki K. 2015. Genetic diversity in the feline leukemia virus gag gene. Virus Res. 204: 74-81.

Kipar A, Meli ML, Baptiste KE, Bowker LJ and Lutz H. 2010. Sites of feline coronavirus persistence in healthy cats. J Gen Virol. 91(Pt 7): 1698-1707.

Ksiazek TG, Erdman D, Goldsmith CS, Zaki SR, Peret T, Emery S, Tong S, Urbani C, Comer JA, Lim W, Rollin PE, Dowell SF, Ling AE, Humphrey CD, Shieh WJ, Guarner J, Paddock CD, Rota P, Fields B, DeRisi J, Yang JY, Cox N, Hughes JM, LeDuc JW, Bellini WJ, Anderson LJ and Group SW. 2003. A novel coronavirus associated with severe acute respiratory syndrome. N Engl J Med. 348(20): 1953-1966.

Kumar R, Herbert PE and Warrens AN. 2005. An introduction to death receptors in apoptosis. Int J Surg. 3(4): 268-277.

Kurts C, Panzer U, Anders HJ and Rees AJ. 2013. The immune system and kidney disease: basic concepts and clinical implications. Nat Rev Immunol. 13(10): 738-753.

Lacharoje S, Techangamsuwan S and Chaichanawongsaroj N. 2021. Rapid

characterization of feline leukemia virus infective stages by a novel nested recombinase polymerase amplification (RPA) and reverse transcriptase-RPA. Sci Rep. 11(1): 22023.

Landmann M, Scheibner D, Graaf A, Gischke M, Koethe S, Fatola OI, Raddatz B, Mettenleiter TC, Beer M, Grund C, Harder T, Abdelwhab EM and Ulrich R. 2021. A Semiquantitative Scoring System for Histopathological and Immunohistochemical Assessment of Lesions and Tissue Tropism in Avian Influenza. Viruses. 13(5).

Lavorente FLP, de Matos A, Lorenzetti E, Oliveira MV, Pinto-Ferreira F, Michelazzo MMZ, Viana NE, Lunardi M, Headley SA, Alfieri AA and Alfieri AF. 2021. First detection of Feline morbillivirus infection in white-eared opossums (Didelphis albiventris, Lund, 1840), a non-feline host. Transbound Emerg Dis.

Lawson J, Elliott J, Wheeler-Jones C, Syme H and Jepson R. 2015. Renal fibrosis in feline chronic kidney disease: known mediators and mechanisms of injury. Vet J. 203(1): 18-26.

Licitra BN, Millet JK, Regan AD, Hamilton BS, Rinaldi VD, Duhamel GE and Whittaker GR. 2013. Mutation in spike protein cleavage site and pathogenesis of feline coronavirus. Emerg Infect Dis. 19(7): 1066-1073.

Long TE, Sigurdsson MI, Sigurdsson GH and Indridason OS. 2016. Improved long-term survival and renal recovery after acute kidney injury in hospitalized patients: A 20 year experience. Nephrology (Carlton). 21(12): 1027-1033.

Ludes PO, de Roquetaillade C, Chousterman BG, Pottecher J and Mebazaa A. 2021. Role of Damage-Associated Molecular Patterns in Septic Acute Kidney Injury, From Injury to Recovery. Front Immunol. 12: 606622.

Maclachlan N, Dubovi E and Fenner F. 2017. Fenner's veterinary virology. 5th ed. In: ELSEVIER, San Diego, California.

Makris K and Spanou L. 2016. Acute Kidney Injury: Definition, Pathophysiology and Clinical Phenotypes. Clin Biochem Rev. 37(2): 85-98.

Marcacci M, De Luca E, Zaccaria G, Di Tommaso M, Mangone I, Aste G, Savini G, Boari A and Lorusso A. 2016. Genome characterization of feline morbillivirus from Italy. J Virol Methods. 234: 160-163.

McCallum KE, Stubbs S, Hope N, Mickleburgh I, Dight D, Tiley L and Williams TL. 2018. Detection and seroprevalence of morbillivirus and other paramyxoviruses in geriatric cats with and without evidence of azotemic chronic kidney disease. J Vet Intern Med. 32(3): 1100-1108.

McLeland SM, Cianciolo RE, Duncan CG and Quimby JM. 2015. A Comparison of Biochemical and Histopathologic Staging in Cats With Chronic Kidney Disease. Veterinary Pathology. 52(3): 524-534.

Mochizuki M, Horiuchi M, Hiragi H, San Gabriel MC, Yasuda N and Uno T. 1996. Isolation of canine parvovirus from a cat manifesting clinical signs of feline panleukopenia. J Clin Microbiol. 34(9): 2101-2105.

Mohd Isa NH, Selvarajah GT, Khor KH, Tan SW, Manoraj H, Omar NH, Omar AR and Mustaffa-Kamal F. 2019. Molecular detection and characterisation of feline morbillivirus in domestic cats in Malaysia. Vet Microbiol. 236: 108382.

Monaghan K, Nolan B and Labato M. 2012. Feline acute kidney injury: 1. Pathophysiology, etiology and etiology-specific management considerations. J Feline Med Surg. 14(11): 775-784.

Muratore E, Cerutti F, Colombino E, Biasibetti E, Caruso C, Brovida C, Cavana P, Poncino L, Caputo MP, Peletto S, Masoero L and Capucchio MT. 2020. Feline morbillivirus in northwestern Italy: first detection of genotype 1-B. J Feline Med Surg. 1098612X20969360.

Naim HY. 2015. Measles virus. Hum Vaccin Immunother. 11(1): 21-26.

Nambulli S, Rennick LJ, Acciardo AS, Tilston-Lunel NL, Ho G, Crossland NA, Hardcastle K, Nieto B, Bainbridge G, Williams T, Sharp CR and Duprex WP. 2022. FeMV is a cathepsin-dependent unique morbillivirus infecting the kidneys of domestic cats. Proceedings of the National Academy of Sciences. 119(43): e2209405119.

Neumann S, El Maadidi S, Faletti L, Haun F, Labib S, Schejtman A, Maurer U and Borner C. 2015. How do viruses control mitochondria-mediated apoptosis? Virus Res. 209: 45-55.

Newman S. 2012. The Urinary System. In: Pathologic Basis of Veterinary. 5th ed. Zachary JF and McGavin, MD (ed.). Missouri: ELSEVIER MOSBY. 589-659.

Nikolin V, Hatsue Sobreda Doi L, Sieg M, Busch J, Bottcher D, Tedeschi L, Poulard A,

Staszewski V, Vahlenkamp T and Poulet H. 2022. In Vitro Growth, Receptor Usage and Pathogenesis of Feline Morbillivirus in the Natural Host. Viruses. 14(7).

O'Neill DG, Church DB, McGreevy PD, Thomson PC and Brodbelt DC. 2014. Prevalence of disorders recorded in cats attending primary-care veterinary practices in England. Vet J. 202(2): 286-291.

Obeng E. 2021. Apoptosis (programmed cell death) and its signals - A review. Braz J Biol. 81(4): 1133-1143.

Park ES, Suzuki M, Kimura M, Mizutani H, Saito R, Kubota N, Hasuike Y, Okajima J, Kasai H, Sato Y, Nakajima N, Maruyama K, Imaoka K and Morikawa S. 2016. Epidemiological and pathological study of feline morbillivirus infection in domestic cats in Japan. BMC Vet Res. 12(1): 228.

Pedersen NC, Elliott JB, Glasgow A, Poland A and Keel K. 2000. An isolated epizootic of hemorrhagic-like fever in cats caused by a novel and highly virulent strain of feline calicivirus. Vet Microbiol. 73(4): 281-300.

Pedersen NC, Ho EW, Brown ML and Yamamoto JK. 1987. Isolation of a T-lymphotropic virus from domestic cats with an immunodeficiency-like syndrome. Science. 235(4790): 790-793.

Pesavento PA, Chang KO and Parker JS. 2008. Molecular virology of feline calicivirus. Vet Clin North Am Small Anim Pract. 38(4): 775-786, vii.

Pfeffer CM and Singh ATK. 2018. Apoptosis: A Target for Anticancer Therapy. Int J Mol Sci. 19(2).

Piewbang C, Chaiyasak S, Kongmakee P, Sanannu S, Khotapat P, Ratthanophart J, Banlunara W and Techangamsuwan S. 2020. Feline Morbillivirus Infection Associated With Tubulointerstitial Nephritis in Black Leopards (Panthera pardus). Vet Pathol. 57(6): 871-879.

Piewbang C, Kasantikul T, Pringproa K and Techangamsuwan S. 2019. Feline bocavirus-1 associated with outbreaks of hemorrhagic enteritis in household cats: potential first evidence of a pathological role, viral tropism and natural genetic recombination. Sci Rep. 9(1): 16367.

Piewbang C, Wardhani SW, Chanseanroj J, Yostawonkul J, Boonrungsiman S, Saengkrit N, Kongmakee P, Banlunara W, Poovorawan Y, Kasantikul T and Techangamsuwan

S. 2021a. Natural infection of parvovirus in wild fishing cats (Prionailurus viverrinus) reveals extant viral localization in kidneys. Plos One. 16(3): e0247266.

Piewbang C, Wardhani SW, Dankaona W, Yostawonkul J, Boonrungsiman S, Surachetpong W, Kasantikul T and Techangamsuwan S. 2021b. Feline morbillivirus-1 in dogs with respiratory diseases. Transbound Emerg Dis.

Polani S, Roca AL, Rosensteel BB, Kolokotronis SO and Bar-Gal GK. 2010. Evolutionary dynamics of endogenous feline leukemia virus proliferation among species of the domestic cat lineage. Virology. 405(2): 397-407.

Prasad N and Patel MR. 2018. Infection-Induced Kidney Diseases. Front Med (Lausanne). 5: 327.

Quimby J, Gowland S, Carney HC, DePorter T, Plummer P and Westropp J. 2021. 2021 AAHA/AAFP Feline Life Stage Guidelines. J Feline Med Surg. 23(3): 211-233.

Rayhel LH, Quimby JM, Cianciolo RE, Cleroux A, McLeland SM and Franken T. 2020. Clinicopathologic and pathologic characteristics of feline proteinuric kidney disease. J Feline Med Surg. 22(12): 1219-1229.

Reubel GH, Hoffmann DE and Pedersen NC. 1992. Acute and chronic faucitis of domestic cats. A feline calicivirus-induced disease. Vet Clin North Am Small Anim Pract. 22(6): 1347-1360.

Reynolds BS and Lefebvre HP. 2013. Feline CKD: Pathophysiology and risk factors--what do we know? J Feline Med Surg. 15 Suppl 1: 3-14.

Rima B, Balkema-Buschmann A, Dundon WG, Duprex P, Easton A, Fouchier R, Kurath G, Lamb R, Lee B, Rota P, Wang L and Ictv Report C. 2019. ICTV Virus Taxonomy Profile: Paramyxoviridae. J Gen Virol. 100(12): 1593-1594.

Rossi F, Aresu L, Martini V, Trez D, Zanetti R, Coppola LM, Ferri F and Zini E. 2019. Immune-complex glomerulonephritis in cats: a retrospective study based on clinico-pathological data, histopathology and ultrastructural features. BMC Vet Res. 15(1): 303.

Roulston A, Marcellus RC and Branton PE. 1999. Viruses and apoptosis. Annu Rev Microbiol. 53: 577-628.

Roy S and Nicholson DW. 2000. Cross-talk in cell death signaling. J Exp Med. 192(8): F21-25.

Sahoo M, M D, Thakor JC, Baloni S, Saxena S, Shrivastava S, Dhama K, Singh K and Singh R. 2020. Neuropathology mediated through caspase dependent extrinsic pathway in goat kids naturally infected with PPRV. Microbial Pathogenesis. 140: 103949.

Sakaguchi S, Nakagawa S, Mitsuhashi S, Ogawa M, Sugiyama K, Tamukai K, Koide R, Katayama Y, Nakano T, Makino S, Imanishi T, Miyazawa T and Mizutani T. 2020. Molecular characterization of feline paramyxovirus in Japanese cat populations. Arch Virol. 165(2): 413-418.

Samal SK. 2008. Paramyxoviruses of Animals. Encyclopedia of Virology. 40-47.

Sato Y, Ohe K, Murakami M, Fukuyama M, Furuhata K, Kishikawa S, Suzuki Y, Kiuchi A, Hara M, Ishikawa Y and Taneno A. 2002. Phylogenetic analysis of field isolates of feline calcivirus (FCV) in Japan by sequencing part of its capsid gene. Vet Res Commun. 26(3): 205-219.

Scalon MC, da Silva TF, Aquino LC, Carneiro FT, Lima MG, Lemos MD and Paludo GR. 2014. Touchdown polymerase chain reaction detection of polycystic kidney disease and laboratory findings in different cat populations. J Vet Diagn Invest. 26(4): 542-546.

Schober P, Boer C and Schwarte LA. 2018. Correlation Coefficients: Appropriate Use and Interpretation. Anesth Analg. 126(5): 1763-1768.

Segev G. 2022. "Subject: Differentiation between Acute kidney injury and chronic kidney disease" (online). Available: http://www.iris-kidney.com/education/differentiation_acute_kidney_injury_chronic_kidney_disease.html.

Sharp CR, Nambulli S, Acciardo AS, Rennick LJ, Drexler JF, Rima BK, Williams T and Duprex WP. 2016. Chronic Infection of Domestic Cats with Feline Morbillivirus, United States. Emerg Infect Dis. 22(4): 760-762.

Sieg M, Busch J, Eschke M, Bottcher D, Heenemann K, Vahlenkamp A, Reinert A, Seeger J, Heilmann R, Scheffler K and Vahlenkamp TW. 2019. A New Genotype of Feline Morbillivirus Infects Primary Cells of the Lung, Kidney, Brain and Peripheral Blood. Viruses. 11(2).

Sieg M, Heenemann K, Ruckner A, Burgener I, Oechtering G and Vahlenkamp TW. 2015. Discovery of new feline paramyxoviruses in domestic cats with chronic kidney disease. Virus Genes. 51(2): 294-297.

Sieg M, Sacristan I, Busch J, Terio KA, Cabello J, Hidalgo-Hermoso E, Millan J, Bottcher D, Heenemann K, Vahlenkamp TW and Napolitano C. 2020. Identification of Novel Feline Paramyxoviruses in Guignas (Leopardus guigna) from Chile. Viruses. 12(12).

Soos TJ, Sims TN, Barisoni L, Lin K, Littman DR, Dustin ML and Nelson PJ. 2006. CX3CR1+ interstitial dendritic cells form a contiguous network throughout the entire kidney. Kidney International. 70(3): 591-596.

Sterneberg-van der Maaten T, Turner D, Van Tilburg J and Vaarten J. 2016. Benefits and Risks for People and Livestock of Keeping Companion Animals: Searching for a Healthy Balance. J Comp Pathol. 155(1 Suppl 1): S8-S17.

Strutz F and Zeisberg M. 2006. Renal fibroblasts and myofibroblasts in chronic kidney disease. J Am Soc Nephrol. 17(11): 2992-2998.

Sugisawa R, Hiramoto E, Matsuoka S, Iwai S, Takai R, Yamazaki T, Mori N, Okada Y, Takeda N, Yamamura KI, Arai T, Arai S and Miyazaki T. 2016. Impact of feline AIM on the susceptibility of cats to renal disease. Sci Rep. 6: 35251.

Sukhumavasi W, Bellosa ML, Lucio-Forster A, Liotta JL, Lee AC, Pornmingmas P, Chungpivat S, Mohammed HO, Lorentzen L, Dubey JP and Bowman DD. 2012. Serological survey of Toxoplasma gondii, Dirofilaria immitis, Feline Immunodeficiency Virus (FIV) and Feline Leukemia Virus (FeLV) infections in pet cats in Bangkok and vicinities, Thailand. Vet Parasitol. 188(1-2): 25-30.

Sun M, Rothermel TA, Shuman L, Aligo JA, Xu S, Lin Y, Lamb RA and He B. 2004. Conserved cysteine-rich domain of paramyxovirus simian virus 5 V protein plays an important role in blocking apoptosis. J Virol. 78(10): 5068-5078.

Sutummaporn K, Suzuki K, Machida N, Mizutani T, Park ES, Morikawa S and Furuya T. 2019. Association of feline morbillivirus infection with defined pathological changes in cat kidney tissues. Vet Microbiol. 228: 12-19.

Sutummaporn K, Suzuki K, Machida N, Mizutani T, Park ES, Morikawa S and Furuya T. 2020. Increased proportion of apoptotic cells in cat kidney tissues infected with feline morbillivirus. Arch Virol. 165(11): 2647-2651.

Sykes JE. 2014. Canine and Feline Infectious Diseases. In: Elsevier Saunders, St. Louis, Missouri.

Syntichaki P and Tavernarakis N. 2002. Death by necrosis. Uncontrollable catastrophe, or is there order behind the chaos? EMBO Rep. 3(7): 604-609.

Tekes G, Hofmann-Lehmann R, Stallkamp I, Thiel V and Thiel HJ. 2008. Genome organization and reverse genetic analysis of a type I feline coronavirus. J Virol. 82(4): 1851-1859.

Thibault PA, Watkinson RE, Moreira-Soto A, Drexler JF and Lee B. 2017. Zoonotic Potential of Emerging Paramyxoviruses: Knowns and Unknowns. Adv Virus Res. 98: 1-55.

Thomsen JL, Kristensen IB and Ottosen PD. 2006. The histological demonstration of lipids in the proximal renal tubules of patients with diabetic coma. Forensic Sci Med Pathol. 2(4): 249-252.

Tong S, Chern SW, Li Y, Pallansch MA and Anderson LJ. 2008. Sensitive and broadly reactive reverse transcription-PCR assays to detect novel paramyxoviruses. J Clin Microbiol. 46(8): 2652-2658.

Valones MA, Guimaraes RL, Brandao LA, de Souza PR, de Albuquerque Tavares Carvalho A and Crovela S. 2009. Principles and applications of polymerase chain reaction in medical diagnostic fields: a review. Braz J Microbiol. 40(1): 1-11.

Vanmechelen B, Bletsa M, Laenen L, Lopes AR, Vergote V, Beller L, Deboutte W, Korva M, Avsic Zupanc T, Gouy de Bellocq J, Gryseels S, Leirs H, Lemey P, Vrancken B and Maes P. 2018. Discovery and genome characterization of three new Jeilongviruses, a lineage of paramyxoviruses characterized by their unique membrane proteins. BMC Genomics. 19(1): 617.

Wardhani SW, Wongsakul B, Kasantikul T, Piewbang C and Techangamsuwan S. 2021. Molecular and Pathological Investigations of Selected Viral Neuropathogens in Rabies-Negative Brains of Cats and Dogs Revealed Neurotropism of Carnivore Protoparvovirus-1. Front Vet Sci. 8: 710701.

Woo PC, Lau SK, Wong BH, Fan RY, Wong AY, Zhang AJ, Wu Y, Choi GK, Li KS, Hui J, Wang M, Zheng BJ, Chan KH and Yuen KY. 2012. Feline morbillivirus, a previously undescribed paramyxovirus associated with tubulointerstitial nephritis

in domestic cats. Proc Natl Acad Sci U S A. 109(14): 5435-5440.

Yabuki A, Mitani S, Fujiki M, Misumi K, Endo Y, Miyoshi N and Yamato O. 2010. Comparative study of chronic kidney disease in dogs and cats: induction of myofibroblasts. Res Vet Sci. 88(2): 294-299.

Yang S and Rothman RE. 2004. PCR-based diagnostics for infectious diseases: uses, limitations, and future applications in acute-care settings. Lancet Infect Dis. 4(6): 337-348.

Yilmaz H, Tekelioglu BK, Gurel A, Bamac OE, Ozturk GY, Cizmecigil UY, Altan E, Aydin O, Yilmaz A, Berriatua E, Helps CR, Richt JA and Turan N. 2017. Frequency, clinicopathological features and phylogenetic analysis of feline morbillivirus in cats in Istanbul, Turkey. J Feline Med Surg. 19(12): 1206-1214.

Zwart MP and Elena SF. 2015. Matters of Size: Genetic Bottlenecks in Virus Infection and Their Potential Impact on Evolution. Annu Rev Virol. 2(1): 161-179.

APPENDIX

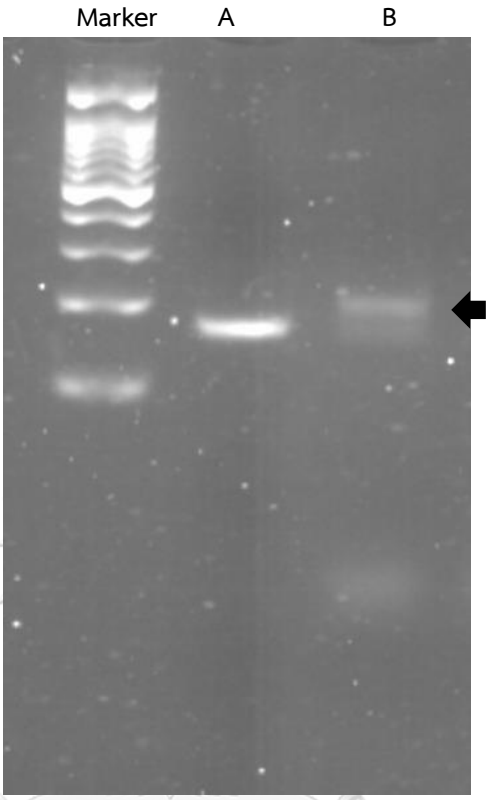

Supplementary Figure 1 Probe construction of partial of L-gene of FeMV-1. A: purified RT-PCR product of partial of L-gene (155 bp); B: DIG-labelled probe. The probe would have bigger molecular weight compared to purified RT-PCR product due to containment of DIG (Arrow).

VITA

NAME	Aisyah Nikmatuz Zahro
DATE OF BIRTH	05 November 1995
PLACE OF BIRTH	Trenggalek, East Java, Indonesia
INSTITUTIONS ATTENDED	Faculty of Veterinary Medicine, Airlangga University, East Java, Indonesia
HOME ADDRESS	Rt 01 Rw 01, Dusun Bakalan, Desa Panggul, Kecamatan Panggul, Kabupaten Trenggalek, East Java, Indonesia, 66364
PUBLICATION	Eosinophilic Intracytoplasmic Inclusion Bodies in Feline Kidneys with Morbillivirus Screening "Proceedings of The Chulalongkorn University Veterinary Conference CUVC 2022: Innovation for Veterinary Society" (Thai Journal Veterinary Medicine Supplement, Volume 52, 2022).
AWARD RECEIVED	Scholarship program for ASEAN countries Chulalongkorn University 90th Anniversary of Chulalongkorn University Scholarship under the Ratchadapisek Somphot Endowment Fund